

Flexible objective controllers for semi-active suspensions with preview

Citation for published version (APA):

Muijderman, J. H. E. A. (1997). *Flexible objective controllers for semi-active suspensions with preview*. [Phd Thesis 1 (Research TU/e / Graduation TU/e), Mechanical Engineering]. Technische Universiteit Eindhoven. <https://doi.org/10.6100/IR502868>

DOI:

[10.6100/IR502868](https://doi.org/10.6100/IR502868)

Document status and date:

Published: 01/01/1997

Document Version:

Publisher's PDF, also known as Version of Record (includes final page, issue and volume numbers)

Please check the document version of this publication:

- A submitted manuscript is the version of the article upon submission and before peer-review. There can be important differences between the submitted version and the official published version of record. People interested in the research are advised to contact the author for the final version of the publication, or visit the DOI to the publisher's website.
- The final author version and the galley proof are versions of the publication after peer review.
- The final published version features the final layout of the paper including the volume, issue and page numbers.

[Link to publication](#)

General rights

Copyright and moral rights for the publications made accessible in the public portal are retained by the authors and/or other copyright owners and it is a condition of accessing publications that users recognise and abide by the legal requirements associated with these rights.

- Users may download and print one copy of any publication from the public portal for the purpose of private study or research.
- You may not further distribute the material or use it for any profit-making activity or commercial gain
- You may freely distribute the URL identifying the publication in the public portal.

If the publication is distributed under the terms of Article 25fa of the Dutch Copyright Act, indicated by the "Taverne" license above, please follow below link for the End User Agreement:

www.tue.nl/taverne

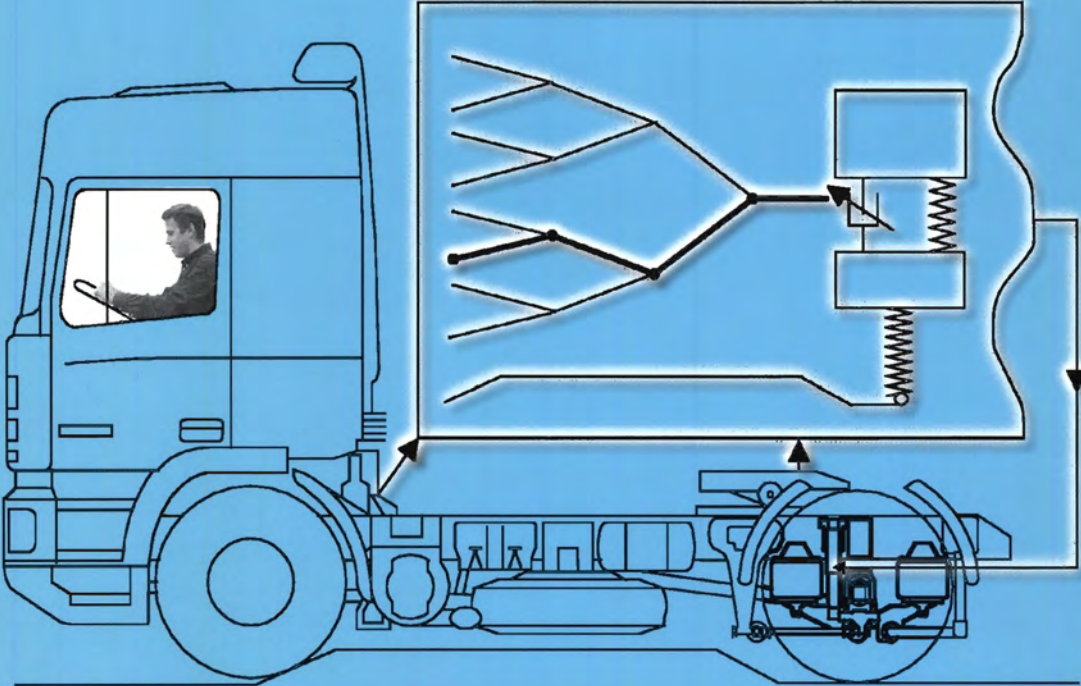
Take down policy

If you believe that this document breaches copyright please contact us at:

openaccess@tue.nl

providing details and we will investigate your claim.

Flexible objective controllers for semi-active suspensions with preview



Hans Muijderman

Flexible objective controllers
for
semi-active suspensions with preview

CIP-DATA LIBRARY TECHNISCHE UNIVERSITEIT EINDHOVEN

Muijderman, Johannes Hendrik Everhardus Aldegonda

Flexible objective controllers for semi-active suspensions with preview /

Johannes Hendrik Everhardus Aldegonda Muijderman. - Eindhoven :

Technische Universiteit Eindhoven, 1997

Proefschrift. - ISBN 90-386-0600-1

NUGI 834

Trefw.: wielophanging / semi-actieve vering / regelsystemen ; optimalisering

Subject headings: vehicle suspensions / semi-active suspensions / control systems

Druk: Universiteitsdrukkerij TU Eindhoven

This study is performed in the context of the European research project CASCOV, made possible through the CEC Bríte/Euram programme.

Flexible objective controllers
for
semi-active suspensions with preview

PROEFSCHRIFT

ter verkrijging van de graad van doctor
aan de Technische Universiteit Eindhoven,
op gezag van de Rector Magnificus,
prof.dr. M. Rem, voor een commissie
aangewezen door het College voor Promoties
in het openbaar te verdedigen op
dinsdag 4 november 1997 om 16.00 uur

door

Johannes Hendrik Everhardus Aldegonda Muijderman

geboren te Veldhoven

Dit proefschrift is goedgekeurd door de promotoren:

prof.dr.ir. J.J. Kok

prof.dr.ir. P.P.J. van den Bosch

Copromotor:

dr.ir. F.E. Veldpaus

Voor mijn vader en moeder

Contents

Summary	ix
Notation	xi
1 Introduction	1
2 System and problem description	7
2.1 Conventional vehicle with driver	7
2.2 Alternative semi-active tractor rear axle suspension	15
2.3 Road excitations	16
2.4 Assessment of vehicle performance	18
2.4.1 Comfort of the occupants	18
2.4.2 Load on chassis components and cargo	19
2.4.3 Suspension working space	20
2.4.4 Handling	21
2.4.5 Road damage	22
3 Selection of the control method for the semi-active system	25
3.1 Modeling	26
3.1.1 Vehicle model for controller and control method selection	26
3.1.2 Road models for control method selection	28
3.2 Control objective	28
3.3 Control concepts for a multi-level damper	32
3.3.1 Direct calculation controller	32
3.3.2 Branch-and-bound controller	33
3.4 Control concept for a continuously variable damper	35
3.5 Choice of values for some controller parameters	38
3.5.1 Subinterval length Δh_i	38
3.5.2 Application interval length $s\Delta h_i$	46
3.5.3 Sample interval length Δh_c and integration routine	48
3.5.4 Conclusions	50

3.6	Concept choice	51
3.7	Applicable direct calculation controller	66
3.7.1	Concept	66
3.7.2	Reduction of computation time	68
3.7.3	Required preview information for the wave	71
3.7.4	Conclusions	73
4	Performance of the passive and the semi-active 3D vehicle model	75
4.1	Verification of the vehicle model	75
4.2	Configuration of the semi-active system	80
4.3	Performance for the passive and the semi-active 3D vehicle model	81
4.3.1	Performance for the laden vehicle	81
4.3.2	Performance for the un-laden vehicle	89
4.3.3	Conclusions	94
5	Review, conclusions and recommendations	97
5.1	Review	97
5.2	Conclusions	102
5.3	Recommendations	103
A	Determination of the penalty factors in the control objective criterion	107
B	Performance of the 3D vehicle model	109
	References	115
	Samenvatting	119
	Acknowledgments	121
	Curriculum Vitae	123

Summary

The suspension systems in a tractor-semitrailer combination are to a large extent responsible for the occupants comfort, the handling properties of the vehicle, the required suspension working space, the load on the road, the load on the cargo and the load on the chassis components. The performance of these suspension systems can be improved by using controlled, fast adjustable dampers.

Common controller design methods assume quadratic criteria, expressing the control objective, and assume linear models, characterizing the system behavior. The development of controllers for adjustable dampers is complicated because a suitable mathematical representation of notions like comfort and handling is not available. Furthermore, the switching dynamics and the nonlinear characteristics of the adjustable damper make the use of the common controller design methods even more difficult.

This thesis presents model-based control methods, resembling Model Predictive Control methods, for fast adjustable dampers. These methods can handle a broad class of criteria and can take into account the nonlinearities in the suspension. They use the damper either as continuously variable damper or as multi-level damper. All methods are based on knowledge of the road surface between the front and the rear wheels of the tractor at each time point. This so-called preview information may be obtained by reconstruction from measurements at the vehicle. The controllers divide the time interval for which the road surface is known, the preview interval, in equal subintervals and determine an optimal constant damper setting, *i.e.* a fixed force-relative velocity curve of the damper, for each of these subintervals.

For further development of the control methods and to enable a mutual comparison of the different suspension systems, a specific control objective and a controller internal model with two degrees of freedom (two-DOF model) are chosen. The chosen control objective contains the minimization of the maximum absolute acceleration of the sprung mass, without tire lift-off and without reaching the bounds on the suspension deflection. If tire lift-off is inevitable then the lift-off time must be as small as possible. If it is impossible to prevent the suspension deflection from reaching its bounds then the resulting impact force has to be as small as possible.

A two-DOF simulation model and a specific control method are used to determine

suitable lengths for the subintervals and the update interval for the preview information. From this investigation it appears that a better performance of the semi-active system than that of a good passive system is only obtained for subinterval lengths smaller than or at least close to the smallest natural oscillation time of the linearized model. Therefore, the length of a subinterval is chosen somewhat smaller than this natural oscillation time. Furthermore, the performance of the semi-active system strongly decreases if the update interval for the preview information is larger than the mentioned smallest natural oscillation time. The length of this update interval is therefore taken equal to the length of a subinterval.

The two-DOF simulation model is also used to compare the controlled semi-active systems. From this investigation it appears that the system with the controlled two-level damper is preferable to the system with the controlled continuously variable damper, as the performance is nearly equal and the computational burden for the controller of the two-level damper is much lower.

Finally, the performance of an elaborated three-dimensional model (3D model) of a tractor-semitrailer with conventional passive dampers is compared to that of a 3D model with a two-level damper at both the left and the right side in the tractor rear axle suspension. Each damper is controlled by its own controller. Each controller uses a two-DOF internal vehicle model, representing half the rear side of the tractor, and is provided with the preview information on the road surface between the front and the rear wheels of the tractor at the side of the controlled damper. Comparison of the results for the conventional passive vehicle and the vehicle with the semi-active tractor rear axle suspension shows that the semi-active system can reduce the tire lift-off time and a number of high peaks in the chassis acceleration at the rear side of the tractor, both for symmetric and for asymmetric incidental road excitations. The reduction of the peaks in the chassis acceleration at both the left and the right rear side of the tractor leads to a reduction of the peak load on the cargo for symmetric road excitations and to a reduction of the fatigue load on the chassis components at the rear side of the tractor, but not automatically to improved comfort in the cabin and not automatically to a reduction of the peak load on the cargo for asymmetric road excitations. More elaborated internal models for the controller will be required to improve the performance of the developed semi-active suspension with respect to these two aspects.

Notation

Conventions

\dot{a}	first time derivative of a
\ddot{a}	second time derivative of a
\dddot{a}	third time derivative of a
\underline{a}	column of scalars
$[a, b]$	collection of the elements in the range a to b
$\{a, b\}$	collection of the elements a and b

Abbreviations

3D	three-Dimensional
ADCC	Applicable DCC
BBC	Branch-and-Bound Controller
CASCOV	Controlled Axle Suspensions for COmmercial Vehicles
CPU	Central Processing Unit
CR	Computational Requirement
DCC	Direct Calculation Controller
DOF	Degrees Of Freedom
HWIL	HardWare-In-the-Loop
PASM	PASSive Medium system
PM	Palmgren-Minor (number)
RMS	Root Mean Square (value)
SQP	Sequential Quadratic Programming
SQPCO	SQP Controller with 'Original' control objective
SQPCE	SQP Controller with 'Explicit' control objective
VD	Vibration Dose (value)

Chapter 1

Introduction

The long-distance cargo road transport has been growing considerably in recent years and a further growth is expected for the next years. Two reasons for this are the opening up of Eastern Europe and the unification of Western Europe, resulting in an enlargement of the market for many industries. Long-distance cargo transport is done partly by aircraft, train and ship. However, a large amount of this cargo is transported by commercial vehicles. The increased use of commercial vehicles has a negative impact on the environment and on the traffic safety. This is unacceptable according to the latest European standards. Furthermore, nowadays more attention is paid to the well-being and the health of the occupants of commercial vehicles. Therefore, the road cargo transport must become more efficient, safer and less harmful for the occupants and the environment. More cargo must be transported with the same vehicle, the handling capabilities of the vehicle and, if possible, the comfort of the occupants must be improved whereas the fuel consumption, the exhaust emissions and the road damage for equal freight must be reduced.

Increasing the cargo volume of a commercial vehicle within the legal constraints is possible only if the floor of the cargo deck is lowered. This requires a reduction of the necessary working space of the suspension systems beneath the cargo deck. Besides, the effective cargo volume increases if less packaging materials are needed. This is possible if the accelerations of the cargo are lowered. Nowadays, however, often the cargo weight instead of the cargo volume limits the cargo capacity of a commercial vehicle. The use of less packaging materials of course also reduces the weight of the total cargo and enables an increase of the effective cargo. However, a considerable increase of the effective cargo weight is possible only if the vehicle itself is lighter. A low weight design of the vehicle without a reduction of the operational life is possible if the accelerations of the vehicle chassis are reduced. Lower accelerations of the vehicle chassis may also reduce the accelerations in the cabin, *i.e.* improve the comfort for the occupants. A low weight design of the vehicle also results in less fuel consumption, less exhaust emissions and less road damage for the same cargo. Road damage depends on the static and the

dynamic wheel load and is reduced if the dynamic wheel load is reduced. Moreover, a reduction of the dynamic wheel load improves the handling capability of a vehicle and consequently the safety of the vehicle.

The mentioned improvements require reduced suspension working spaces, lower chassis and cabin accelerations and lower dynamic tire forces. These quantities are strongly affected by the suspension systems of the vehicle.

The Eindhoven University of Technology (The Netherlands) and three companies, *i.e.* DAF Trucks N.V. (The Netherlands), ContiTech Formteile GmbH (Germany) and Monroe (Belgium), co-operate in a Brite/Euram II project, called CASCOV (Controlled Axle Suspensions for COmmercial Vehicles), to acquire technology for improving the dynamic behavior of tractor-semitrailer combinations with respect to five aspects: comfort of the occupants, load on chassis components and cargo, dynamic suspension travel, handling capabilities and road damage. A tractor-semitrailer is used in this project because this kind of commercial vehicle is commonly used for long-distance cargo transport. Although the acquired technology may also be of importance for the semitrailer suspensions, the investigations for the CASCOV project focus on the tractor suspensions, because these suspensions are of primary importance for the truck manufacturer. The attention is focussed on the tractor rear axle suspension because this suspension most strongly affects all five aforementioned aspects (Vael [39]). Three research areas are distinguished in the CASCOV project: passive suspensions, adaptive suspensions and (semi-)active suspensions. The investigation described in this thesis concerns (semi-)active suspensions. It is chosen to focus the investigations in passive and adaptive suspensions at a better average performance of the vehicle and the investigations in (semi-)active suspensions at a better performance for incidental road excitations. The impression of the occupants about the suspension performance is largely determined by the performance on the incidental road excitations because the performance on these excitations is much worse than the average performance of the suspension. The cost-benefit ratio and the reliability of a commercial vehicle are rather important. Since active suspensions are much more expensive and less reliable than semi-active suspensions, attention is focussed on semi-active suspensions, *i.e.* suspensions with controlled adjustable dampers. As the controlled dampers are mounted in the rear axle suspension of the tractor, it is possible to use wheelbase preview. Wheelbase preview implies that the road surface between the front and the rear wheels of the tractor is reconstructed before it enters the rear wheels. This reconstruction is based on measurements of accelerations and relative displacements at the tractor. One problem using wheelbase preview is that the tracks of the rear wheels are not always equal to the tracks of the front wheels, especially in cornering or when the rear axle is 'twin mounted' whereas the front axle is not. However, according to many investiga-

tions (Bender [4], Hać et al. [13], Huisman [19]), controlled suspensions with wheelbase preview show considerable advantages in comparison to controlled suspensions without preview. Therefore, it was decided to use wheelbase preview for the controllers of the adjustable dampers at the rear axle of the tractor.

Literature on semi-active suspensions

Semi-active suspension systems consisting of adjustable dampers and passive spring elements have been proposed for many years as a cheap and reliable alternative to active suspensions for cars, trains, busses and motorcycles.

In the early seventies (semi-)active suspension systems which approximate the behavior of a passive system with a so-called 'skyhook damper' are proposed (Karnopp et al. [22]). The idea is to design a damper controller which makes the damper behave like a passive damper with one end connected to the sprung mass and the other end to an inertial reference in the sky. Then the damper force is proportional to the sprung mass velocity. Linear optimal control theory, applied to a one degrees of freedom (one-DOF) vehicle model with a quadratic performance index, defined as the weighted sum of the vertical sprung mass velocity and the suspension deflection, has shown the optimality of a one-mass-spring-damper system with the spring connected to the road surface and the damper connected to the sky. Of course, a skyhook damper is not possible in real vehicle suspension systems, but an active device, parallel to the spring in this one-DOF system, might imitate the skyhook damper.

Semi-active systems use an adjustable damper instead of the active device. Many investigations (Karnopp et al. [22], Margolis [26]) propose adjustable dampers which produce the same force as the active device if the damper has to dissipate energy and a force as small as possible otherwise. Nowadays, controllers for semi-active systems which determine the desired damping force by passing 'the optimal active force' through a limiter are known as 'clipped optimal' controllers (Butsuen et al. [6], Tomizuka et al. [36], Tseng et al. [37]).

Semi-active systems, based on the principle of the 'skyhook damper', show an improved isolation of the sprung mass for road excitations compared to passive systems at the expense of a significant increase in dynamic tire force. Therefore, in the eighties control strategies for semi-active suspensions which take into account comfort, suspension deflection and dynamic tire force are developed. Butsuen and Hedrick [6] determine the 'optimal' control strategy for the damping coefficient of a semi-active two-DOF vehicle model with continuously variable damper, using a quadratic performance index which accounts for passenger acceleration, suspension working space, tire deflection and sprung and unsprung mass velocities. The performance of the semi-active system with

this controller is shown to be superior to that of the 'clipped optimal' controlled system with the same performance index, but the difference is small in the case of large ranges for the damping coefficient.

The advantage of the use of preview information to control active suspension systems is already shown by Bender [4] in the late sixties. Hać and Youn [13] determine the effect of preview control on the performance of a semi-active two-DOF vehicle model with continuously variable damping coefficient, using a quadratic performance index which accounts for passenger acceleration, suspension working space and tire deflection. A substantial performance improvement is reported for the semi-active system with preview compared to the semi-active system without preview, especially on a randomly profiled road.

Research objective

As mentioned before, the investigation described in this thesis focuses on the rear axle suspension of the tractor of a tractor-semitrailer combination. A difficulty in the development of a semi-active tractor rear axle suspension is the choice of the control objective. There is still a lot of discussion about how to translate subjective requirements with respect to comfort on incidental road excitations, handling, load on chassis components and on cargo and road damage into specifications that can be used within a mathematical context. For example, in literature comfort of the occupants on incidental road excitations is related to both accelerations and 'jerk' (third time derivative of the displacement). Besides, often only an approximation of the chosen criterion into the control objective is possible due to restrictions imposed by the controller design methods. For example, control objectives which aim to minimize the maximum absolute acceleration of the occupants under hard constraints on the suspension deflection and on the tire force are not suitable for controllers based on (bi)linear optimal control theory.

A main objective of the research described in this thesis is to develop and evaluate controllers which use wheelbase preview and can handle a broad class of control objectives. These controllers must be able to handle constraints on vehicle performance criteria. Furthermore, the nonlinear characteristics of the dampers and the air springs must be taken into account and the practicability of the controller is important. The latter implies that also the computational burden for the hardware is of importance.

Within the framework of the CASCOV project, it has to be decided whether dampers with an infinite number of force-relative velocity characteristics, so-called continuously variable dampers, are necessary or whether dampers with a finite number of possible force-relative velocity characteristics, so-called multi-level dampers, are sufficient.

The performance of the tractor-semitrailer with optimized semi-active tractor rear axle suspension has to be determined and must be compared to the performance of a tractor-semitrailer with a passive suspension for vertical, incidental road input to the vehicle by driving straight ahead. In this thesis, it is assumed that the preview information, *i.e.* the road surface between the front and the rear wheels of the tractor, is exactly known by the controller of the semi-active suspension.

Outline of the thesis

The investigation described in this thesis uses a 3D (three-Dimensional) model as a substitute for the real tractor-semitrailer. An outline of the real tractor-semitrailer together with an overview of the degrees of freedom of the 3D model is given in Chapter 2. In this 3D model the original passive tractor rear axle suspension can be replaced by a semi-active suspension, which is also described in Chapter 2. Besides, this chapter specifies models of those 'realistic' incidental road excitations for which the responses of the passive and the semi-active vehicle model will be determined. These responses are analyzed and evaluated, not only with respect to criteria closely related to the control objective but also to a large number of other criteria, which are mentioned in Chapter 2.

Chapter 3 describes several model-based controllers with wheelbase preview for semi-active suspensions. These controllers can handle a broad class of control objectives. Their performances and an important hardware requirement are compared and the most promising concept is optimized. A nonlinear two-DOF model is used as internal vehicle model for the controllers. Although many control objectives can be used by the controllers, only one is used for the comparison and the optimization, being the minimization of the maximum absolute sprung mass acceleration under hard constraints on the suspension deflection and on the tire lift-off time. The 'simple' nonlinear two-DOF vehicle model is also used as the vehicle simulation model instead of the more extensive 3D model to restrict simulation times in this comparison and optimization stage.

The selected and optimized controller with the two-DOF model as internal vehicle model, is applied in Chapter 4 to the semi-active tractor rear axle suspension of the extensive 3D model. The behavior of this semi-active system is compared to the behavior of the 3D model with passive suspensions for the incidental road excitations mentioned in Chapter 2.

What's new?

Model-based control strategies for multi-level and for continuously variable dampers with nonlinear force-relative velocity characteristics are developed, using wheelbase preview of the road. A broad class of control objectives can be handled. Nonlinear vehicle

models may be used for controller design, although the order of these models is limited to obtain practicable controllers. The control strategies for the multi-level damper result in the optimum damper setting sequence over the preview interval whereas the control strategies for the continuously variable damper yield a suboptimal damper setting sequence over the preview interval. An estimate of the required switching frequency and of the optimum sampling interval for the preview information are determined.

The performance of an elaborated 3D tractor-semitrailer model with controlled two-level dampers at the rear axle of the tractor is evaluated for both the laden and the un-laden situation for incidental road excitations.

Chapter 2

System and problem description

The objective of the research described in this thesis is to develop a practicable control strategy for a semi-active suspension at the rear axle of the tractor of a tractor-semitrailer combination to improve the performance, compared to the vehicle with a conventional passive suspension, on incidental road excitations. The notions 'passive suspension', 'semi-active system', 'road excitations' and 'improved vehicle performance' are elucidated in this chapter. Until now it is not possible to experiment with a real vehicle on real road surfaces. Therefore, a model of the vehicle with passive suspension, a model of the semi-active suspension and models of the road excitations are presented. Furthermore, quantitative measures for the assessment of the vehicle behavior are established to make a quantitative comparison between the vehicle with a passive suspension and the vehicle with a semi-active suspension possible.

2.1 Conventional vehicle with driver

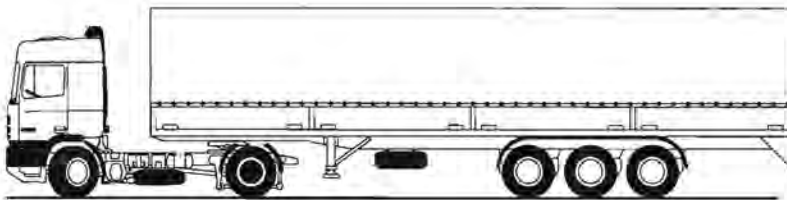


Figure 2.1: DAF95 tractor - semitrailer

The investigated tractor - semitrailer combination is given in Figure 2.1. An elaborated 3D multi-body model of this vehicle, build with the software package DADS (CADSi [7]), is used to describe the vehicle behavior in the frequency range of 0 to 15 Hz (Bekkers [3]). This model is used to analyze the vehicle performance. In this section the connections between the main components of the vehicle, the interactions between

the vehicle and the road surface, the interactions between the vehicle and the driver and their models are discussed.

Tractor chassis

Figure 2.2 shows the tractor chassis. It consists of two side members, connected by cross members. Some of the lowest eigenfrequencies of the chassis lie within the range of 0 to 15 Hz. This makes it desirable to incorporate a flexible body model of the chassis with at least the corresponding eigenmodes in the 3D model. However, a validated flexible body model of the chassis was not available. Therefore, in first instance, the chassis is treated as a rigid body in the 3D model.

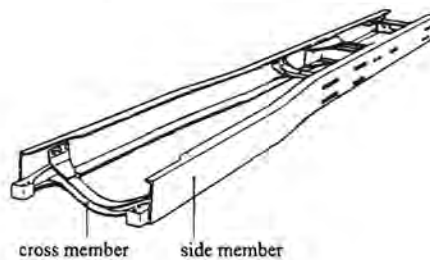


Figure 2.2: Tractor chassis

Cabin suspension

The suspension of the cabin is shown in Figure 2.3. The cabin front suspension contains a roll stabilizer of which the ends are connected to the chassis by means of rubber elements, called 'silent blocks'. The edges of the roll stabilizer are connected to both the chassis and the cabin. The connection to the chassis is realized with spring/damper elements whereas the connection to the cabin is realized with revolute joints. The left and right cabin rear suspension consist of a spring/damper element between the left, respectively the right side of the cabin and the chassis. These spring/damper elements are connected to the cabin with rubber elements which provide lateral stiffness to the cabin with respect to the chassis. The cabin can bounce, pitch and roll with respect to the chassis. However, also small lateral, longitudinal and yaw movements of the cabin with respect to the chassis are possible due to the rubber elements. The cabin is modeled as a rigid body. The six degrees of freedom of the cabin with respect to the chassis are incorporated in the 3D vehicle model using spring/damper models, models for the rubber elements and a model for the roll stabilizer.

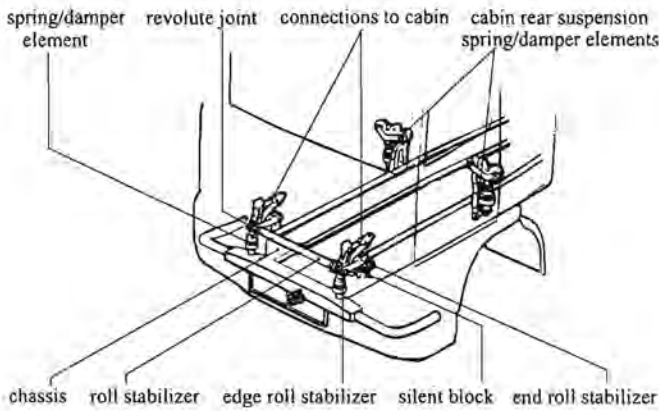


Figure 2.3: Cabin suspension

Engine/transmission suspension

Figure 2.4 shows the suspension of the engine/transmission combination. This combination is connected to the chassis with four rubber elements, two at the front and two at the rear. This results in six degrees of freedom with respect to the chassis. The engine/transmission combination is modeled as one rigid body and the six degrees of freedom are incorporated in the 3D model by using appropriate models for the rubber elements.

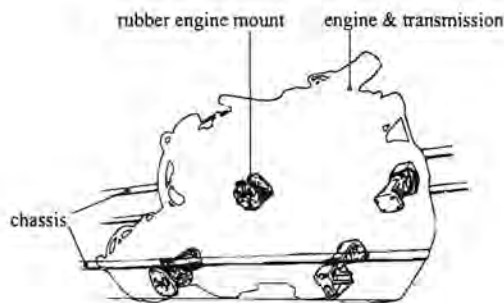


Figure 2.4: Engine/transmission suspension

Tractor front axle suspension

The tractor front axle suspension is shown in Figure 2.5. Two parabolic leaf springs, each with two leaves, are used. The front and the rear side of each leaf spring are connected to the chassis with a revolute joint, respectively by a shackle with two revolute

joints. The middle of each leaf spring is connected rigidly to the front axle. Furthermore, a damper is placed between the chassis and the front axle at both the left and the right side of the vehicle. The front axle and the chassis are also connected by the roll stabilizer whose ends are connected to the chassis with revolute joints. The edges of the roll stabilizer are connected to the front axle with cylindrical joints. The roll stabilizer provides extra roll stiffness between the front axle and the chassis. Furthermore, rubber bump stops are placed on top of each leaf spring to prevent iron to iron contact. Rebound elements in the dampers restrict the maximum suspension deflection at the front axle. Due to the construction of the front axle suspension, the axle can bounce, roll and pitch with respect to the chassis. The pitch degree of freedom is caused by wrap-up of the leaf springs. The front axle is modeled in the 3D model as a rigid body and the three degrees of freedom of this axle are taken into account by appropriate models of the leaf springs, the damper elements, the bump stops, the rebound elements in the dampers and the roll stabilizer.

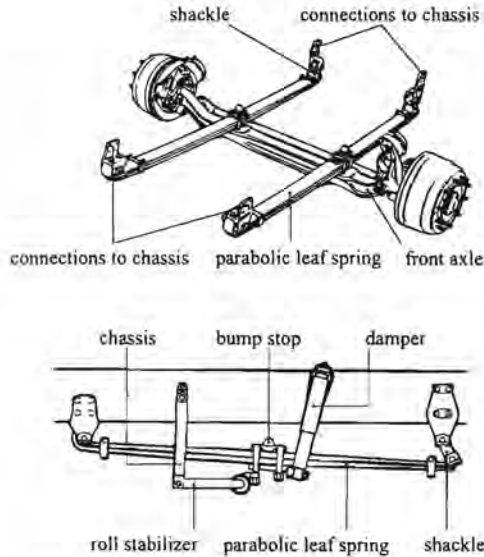


Figure 2.5: Tractor front axle suspension

Tractor rear axle suspension

Figure 2.6 gives an impression of the tractor rear axle suspension. This axle is connected to the chassis with a triangle, two links, a roll stabilizer, four air springs and two dampers. The triangle is connected with spherical joints to the top middle of the rear axle and to the chassis. The two links are connected with tow bar eyes to the chassis

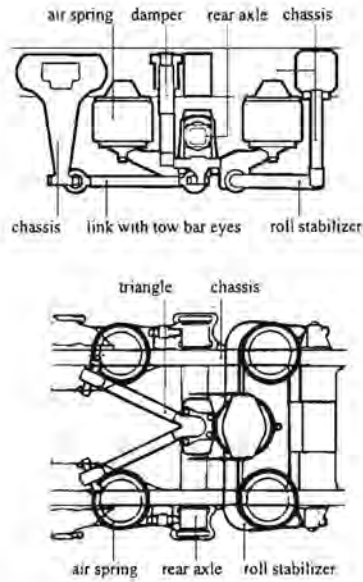


Figure 2.6: Tractor rear axle suspension

and to, respectively, the left and the right bottom of the rear axle. Two air springs and a damper are placed between the rear axle and the chassis at the left and at the right side. The roll stabilizer is used to add extra roll stiffness between the rear axle and the chassis. Each edge of the roll stabilizer is connected to the rear axle by means of a cylindrical joint and each end of the roll stabilizer is connected to the chassis with a revolute joint. Bump stops at the bottom of the chassis prevent iron to iron contact. The maximum suspension deflection is restricted by rebound elements in the dampers. The rear axle can bounce and roll with respect to the chassis movements. It is modeled as a rigid body in the 3D model and the mentioned degrees of freedom are taken into account with appropriate models of the air springs, the dampers, the bump stops, the rebound elements in the dampers, the roll stabilizer and the links. The air spring model accounts for the leveling system of the spring. This system is used to obtain the same distance between the axle and the chassis for different static loads. The relation for the air spring force F_s as a function of the static air spring force $F_{s,stat}$ and the air spring deflection Δq with respect to the static air spring deflection is determined experimentally and can be written as

$$F_s = -F_{s,stat} + f_s(\Delta q) \cdot (1.0428)^{(F_{s,stat})}. \quad (2.1)$$

The function f_s , given in Figure 2.7a, and the values of $F_{s,stat}$ and F_s are in kN. For each damper the relation between the force and the relative velocity is modeled by the characteristic given in Figure 2.7b. A damper with this characteristic shows, according to experienced test drivers, a good average performance on the road surfaces used by the tractor-semitrailer.

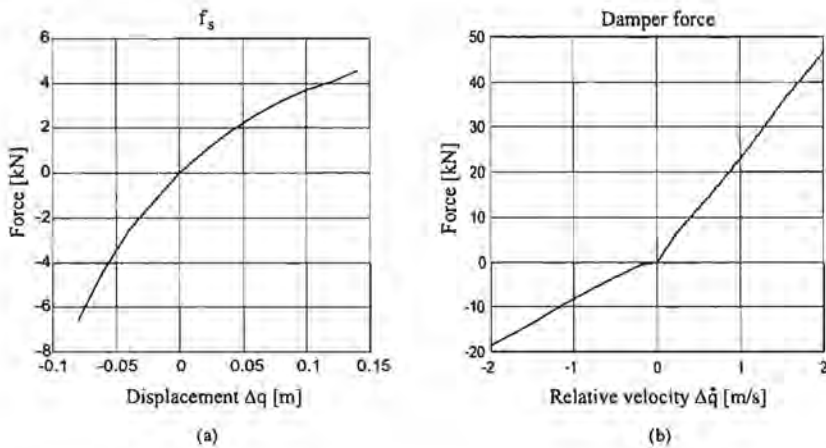


Figure 2.7: Characteristics of the tractor rear axle air spring and damper

Semitrailer frame

Figure 2.8 shows the semitrailer. The connection of this semitrailer with the chassis of the tractor at the kingpin allows for pitch and yaw with respect to the tractor. The flexible semitrailer frame is modeled as an assembly of two rigid bodies in series, connected by a revolute joint with a torsional spring, to account for the finite torsion stiffness of the semitrailer frame. The connection of the frame to the chassis is modeled as a universal joint between the first rigid body and the tractor chassis.

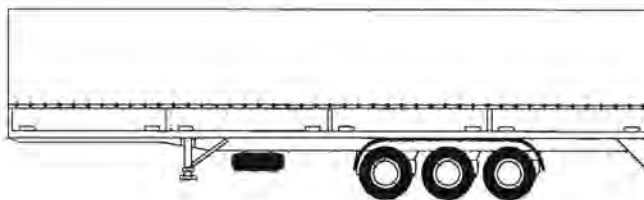


Figure 2.8: Semitrailer

Semitrailer axle suspension

Three axles are connected to the semitrailer. Figure 2.9 shows the layout of the suspension for one axle. Two leaf spring elements are used to connect each axle to the semitrailer frame. The middle of each leaf spring is connected rigidly to the axle. One side of each leaf spring is connected to the frame by a revolute joint whereas air springs with leveling system are placed between the other side of each leaf spring and the frame. Two dampers are placed between each axle and the frame, one at the left side and one at the right side of the vehicle. The minimum suspension deflection is restricted by a bump stop whereas the maximum suspension deflection is restricted by a chain. The

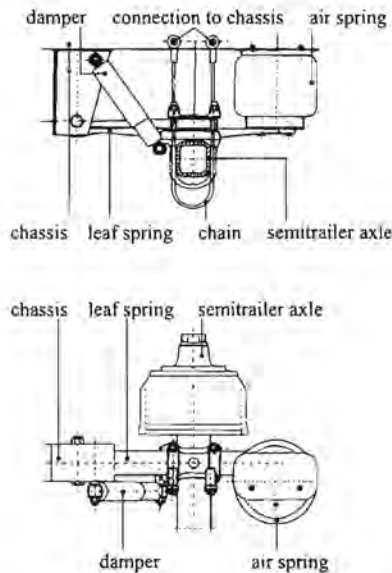


Figure 2.9: Semitrailer axle suspension

axles can bounce and roll with respect to the semitrailer frame. They are modeled as a rigid body in the 3D model. The two degrees of freedom of each axle are incorporated in this model by means of models for the air springs, the dampers, the leaf springs, the bump stops and the chains.

Tires

The tires play a crucial rôle in vehicle dynamics. They have to support the vehicle, filter road irregularities and transmit forces between the vehicle and the road surface. The 3D model uses the most detailed tire model available in DADS (CADSi [7]). Anyway, this model describes the tire behavior (the enveloping effect of road irregularities and

the development of longitudinal, lateral and vertical forces) only roughly. However, Bekkers [3] shows that the responses of the 3D model with this tire model are much alike the measured responses of a real tractor-semitrailer.

Steering system

The steering system is shown in Figure 2.10. Each of the two front wheels of the tractor can rotate about an axis of a so-called swivel body. One swivel body is connected to the left side of the front axle and one to the right side. Each swivel body is connected to the front axle with a revolute joint. The orientation of these revolute joints introduces certain camber, caster and inclination angles. Both swivel bodies contain a tie-rod arm. These arms are connected by a tie-rod with two spherical joints. A steering arm,

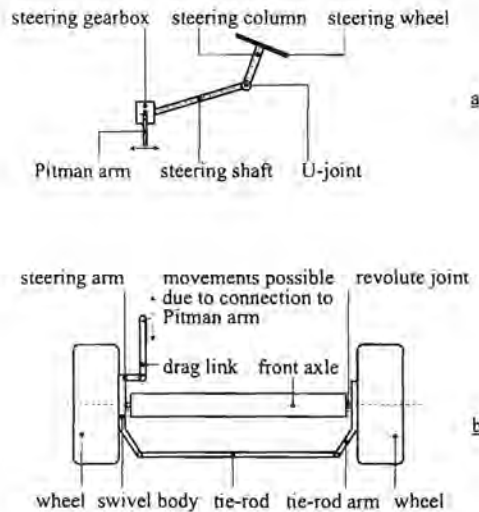


Figure 2.10: Steering system

rigidly attached to the left swivel body, is connected to the lower end of the so-called Pitman arm by a drag link with two spherical joints. The upper end of this Pitman arm is rigidly connected to the output shaft of the steering gearbox. This box is rigidly connected to the chassis and transforms the rotation of the steering shaft into a rotation of the Pitman arm about the axis of the output shaft. The steering shaft is connected to the steering wheel via the steering column and the U-joint. Rotations of the steering wheel result in fore-aft movements of the lower end of the Pitman arm. These fore-aft movements are transmitted to the drag link and result in rotations of the swivel bodies and of the wheels about the axis of 'their' revolute joint. The 3D model incorporates

only a part of the steering system, namely a model of the link mechanism shown in Figure 2.10b and a model of the Pitman arm.

Driver

Each driver has his or her own driving behavior and this behavior is vehicle dependent. This makes the modeling of the driver behavior rather complicated.

In the simulations the vehicle model has to drive straight ahead only. However, in the 3D model this can not be achieved by just fixing the rotation of the Pitman arm such that the front wheels are in straight ahead position. A model of the driver is required to compensate for roll steering caused by asymmetrical distribution of the (un-laden) vehicle mass and asymmetrical road disturbances. Driver models based on assumptions about the physical behavior of a driver have been developed for lateral dynamics (Segel et al.[32], Venhovens [40]). These models incorporate the perceptual time delay and the neuromuscular time constant of a driver and the capability of a driver to observe the future desired path. Furthermore, these models have the possibility to adopt their behavior in response to changes in the vehicle dynamics. The latter is observed in experiments with real man-vehicle systems.

In this thesis a simple proportional controller is used as the driver model, because suitable values for the parameters of the more sophisticated models are not available. The current lateral position of the center of gravity of the front axle with respect to the desired driving line is the input for the controller. The difference of the current angle between the left swivel body and the front axle and this angle for straight on steering is used as the output of the controller. Simple simulations show that the controller can correct small deviations that are caused by the asymmetrical distribution of the vehicle mass and by asymmetrical road disturbances. Furthermore, the behavior of this controller is acceptable if the front wheels of the tractor show tire lift-off.

2.2 Alternative semi-active tractor rear axle suspension

The only difference between the semi-active and the passive tractor rear axle suspension concerns the damper. The damper of the semi-active system is a continuously variable damper with force versus relative velocity characteristics in the marked range in Figure 2.11. The characteristic with the highest absolute damper force at each relative velocity is called the highest damper setting and is denoted by $S_a = 1$. The characteristic denoted by $S_a = 0$ is called the lowest damper setting. All other characteristics are denoted by a value of S_a between 0 and 1. The characteristic with $S_a = 0.5$ is equal to the characteristic of the passive damper in Section 2.1. The functions $f_{d,h} = f_{d,h}(\Delta\dot{q})$ and $f_{d,l} = f_{d,l}(\Delta\dot{q})$ give the damper force F_d for the highest damper setting, respectively

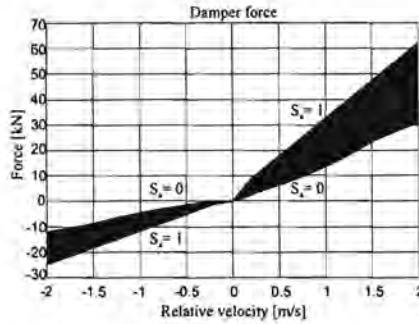


Figure 2.11: Characteristics of the semi-active tractor rear axle damper

the lowest damper setting as a function of the relative velocity $\Delta\dot{q}$ over the damper. The switching from one desired setting S to another is modeled by a first order lag with time constant τ_d . From measurements it is known that $\tau_d = 6.5$ ms is reasonable for a change $\Delta S = 1$ in the desired setting. The value for τ_d will depend on ΔS . However, until now no information about this dependency is available. Therefore, $\tau_d = 6.5$ ms is used in the semi-active damper model for all ΔS . The relation between the desired damper setting S and the actual damper setting S_a is given by

$$\dot{S}_a = \frac{1}{\tau_d} \cdot (-S_a + S). \quad (2.2)$$

The semi-active damper force, corresponding to an actual damper setting S_a , is determined from

$$F_d = S_a \cdot f_{d,h}(\Delta\dot{q}) + (1 - S_a) \cdot f_{d,l}(\Delta\dot{q}). \quad (2.3)$$

Although the semi-active damper is continuously variable, it can also be used as a multi-level damper by restricting the possible settings S . In Chapter 3 it will be investigated whether or not it is advantageous to use the damper as a two-level damper, taking into account both the system performance and the controller CPU times. In Chapter 4 the performance of the 3D vehicle model with a controlled semi-active damper at the rear axle of the tractor is compared to the performance of the passive 3D vehicle model.

2.3 Road excitations

The actual road input to a vehicle is rather diverse and a representative selection of road inputs for simulations, used to get insight into the dynamic behavior of the vehicle, is far from trivial. The majority of the kilometers driven by a tractor-semitrailer are made on motor-ways. The average performance on these motor-ways is judged at a proper level. As a result, the impression of the occupants about the suspension performance

is largely determined by the performance on incidental road excitations, like a brick on the road or the transition from normal asphalt to scraped asphalt.

Models for five different incidental road irregularities are selected for the simulations, namely a standard brick lying on the road surface, a traffic hump, the transition from normal asphalt to scraped asphalt, a road surface with a well of which the lid is missing and a wave. Illustrations together with abbreviated names for these road irregularities are shown in Figure 2.12. The models assume that all tires at one side of the vehicle 'feel' the same road track, even if there is more than one tire per axle side. However, the left and right road tracks can be different. In general, a traffic hump, a scraped road and a wave will excite both the left and the right side of the vehicle, whereas a standard brick and a well only excite one side. The traffic hump, the scraped road and the wave are therefore modeled as symmetric road surfaces, so the road height of the left and the right road track is the same at each cross-section of the road. The standard brick and the well are modeled as asymmetric surfaces, such that the left track contains the irregularity and the right track is flat. A prescribed 'realistic' forward velocity of the vehicle is chosen for each of the irregularities, assuming that the driver does notice the traffic hump, the scraped road and the wave but not the standard brick and the well.

	A	B	C	V
	[m]	[m]	[m]	[km/h]
1. Standard brick	0.105	0.065		80
2. Traffic hump	0.600	1.400	0.100	20
3. Scraped road	0.070			60
4. Well	0.600	0.100		40
5. Wave	25.00	0.500		80

Figure 2.12: 5 deterministic road irregularities

Motorways and brick paved roads are called 'stochastic road surfaces' because they are often characterized by a stochastic description. They are not used in the simulations but are sometimes mentioned in the following text.

2.4 Assessment of vehicle performance

For a quantitative comparison of the performance of the vehicles with the passive and semi-active suspension, performance measures have to be specified. The comfort of the occupants, the load on the chassis components and the cargo, the required suspension working space, the handling properties and the road damage are chosen as the aspects to be evaluated. For incidental road excitations, a generally applicable, commonly accepted translation of these aspects in mathematical criteria, is not available at the moment. In this thesis, some criteria are chosen for each performance aspect, where it is assumed that the vehicle is driving straight on and that only the influence of the road irregularities has to be considered.

2.4.1 Comfort of the occupants

Comfort is a subjective notion. It is often associated with vibrations transmitted to a human body. However, several other factors, like interior noise, interior space, sight, ergonomics, occupants size and weight and the position and orientation of the seats influence the experienced comfort level. Due to its subjective character, comfort is often judged in practical tests with drivers and co-drivers. Besides, many quantitative investigations are carried out. Most quantitative comfort measures are determined as a function of the place, the direction, the frequency, the duration and the acceleration values of the human body excitation. The feet, the seat, the backrest and the hands are, according to Griffin [12], the most important places at which the human body is excited. Important excitation directions are the vertical excitation at the feet support, the excitation in three directions at the seat and the vertical and fore-and-aft vibration at the backrest. Seated human beings are especially sensitive to vertical excitations in the frequency range between 4 and 8 Hz and to horizontal excitations in the frequency range up to 2 Hz. The high sensitivity for vertical excitations between 4 and 8 Hz is caused by the vertical resonance of the abdominal cavity whereas the high sensitivity for horizontal excitations is caused by the fore-and-aft resonance of the upper torso (Venhovens [40]). For vertical excitations in the frequency range below 1 Hz 'motion sickness' may occur. The excitation duration also has its influence on comfort. Many investigations (Griffin et al. [11], Kjellberg et al. [24], Miwa [28]) indicate that certainly at the beginning of an excitation the comfort level decreases if the duration of the excitation increases. Although some comfort measures are related to the jerk of the excitation, most of them are related to the acceleration of the excitation.

An often used approach on stochastic road surfaces is to use a location, direction and frequency dependent weighting of the accelerations in the main directions of the main excitation places and to use the RMS (Root Mean Square) values of these weighted

accelerations as comfort measures. There is however not much known about the judgment of comfort on incidental road excitations. Huisman [19] used maximum absolute values of non-weighted accelerations and time response plots of displacements. Griffin [12] and Howarth and Griffin [17] recommend to use so-called VD (Vibration Dose) values. The VD value of an, eventually weighted, acceleration signal a over the time interval $[0, T]$ is defined as

$$VD = \left(\int_0^T a^4(t') dt' \right)^{\frac{1}{4}}. \quad (2.4)$$

The fourth power warrants a strong contribution of peak values to the degree of discomfort and the integration over the total driving time provides the possibility to compare vehicle responses of different duration. Some authors (Hoberock [16], Hrovat [18]) use the jerk as an additional comfort measure to amplify the contribution of high frequency components to the amount of discomfort.

In this thesis, the maximum absolute values, the RMS values and the VD values of the weighted and the non-weighted accelerations, the maximum absolute values of the jerk in longitudinal, lateral and vertical direction at the seat of the driver and the time response plots of the displacements in these directions are used to judge the occupants comfort on the incidental road excitations. Both the weighted and the non-weighted accelerations are taken into account because the real accelerations of the occupants are unknown, due to the fact that no chair suspension and human body dynamics are taken into account by the vehicle model. Weighting of the accelerations is performed according to ISO 2631 [20].

2.4.2 Load on chassis components and cargo

Chassis components can be damaged by fatigue and both chassis components and cargo can be damaged by incidental loads.

Fatigue is the phenomenon of crack initiation and crack growth in constructions due to variable loads for a longer period of time, where the magnitude of the variable loads is much lower than the static yield load. The acceleration history of a chassis component as a function of time is often used to judge the fatigue damage of this component. This acceleration signal is translated into an equivalent acceleration signal with a constant amplitude, using a so-called rainflow counting method (Suresh [35]) and the Palmgren-Minor-rule for equivalent damage. The number of cycles in this transformed acceleration signal, the PM (Palmgren-Minor) number, is used as a measure for the fatigue damage. The PM numbers for the vertical accelerations at the four corner points of the tractor chassis are chosen to judge the fatigue damage of the chassis components.

High incidental loads also cause damage to the chassis components and may lead to instantaneous failure of the vehicle. Furthermore, these loads are the main cause of

cargo damage. A reduction of these loads on the cargo gives the possibility to use less packaging materials and to increase the valuable cargo. According to Snowdon [33], the maximum absolute acceleration of the mass of a damage-prone element due to an incidental load is a suitable measure for the damaging potential of this incidental load on this element. Here, the maximum absolute acceleration at the kingpin is used as a measure for the damage on the cargo and the maximum absolute accelerations at the left and right rear side of the chassis are used as a measure for the damage on the chassis components caused by an incidental load.

2.4.3 Suspension working space

The minimum suspension deflections, both at the tractor and at the semitrailer, are restricted by bump stops whereas the maximum suspension deflections are bounded by rebound elements in the dampers (tractor) or by chains (semitrailer). The difference between these extremes is called the suspension working space. A reduced suspension working space allows the designer to lower the floor of the semitrailer. Since the maxima of the height, the width and the length of a semitrailer are restricted by law, a lower floor is the only possibility to increase the payload volume. High chassis and axle accelerations may result if the bounds of the suspension working space are reached.

On a stochastic road surface the RMS value of the relative suspension deflection, *i.e.* the suspension deflection with respect to the static suspension deflection, is often used to judge the behavior of the suspension deflection. For linear systems with Gaussian distributed road input, the suspension deflection will remain between predefined symmetric bounds around the static suspension deflection for a certain percentage of the driving time if the corresponding RMS value of the relative suspension deflection does not exceed a predefined value. In this thesis, the behavior of a nonlinear vehicle model with asymmetric suspension deflection bounds around the static suspension deflection is studied for incidental road excitations. The meaning of the RMS value of the relative suspension deflection is not so straightforward in this case due to the nonlinear model and the short duration of the incidental road excitations. Therefore, next to the RMS value of the relative suspension deflection, the number of times that a predefined suspension deflection bound is reached and a measure for the severity of the impact are used to judge the behavior of the suspension deflection at the left and the right rear side of the tractor. The measure for the severity of the impact is the relative velocity between the chassis and the axle just before the impact.

2.4.4 Handling

Like comfort, handling is a subjective notion. It indicates the ease of keeping a vehicle on the desired course during driving straight on, cornering, accelerating, braking and all other manoeuvres. A vehicle with good handling properties has sufficient possibilities to perform the desired actions, gives clear and correct information about the vehicle status and does not ask too much effort of the driver. Many aspects influence handling, for example, the road-holding of a vehicle, the roll, pitch and yaw behavior of the vehicle body, the steering effort and the tire properties. Handling is usually evaluated in tests, using a real vehicle with test drivers or a real vehicle with a steering/braking machine. The latter gives a good reproducibility of the test and eliminates the influence of the driver on the vehicle response. Typical tests are straight line keeping, straight line braking, lane change driving, sinus steering and steady state turning. Usually subjective opinions are used to evaluate the test results. However, sometimes quantitative signals like steering wheel angle, roll, pitch and yaw angle/rate of the vehicle body, maximum lane change velocity, deviation from the desired course and lateral and longitudinal acceleration are used as additional information to judge the handling. Recently, the mentioned tests are partially replaced by simulations with models that contain an extensive model of the vehicle and the driver. Moreover, so-called inverse dynamics is applied to vehicle models to calculate the required steering behavior of a driver, given a prescribed path of the vehicle. This thesis investigates the response of a vehicle (with a constant forward velocity) to the road surfaces mentioned in Section 2.3 and only the road-holding capability is used as a handling measure. The influences of the other quantities on the handling are beyond the scope of this investigation. The representative quantity to judge road-holding is the tire force, *i.e.* the normal force exerted by the road on the tire. Together with the friction between the tire and the road this force strongly influences the maximum lateral and longitudinal force in the contact plane between road and tire. If the tire force is too low over a longer period of time risky situations may occur in braking/accelerating and in steering corrections. An acceptable lower bound on the tire force and an acceptable length of the low tire force period are unknown at this moment.

On stochastic road surfaces the RMS value of the dynamic tire force is often used to judge the road-holding. For linear systems with Gaussian distributed road input, it can be guaranteed that the vertical tire force remains above a predefined value for a certain percentage of the driving time if the RMS value of the dynamic tire force does not exceed a predefined value. Like the RMS value of the relative suspension deflection, the meaning of the RMS value of the dynamic tire force is not obvious for the nonlinear vehicle model at incidental road excitations. Therefore, next to the RMS values of

the dynamic tire force, the tire lift-off time and the time for which less than 75 % of the static tire force is available for the rear tires of the tractor are used to judge the road-holding of the vehicle (see Figure 2.13). The no-tire-lift-off requirement may be too weak whereas requiring no excess of the 75 % (lower) bound on the static tire force may be too strong to guarantee sufficient road-holding in abrupt handling manoeuvres. However, better measures for road-holding are not available at this moment.

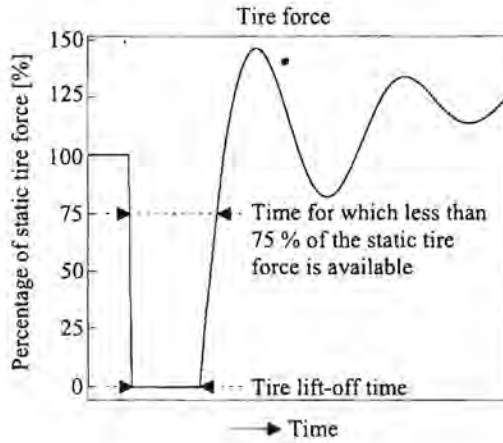


Figure 2.13: Two road-holding criteria

2.4.5 Road damage

Road damage is mainly caused by heavy commercial vehicles. The maintenance and rebuilding costs of road surfaces will considerably reduce if the forces on the road by these vehicles are reduced. The road damage caused by a vehicle depends on several aspects, such as the vehicle velocity, the tire-road contact areas, the distance between the axles and the magnitude of the tire forces. Here, only the influence of the dynamic and static tire force on the road damage is considered. Göktaş and Mitschke [10] use the so-called 'road stress factor' to combine the influence of several aspects on the road damage. According to this factor, the road damage is proportional to $\eta F_{tire,stat}^4$ where $F_{tire,stat}$ is the static tire force and η is related to the dynamic tire force. Usually one of two values is used for η . The first is called η_{max} and is defined as

$$\eta_{max} = \left(\frac{\max(F_{tire})}{F_{tire,stat}} \right)^4, \quad (2.5)$$

where F_{tire} is the total tire force and $\max(F_{tire})$ is the maximum value of F_{tire} over the total driving time. The second value is called $\eta_{average}$ and is defined as

$$\eta_{average} = 1 + 6 \left(\frac{\text{RMS}(F_{tire,dyn})}{F_{tire,stat}} \right)^2, \quad (2.6)$$

with $F_{tire,dyn}$ the dynamic tire force and $\text{RMS}(F_{tire,dyn})$ the Root Mean Square value of $F_{tire,dyn}$ over the total driving time. $\eta_{average}$ is used for homogeneously damaged roads whereas η_{max} is used for the other roads. The real value of η is in between η_{max} and $\eta_{average}$. In this thesis, the sum over the tractor rear tires of $\eta_{max}(F_{tire,stat})^4$ is used to judge the road damage caused by the rear side of the tractor whereas the sum over all tractor-semitrailer tires of $\eta_{max}(F_{tire,stat})^4$ is used to judge the total road damage caused by the vehicle.

Selection of the control method for the semi-active system

In this chapter, the control method for the semi-active damper in the tractor rear axle suspension is established. The method is selected from a number of model-based control methods, which all assume that the road surface between the front and the rear wheels of the tractor is exactly known to the controller. All methods split the time interval for which the oncoming road surface is known, the preview interval, in subintervals of equal length and determine an optimal constant damper setting for each of these subintervals. The methods can handle a broad class of control objectives. This is important for at least two reasons. First of all, it makes it possible to adapt the controller to other mathematical specifications of performance. This is desirable, because there is still a lot of discussion about how to translate subjective performance requirements into mathematical specifications. Secondly, it makes the controller easily adaptable to different driving conditions. This is important, because the performance aspects to be optimized depend on the driving condition. Comfort, for example, is important in straight on driving whereas handling is more important at cornering and braking.

The developed control methods use the damper either as a continuously variable damper or as a multi-level damper. The continuously variable damper of Chapter 2 can be used as a multi-level damper by imposing restrictions on the damper setting S . The control methods for the multi-level damper are elucidated for a two-level damper but the extension to dampers with more levels is straightforward.

A chosen control objective, a two-DOF internal vehicle model for the controller and an identical simulation model are used to explain the control methods, to determine the control parameters and to compare the performances and the computational burdens of the developed control methods. The most promising method is chosen and the behavior of the semi-active 3D vehicle model, controlled with a practicable version of this optimal concept, is compared to the behavior of the passive 3D vehicle model in Chapter 4.

3.1 Modeling

3.1.1 Vehicle model for controller and control method selection

The controller uses a model with two degrees of freedom (two-DOF model) which describes the behavior of the vehicle for the wheel-hop frequency (about 10 Hz) and for the chassis resonant frequency (in the 1 to 2 Hz range). Theoretically, the control methods may use any internal vehicle model. However, large vehicle models like the 3D model are not practicable because they require too much computation time for real-time application. A two-DOF model is the simplest model that shows the conflict between comfort, suspension working space and tire force. Furthermore, according to Huisman [19], the performance of an active suspension improves only marginally when the controller uses an internal model with more than two degrees of freedom. Because the behavior of the semi-active damper is strongly nonlinear, the nonlinear two-DOF model of Figure 3.1 is used by the controller. It describes the dynamic behavior of half the rear side of the tractor. The quantities m_{cr} and m_{ar} represent the sprung

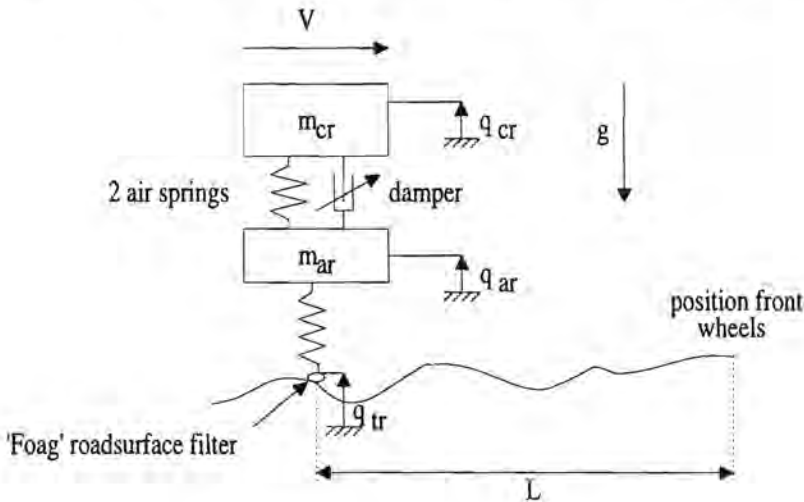


Figure 3.1: Nonlinear two-DOF model

and unsprung mass, while q_{cr} and q_{ar} are the vertical displacements of the sprung and unsprung mass such that the springs are unstrained if $q_{cr} = q_{ar} = q_{tr}$. Here, q_{tr} is the displacement of the lower end of the tire spring. Two air springs and one semi-active damper are positioned between the sprung and the unsprung mass.

The air spring force F_s is calculated using Equation (2.1). It is a function of the static load $F_{s,stat}$ on the air spring and the deflection Δq of the air spring with respect

to the static air spring deflection. However, the leveling system of the air spring keeps the static air spring deflection ($q_{cr,stat} - q_{ar,stat}$) equal to zero and therefore

$$\Delta q = (q_{cr} - q_{ar}) - (q_{cr,stat} - q_{ar,stat}) = (q_{cr} - q_{ar}).$$

The semi-active damper model is discussed earlier in Chapter 2. The desired damper setting S is filtered by a first order filter with time constant $\tau_d = 6.5$ ms and the damper force F_d is determined as a function of the relative velocity $\Delta \dot{q}$ and the filtered value of the damper setting S , according to Equation (2.3). The bump stops and the rebound elements in the dampers are not incorporated in the model.

The tire is modeled as a linear spring with stiffness k_{tire} . However, tire lift-off is incorporated in the model. To incorporate the effect of the finite tire/road contact length in the controller model, the real road elevation q_{rr} is filtered by a low pass filter, resulting in a displacement q_{tr} of the lower end of the tire spring. Here, a first order filter as proposed by Foag [9] is used, because a simple, more accurate description of the influence of the finite contact length is not available. Foag [9] proposes a time constant $\tau_r = \frac{l}{3V}$, where V is the forward velocity of the vehicle and l is the length of the tire footprint:

$$\dot{q}_{tr} = \left(\frac{1}{\tau_r}\right) \cdot (-q_{tr} + q_{rr}). \quad (3.1)$$

The relation between the tire force F_t and the spring deflection $q_{ar} - q_{tr}$ is given by

$$F_t = \begin{cases} 0 & \text{if } \dot{q}_{ar} - \dot{q}_{tr} > 0 \\ k_{tire} \cdot (q_{ar} - q_{tr}) & \text{if } \dot{q}_{ar} - \dot{q}_{tr} < 0. \end{cases}$$

The road elevation $q_{rr}(t)$ at time t at the rear wheels is assumed to be the same as at the front wheels except for a time delay t_p , the preview time, that is equal to the quotient of the wheelbase L of the tractor and the forward vehicle velocity V .

With the state vector \underline{x} ,

$$\underline{x} = \left(q_{cr} \quad q_{cr} - q_{ar} \quad \dot{q}_{cr} \quad \dot{q}_{cr} - \dot{q}_{ar} \quad S_a \quad q_{tr} \right)^T,$$

the system equations are given by:

$$\dot{x}_1 = x_3 \quad (3.2)$$

$$\dot{x}_2 = x_4 \quad (3.3)$$

$$\dot{x}_3 = \frac{1}{m_{cr}} \cdot (-2F_s - F_d) - g \quad (3.4)$$

$$\dot{x}_4 = \frac{1}{m_{cr}} \cdot (-2F_s - F_d) - \frac{1}{m_{ar}} \cdot (+2F_s + F_d - F_t) \quad (3.5)$$

$$\dot{x}_5 = \frac{1}{\tau_d} \cdot (-x_5 + S); \quad S \in A \subset [0, 1] \quad (3.6)$$

$$\dot{x}_6 = \frac{1}{\tau_r} \cdot (-x_6 + q_{rr}). \quad (3.7)$$

The possible values of S depend on whether the semi-active damper is used as a continuously variable damper ($S \in [0, 1]$) or as a multi-level damper ($S \in \{0, 1\}$). The sprung mass m_{cr} and the static spring force $F_{s,stat} = m_{cr}g$ depend on the payload. The mass m_{cr} for a fully laden and for an un-laden vehicle is determined from simulations with many different values for m_{cr} such that the behavior of the two-DOF model resembles the behavior of half the rear side of the tractor of the 3D vehicle model. The values of m_{cr} and the other quantities, used in the two-DOF vehicle model, are given in Table 3.1. The forward velocity V of the vehicle depends on the road surface.

Table 3.1: Parameter values of the two-DOF vehicle model.

quantity	symbol	value	unit
unsprung mass	m_{ar}	700	[kg]
sprung mass (un-laden)	m_{cr}	955	[kg]
sprung mass (laden)	m_{cr}	4272.5	[kg]
tire stiffness	k_{tire}	$2.4 \cdot 10^6$	[N/m]
damper time constant	τ_d	0.0065	[s]
tire footprint length	l	0.3	[m]
tractor wheelbase	L	3.5	[m]

In this chapter, the same nonlinear two-DOF vehicle model is used to evaluate the performance of the controlled semi-active systems and the same model with $S = 0.5$ is used to evaluate the performance of the vehicle with a conventional passive suspension, unless mentioned otherwise.

3.1.2 Road models for control method selection

For the evaluation of the system performance, the nonlinear two-DOF vehicle simulation model uses the left tracks of the road models in Section 2.3 as road inputs. The forward velocity of the vehicle model on each of these road surfaces is specified in Section 2.3.

3.2 Control objective

The control objective reflects the performance aspects for which the suspension has to be optimized. The chosen objective is to improve occupants comfort and to reduce the incidental load on the chassis components and on the cargo, without a bump stop or a rebound element coming into effect and without tire lift-off. If it is impossible to prevent the suspension deflection from reaching its bounds then the resulting impact force has to be as small as possible. Furthermore, if tire lift-off is inevitable then the lift-off time must be as short as possible.

According to Chapter 2, the comfort of the occupants and the incidental load on the chassis components and cargo is related to (maximum) absolute accelerations of the occupants and of the vehicle body. Therefore, the maximum absolute acceleration $|\ddot{q}_{cr}| = |\dot{x}_3|$ of the sprung mass in the internal controller model is used as a measure for both comfort and incidental load on the chassis components and cargo.

In practice, either a bump stop or a rebound element comes into effect if a bound on the suspension working space $[l^l, l^u]$ is reached. The impact force depends on the relative velocity of the axle and the chassis at the moment of the impact. In the internal model, however, bump stops and rebound elements are not taken into account, so it is not possible to determine impact forces in this model and to use these forces in the performance index. Furthermore, the suspension deflection $x_2 = q_{cr} - q_{ar}$, as calculated in this model, can be outside the allowed range $[l^l, l^u]$. Let δ^l and δ^u be defined by

$$\delta^l = (l^l - x_2) \cdot \varepsilon(l^l - x_2); \quad \delta^u = (x_2 - l^u) \cdot \varepsilon(x_2 - l^u), \quad (3.8)$$

where ε is the unit step function, *i.e.* $\varepsilon(y) = 0$ if $y < 0$ and $\varepsilon(y) = 1$ if $y \geq 0$. Then $\delta^l \neq 0$ ($\delta^u \neq 0$) represents an excess of the negative (positive) suspension deflection bound. Without thorough analysis it is assumed that these virtual excesses are a suitable measure for the impact force. The values for the bounds on the suspension deflection, *i.e.* l^l and l^u , are given in Table 3.2.

Table 3.2: Values for the bounds on the suspension working space.

quantity	parameter	value	unit
lower bound suspension deflection	l^l	-0.09	[m]
upper bound suspension deflection	l^u	+0.14	[m]

The road height between the front and the rear wheels of the tractor is estimated by a 'reconstructor' from measurements of, *e.g.*, accelerations and suspension deflections at the front side of the tractor. This reconstructor delivers the road surface over the preview interval $(t, t + t_p]$ only. It was decided not to make assumptions about the oncoming road surface outside this interval. Therefore, the controller does not find the optimum over the total driving time but only over the preview interval $(t, t + t_p]$.

The control objective is translated now in finding the *function* $S : (t, t + t_p] \rightarrow A$ which minimizes the performance index J , defined by

$$J = \max_{v \in (t, t+t_p]} c_1(t') + \int_t^{t+t_p} c_2(t') dt' + J_{ext}(t + t_p), \quad (3.9)$$

where $c_1(t')$ and $c_2(t')$ are given by

$$c_1(t') = |\dot{x}_3(t')| + V_1 \cdot \delta^l(t') + V_2 \cdot \delta^u(t') \quad (3.10)$$

$$c_2(t') = W \cdot \varepsilon(F_i(t')). \quad (3.11)$$

The quantity $c_1(t')$ is the sum of the maximum absolute acceleration of the sprung mass at time t' and two terms to penalize an eventual excess of the suspension deflection bounds at time t' . The quantity $c_2(t')$ penalizes eventual tire lift-off at time t' . The penalty factors V_1 , V_2 and W are large, positive numbers. Furthermore, the term $J_{ext}(t + t_p)$ accounts for the expected performance for $t' > t + t_p$. It may be a function of the state quantities at $t + t_p$ and possibly of the road surface in the preview interval. However, in this thesis the term is taken equal to zero.

A numerical elaboration of the stated problem is hampered by the fact that the design variable to be found is the *function* $S : (t, t + t_p] \rightarrow A$ and not a parameter or a vector of parameters. To deal with this problem discretization is used. The preview interval $(t, t + t_p]$ is divided in I subintervals of fixed length Δh_i (plus a possibly remaining subinterval smaller than Δh_i) by generating equidistant time points

$$t_k = t + k\Delta h_i, \quad k \in \{1, 2, \dots, I\},$$

such that $t_p - \Delta h_i < I\Delta h_i \leq t_p$ (see Figure 3.2). In each subinterval $k \in \{1, 2, \dots, I\}$ the *function* $S(t')$ is approximated by a constant $S_k \in A$, whereas the damper setting for the interval $(t + I\Delta h_i, t + t_p]$ is left out of consideration, so the controller determines the optimum not for $(t, t + t_p]$, but for $(t, t + I\Delta h_i]$. The set $\underline{S} = [S_1, S_2, \dots, S_I]$ is called a damper setting combination.

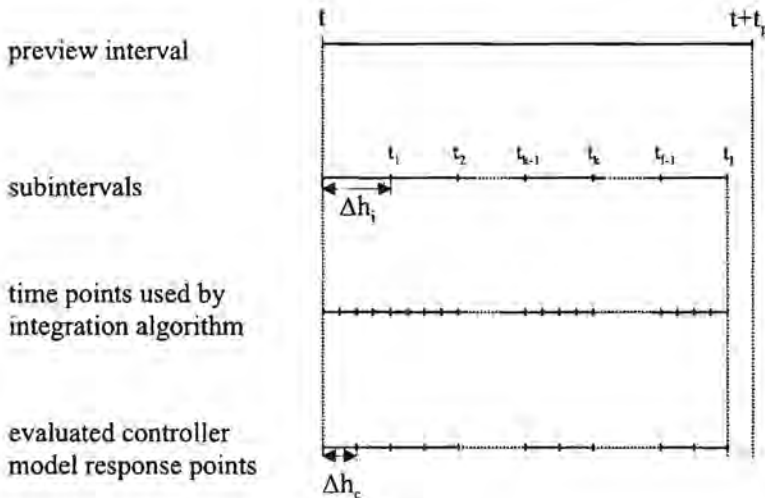


Figure 3.2: The preview interval

The controller solves the system equations (3.2) to (3.7) with a numerical integration algorithm, given the state at time t (= current state) of the controlled vehicle, the road

height for the preview interval and a chosen damper setting combination \underline{S} . In general, the reconstructor will give the road height only at a number of discrete time points which do not coincide with the discrete time points, used by the integration algorithm. Then an interpolation algorithm is required to estimate the road height at the discrete time points of the integration algorithm. In the remainder of this thesis it is assumed that the road height is known at the discrete time points of the integration algorithm.

The state of the model is determined at C discrete time points $t+\Delta h_c, t+2\Delta h_c, \dots, t+C\Delta h_c$, where $C\Delta h_c = I\Delta h_i$ and, to get usable results, $C > I$ (see Figure 3.2). At each of these time points the functions c_1 and c_2 are evaluated and used to calculate the performance index J . The integral in Equation (3.9) is approximated by

$$\int_t^{t+C\Delta h_c} c_2(t')dt' \approx \Delta h_c \cdot \left[\frac{1}{2}c_2(t) + \sum_{j=1}^{C-1} c_2(t+j\Delta h_c) + \frac{1}{2}c_2(t+C\Delta h_c) \right]. \quad (3.12)$$

The first term in this approximation, *i.e.* $\frac{1}{2}\Delta h_c c_2(t)$, is the same for all possible damper settings in the interval $(t, t+t_p]$ and is therefore irrelevant. Hence, the performance index for the discrete problem is approximated by¹

$$J = \max_{j \in \{1, 2, \dots, C\}} c_1(t+j\Delta h_c) + \Delta h_c \sum_{j=1}^{C-1} c_2(t+j\Delta h_c) + \frac{1}{2}\Delta h_c c_2(t+C\Delta h_c) + J_{ext}(C\Delta h_c) \quad (3.13)$$

and the original control objective is now approximated by

using the definitions for c_1 and c_2 , the state $\underline{x}(t)$ and the reconstructed road surface q_{rr} at the discrete time points of the integration algorithm in $(t, t+t_p]$, determine the damper settings $S_k \in A$ for $k \in \{1, 2, \dots, I\}$ which minimize this performance index under the constraints of the system equations (3.2) to (3.7).

The choice of the penalty factors V_1 , V_2 and W in the expressions for c_1 and c_2 is rather difficult. It is useful to scale and make the penalty factors non-dimensional by the order of magnitude of the quantities to be penalized. This strategy for determining the penalty factors is presented in Appendix A. The values for V_1 , V_2 and W are given in Table 3.3. They are selected from a large number of possible non-dimensional (V_1^*, V_2^*, W^*) -combinations such that the behavior of the controlled system is satisfactorily if one of the constraints is violated in a preview interval.

¹A conceptually more charming alternative for approximating $\max c_1(t')$ for $t' \in (t, t+t_p]$ in Equation (3.9) is to use evaluated function values of c_1 at the discrete time points of the integration algorithm. A conceptually attractive alternative to determine the integral in Equation (3.9) is solving $\dot{J}_{part}(t') = c_2(t')$ for $t' \in (t, t+t_p]$ with $J_{part}(t) = 0$ together with the system equations (3.2) to (3.7) of the controller internal model.

Table 3.3: Values for penalty factors.

penalized quantity	penalty factor	value	unit
excess of bound on negative suspension deflection	V_1	10^4	[1/m]
excess of bound on positive suspension deflection	V_2	10^4	[1/m]
excess of bound on tire lift-off time	W	10^4	[1/s]

3.3 Control concepts for a multi-level damper

The semi-active damper of Chapter 2 can be used as a multi-level damper by restricting the set of possible damper settings. In this section, two control concepts are presented whereas a third developed concept, the dynamic programming controller, is presented by Muijderman et al. [29]. The latter is applicable for control objectives that satisfy Bellman's principle of optimality (Bellman [2]). It is questionable whether or not this is the case for the control objective used in this thesis. However, the dynamic programming controller is applicable for many other control objectives and is then often preferable to the control concepts presented in this section with respect to the required controller computation time if the preview interval contains many subintervals or if a damper with many levels is used. The analysis in this section is restricted to two-level dampers, but can be extended with some minor modifications to dampers with more levels.

3.3.1 Direct calculation controller

The direct calculation controller (DCC) is the most straightforward controller for the problem stated in Section 3.2. This controller is applicable for a broad class of control objectives and always determines the global optimum.

The procedure of the DCC is schematically depicted in Figure 3.3. The DCC calculates for all possible damper setting combinations $\underline{S} = [S_1, S_2, \dots, S_I]$ the response of the controller internal model at the C discrete time points $t + \Delta h_c, t + 2\Delta h_c, \dots, t + C\Delta h_c$ in the interval $(t, t + I\Delta h_i]$ and determines the performance index J , given the state $\underline{x}(t)$ and the road surface at discrete time points in the preview interval. The damper setting combination with the best performance is the optimal control sequence \underline{S}^{opt} for the current preview interval. However, it is not recommended to apply this optimal sequence during the whole interval $(t, t + I\Delta h_i]$ since the time interval for which the road surface is reconstructed steadily increases. Therefore, the obtained optimal damper settings are applied only in the interval $(t, t + s\Delta h_i]$ with $1 \leq s \leq I$. Then a new preview interval, which takes the extra road information into account, is considered and the whole optimization procedure is repeated for this new interval.

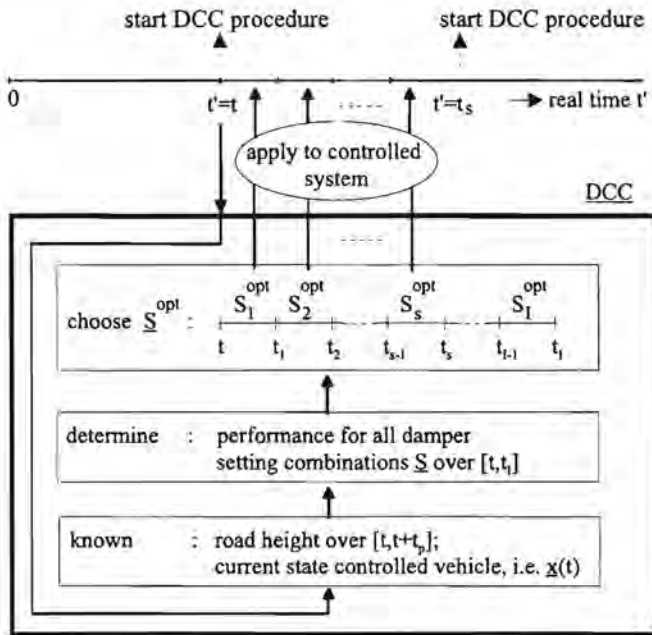


Figure 3.3: DCC procedure

3.3.2 Branch-and-bound controller

The branch-and-bound controller (BBC) is based on a method that was introduced in 1960 by Land and Doig [25] to solve discrete programming problems. The diversity of control objectives that can be handled with the BBC is less than with the DCC. The BBC is applicable to discrete control problems with a monotonously non-decreasing objective function over the preview interval for each damper setting combination (which is the case for the control objective in Section 3.2). For these problems the BBC requires at the utmost the same but in general much less CPU time than the DCC, whereas the performance will be the same. If the allowed controller computation time for determining the optimal control sequence over the preview interval is too small to determine the optimum over the whole interval then it is likely that the obtained optimum of the BBC is 'better', *i.e.* the optimum over a larger part of the preview interval, than the optimum of the DCC because no time is wasted on useless damper setting sequences. Therefore, the BBC is preferable to the DCC for control problems to which it can be applied.

The 'tree diagram' of Figure 3.4 is used to explain the branch-and-bound method for the case of a two-level damper with the objective function of Section 3.2. This figure contains layers with branch points and branches between the layers. Layer $k \in$

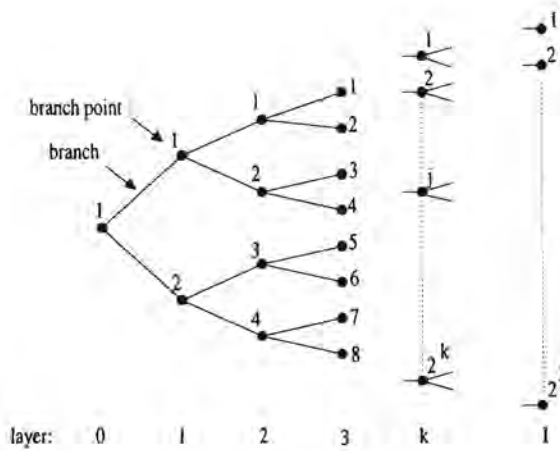


Figure 3.4: Tree diagram

$\{0, 1, 2, \dots, I\}$ corresponds to time point $t_k = t + k\Delta h_i$. From each branch point in layer $k \in \{0, 1, 2, \dots, I - 1\}$ two branches to layer $k + 1$ originate. One of these branches (the upper one in Figure 3.4) corresponds to the low damper setting $S_{k+1} = 0$ in $(t_k, t_{k+1}]$, the other branch (the lower one in Figure 3.4) to the high damper setting $S_{k+1} = 1$. The branch points in layer k are numbered from $j = 1$ at the top to $j = 2^k$ at the bottom. The branch point in layer k with number j is denoted by $P(k, j)$. If $k < I$ then $P(k, j)$ is connected to $P(k + 1, 2j - 1)$ and to $P(k + 1, 2j)$. The unique set of branches, connecting $P(0, 1)$ to $P(k, j)$ is called a trunk and is denoted by $T(k, j)$. If $k < I$ then $T(k, j)$ is a partial trunk whereas $T(I, j)$ is a complete trunk. Each trunk $T(k, j)$ corresponds to a unique control sequence S_1, S_2, \dots, S_k and it can be seen that $j = 1 + 2^{k-1}S_1 + \dots + 2S_{k-1} + S_k$. For each trunk $T(k, j)$, a cost performance index $J_t(k, j)$ is defined. If the number of time points in $(t, t + k\Delta h_i]$, where the state of the controller internal model is determined by the controller, is denoted by n_k (so $n_k \leq C$) then $J_t(k, j)$ is defined by

$$J_t(k, j) = \max_{j \in \{1, 2, \dots, n_k\}} c_1(t + j\Delta h_c) + \Delta h_c \sum_{j=1}^{n_k-1} c_2(t + j\Delta h_c) + \frac{1}{2} \Delta h_c c_2(t + n_k \Delta h_c). \quad (3.14)$$

The optimal control sequence $\underline{S}^{opt} = \{S_1^{opt}, S_2^{opt}, \dots, S_I^{opt}\}$ corresponds to that complete trunk $T(I, j)$ for which $J_t(I, j) = \min(J_t(I, 1), \dots, J_t(I, 2^I))$.

In the procedure to determine the optimal complete trunk the cost performance index is calculated for, in general, a lot of (partial) trunks. A (partial) trunk for which the cost performance index is determined is called a processed (partial) trunk and the

set of all tuples (k, j) for which $T(k, j)$ is processed whereas the branches connected to this trunk are not processed is denoted by D . The essential steps in the branch-and-bound procedure are now given in the following algorithm:

step 1 (initialization): process the partial trunks $T(1, 1)$ and $T(1, 2)$ from the origin to the branch points in layer 1, *i.e.* determine $J_t(1, 1)$ and $J_t(1, 2)$, and initialize D with $D = \{(1, 1), (1, 2)\}$

step 2: select the tuple $(k, j) \in D$ such that

$$J_t(k, j) = \min_{(p, q) \in D} J_t(p, q) \quad (3.15)$$

step 3: if $k < I$ then process the branches from $P(k, j)$ to $P(k + 1, 2j - 1)$ and to $P(k + 1, 2j)$, *i.e.* determine $J_t(k + 1, 2j - 1)$ and $J_t(k + 1, 2j)$, extend D with the tuples $(k + 1, 2j - 1)$ and $(k + 1, 2j)$ and remove (k, j) from D

step 4: repeat step 2 and step 3 until $k = I$. Call this tuple (I, Q) .

The trunk $T(I, Q)$ is the optimal trunk. It corresponds to the optimal control sequence $\underline{S}^{opt} = \{S_1^{opt}, S_2^{opt}, \dots, S_I^{opt}\}$ with $1 + 2^{I-1}S_1^{opt} + \dots + 2S_{I-1}^{opt} + S_I^{opt} = Q$. In general this sequence can be found with the given algorithm without having to consider all possible, *i.e.* 2^I , sequences. This optimal control sequence is applied in the interval $(t, t + s\Delta h_i]$ with $1 \leq s \leq I$. Then a new preview interval is considered and the whole optimization procedure is repeated for this new interval.

3.4 Control concept for a continuously variable damper

This section presents the so-called sequential quadratic programming controller (SQPC) for a continuously variable damper. This control concept is based on the sequential quadratic programming (SQP) technique to solve constrained optimization problems with continuous design variables (see also van der Aa [1]). For each preview interval, the SQP technique is used to determine the control sequence $\underline{S} = \{S_1, S_2, \dots, S_I\}$, where the elements $S_k \in [0, 1]$ are treated as design variables.

The SQP algorithm can use a problem description equivalent to that in Section 3.2. However, the maximum value operator in the performance index (3.13) introduces discontinuities in the derivative of this function with respect to the design variables S_k for $k \in \{1, 2, \dots, I\}$. This can cause serious problems with the usual SQP procedure. However, this operator can be easily avoided by means of an additional design variable S_{I+1} . The original performance index (3.13) is then replaced by

$$J = S_{I+1} \quad (3.16)$$

with the additional constraints

$$c_1(t + j\Delta h_c) + \Delta h_c \sum_{k=1}^{C-1} c_2(t + k\Delta h_c) + \frac{1}{2} \Delta h_c c_2(t + C\Delta h_c) \leq S_{I+1}$$

$$\forall j \in \{1, 2, \dots, C\}. \quad (3.17)$$

The original problem is then replaced by the equivalent problem

using the definitions (3.10) and (3.11) for c_1 and c_2 , the state $\underline{x}(t)$ and the reconstructed road surface q_{rr} at the discrete time points of the integration algorithm in $(t, t + t_p]$, determine the damper settings $S_k \in [0, 1]$ for $k \in \{1, 2, \dots, I\}$ and an additional design variable S_{I+1} which minimize the performance index (3.16) under the constraints of the system equations (3.2) to (3.7) and the additional constraints (3.17).

The extra design variable S_{I+1} does not represent a damper setting but can be interpreted as the unknown upper bound of the performance index which is minimized. It can be seen that the performance index (3.16) is differentiable with respect to all design variables. This approach to convert a min-max problem into a smooth problem by using an additional variable appears to be very useful in many applications (Haftka et al. [14], Haug et al. [15]).

The SQP optimization algorithm may perform poorly when the design variables and constraints are scaled improperly. To prevent ill-conditioning, the magnitude of all design variables should be of the same order. Besides, the magnitude of all constraints should be of the same order if they are at similar levels of criticality. The upper limit of S_k , $k \in \{1, 2, \dots, I\}$ is equal to 1. Furthermore, the upper limit of S_{I+1} and of the constraints are scaled to 1.

The procedure of the SQP controller (SQPC) is schematically depicted in Figure 3.5. Starting with an initial guess $\underline{z}^{(0)} = \{\underline{S}^{(0)}, S_{I+1}^{(0)}\}$ for the design variables, the controller determines the response and the performance of the controller internal model over $(t, t + I\Delta h_i]$, using the current state of the controlled vehicle and the preview information.

The SQP algorithm determines the 'optimum' solution \underline{z}^{opt} in an iterative process. In iteration step i ($i \in \{1, 2, \dots\}$), first the original problem is approximated by a quadratic problem in the neighborhood of the last estimation of the optimal solution, *i.e.* $\underline{z}^{(i-1)}$. This quadratic problem is solved, yielding a search direction for the optimal solution of the original problem. Then, a new estimation of the optimal solution, $\underline{z}^{(i)}$ is determined by solving a one-dimensional optimization problem in this search direction. The performance of the internal model for $\underline{z}^{(i)}$ is determined and compared to the performances for previous estimates of the optimal solution. The iterative process

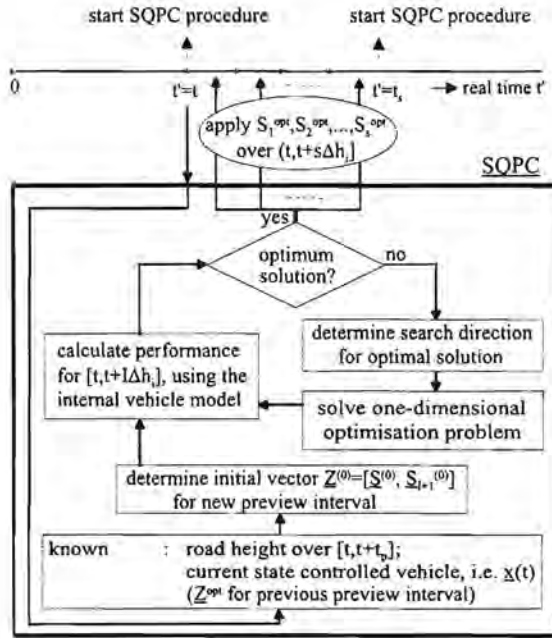


Figure 3.5: SQPC procedure

is finished and $\underline{Z}^{opt} = \{\underline{S}^{opt}, S_{I+1}^{opt}\}$ is established if, according to a chosen criterion, the estimate is close enough to the 'optimal' solution. A more detailed description of this SQP algorithm is available in Haftka et al. [14].

The optimal control sequence \underline{S}^{opt} is applied in the interval $(t, t + s\Delta h_i]$ with $1 \leq s \leq I$. Then a new preview interval is considered and the whole optimization procedure is repeated for this new interval.

The initial values for S_k , $k \in \{1, 2, \dots, I + 1\}$ in the first preview interval and the initial values for S_k , $k \in \{I - s + 1, \dots, I\}$ in the second and subsequent preview intervals are chosen. However, for the second and subsequent preview intervals, the initial value for S_k , $k \in \{1, 2, \dots, I - s\}$ is taken equal to the calculated optimal value S_{k+s} in the previous preview interval whereas the initial value for S_{I+1} is taken equal to the optimal value S_{I+1} of the previous preview interval. An undesirable property of the SQP algorithm is that the optimization may converge to a local minimum if the vector with initial design variables is not close to the global minimum of the optimization problem. Therefore, the performance of the SQPC controller may improve if the optimum control sequence over a preview interval is determined for different values of the initial design variables. However, the computation time of the controller will strongly increase and therefore repeated application of the SQP algorithm for different values of the initial

design variables is omitted in this thesis.

Usually and in contrast to the earlier mentioned control objective, an SQP algorithm takes constraints like those on the suspension deflection and the tire lift-off time explicitly into account. In this chapter the performance of the continuously variable damper with SQPC is compared to the performance of the controlled two-level damper. It is unknown whether the problem description equivalent to that in Section 3.2 or the explicit formulation is more fair for the comparison. Therefore, next to the SQP controller with the above mentioned control objective, called SQPCO, an SQP controller which takes the constraints on the suspension deflection and the tire lift-off time explicitly into account is used for this comparison. The latter is called SQPCE.

3.5 Choice of values for some controller parameters

In this section, suitable values for the parameters Δh_i , $s\Delta h_i$ and Δh_c are determined. The laden two-DOF model with the nonlinear air springs and the DCC controlled nonlinear two-level damper of Section 3.1.1 is used as controller internal model and simulation model. The control objective is the same as in Section 3.2 and the five incidental road excitations with one single vehicle velocity are used. The controlled vehicle response is calculated very accurately with a variable-order variable-step Adams method and a sample interval of 0.0001 s. This small sample interval is used to get accurate tire lift-off times from the controlled vehicle response at equidistant time points. For each of the incidental road excitations, the quantities strongly related to the control objective, *i.e.* the maximum absolute sprung mass acceleration, the excesses of the bounds on the suspension deflection and the tire lift-off time, are determined from the controlled vehicle response. They are used to judge the performance. A quantity called CR (Computational Requirement) is used as a measure for the computational requirement on the controller. The value of this quantity is chosen proportional to the CPU time on a PC with a Pentium 100 processor and 16 MB RAM memory. The value for CR is 1 if 10 s CPU time are required on this machine.

3.5.1 Subinterval length Δh_i

In this section, a suitable subinterval length Δh_i is determined, *i.e.* a Δh_i with 'high' performance and 'low' CR. It will be shown that the CR for a controller reduces considerably if Δh_i is increased and that the performance of the controller decreases if Δh_i is too large.

The influence of control signals with a frequency far above 10 Hz ($\Delta h_i \ll 0.1$ s) on the model response will be negligible, because the highest natural frequency of the linearized two-DOF controller model is about 10 Hz. Therefore, $\Delta h_i \geq 0.025$ s is

chosen. Of course, the maximum length of Δh_i is equal to t_p . The application interval $s\Delta h_i$ is equal to Δh_i , *i.e.* $s = 1$. The road surface is supposed to be known as a continuous function of time over the preview interval and a variable-order variable-step Adams method is used to determine the responses of the controller internal model with $\Delta h_c = 0.0001$ s. Instead of using the prescribed forward velocity V on each incidental road surface, $V = 63$ km/h for all road surfaces in this section, which means $t_p = 0.20$ s. This velocity is close to the average velocity of the vehicle for the different incidental road excitations. Furthermore, for this velocity, the investigated subinterval lengths 0.025 s, 0.050 s, 0.100 s and 0.200 s, all fit an integer number of times in the preview interval, so the whole preview interval is taken into account for all investigated subinterval lengths and none of the subinterval lengths is more advantageous because a larger part of the preview interval is taken into account. For $t_p = 0.20$ s, the controller previews in one preview interval the whole obstacle only for the standard brick, the scraped road and the well. For each preview interval, the controller determines the response of the internal vehicle model for all possible damper setting combinations. Only for the standard brick, the scraped road and the well, there is one preview interval (the first one) which captures for each possible damper setting combination over the total simulation time the response parts which might influence the values of the performance quantities used in this section.

Table 3.4 gives the performance and the CR of the semi-active system with different controllers for the standard brick. The table also gives the performance of a 'passive low', a 'passive medium' and a 'passive high' system. These systems contain conventional passive dampers with force - relative velocity characteristics similar to the semi-active damper characteristic with $S_a = 0$, $S_a = 0.5$ and $S_a = 1$. The suspension deflection remains within the available suspension working space and tire lift-off does not occur, so the controllers will focus on reducing the maximum absolute sprung mass acceleration. This acceleration is for the controllers 2^{aa}, 3^{aa} and 4^{aa} equal to, and for controller 1^{aa} 3.5 % lower than that of the 'best' passive system on this road surface (passive low). However, the CR for controller 1^{aa} is more than 8 times the CR for the other controllers.

Table 3.5 gives the performance and the CR for the traffic hump. The suspension deflection exceeds the available suspension working space and tire lift-off occurs, so the controllers focus on a reduction of these excesses. For all controllers, the semi-active system shows the same maximum excess δ^l as the 'best' passive system on this road surface (passive high). Apparently, it is not possible for the semi-active system to reduce this excess compared to the 'best' passive system. The tire lift-off time of the

Table 3.4: Performance and CR for the standard brick of three passive systems and the DCC controlled semi-active system with different Δh_i and $s\Delta h_i = \Delta h_i$.

Standard brick	Δh_i [s]	$s\Delta h_i$ [s]	$\max \ddot{q}_{cr} $ [m/s ²]	tire lift-off [s]	$\max \delta^u$ [m]	$\max \delta^l$ [m]	CR [-]
controller 1 ^{aa}	0.025	0.025	2.70	0.000	0.00	0.00	13.06
controller 2 ^{aa}	0.050	0.050	2.79	0.000	0.00	0.00	1.49
controller 3 ^{aa}	0.100	0.100	2.79	0.000	0.00	0.00	0.64
controller 4 ^{aa}	0.200	0.200	2.79	0.000	0.00	0.00	0.44
passive low			2.79	0.000	0.00	0.00	
passive medium			3.78	0.000	0.00	0.00	
passive high			4.49	0.000	0.00	0.00	

Table 3.5: Performance and CR for the traffic hump of three passive systems and the DCC controlled semi-active system with different Δh_i and $s\Delta h_i = \Delta h_i$.

Traffic hump	Δh_i [s]	$s\Delta h_i$ [s]	$\max \ddot{q}_{cr} $ [m/s ²]	tire lift-off [s]	$\max \delta^u$ [m]	$\max \delta^l$ [m]	CR [-]
controller 1 ^{aa}	0.025	0.025	18.58	0.067	0.00	0.02	13.06
controller 2 ^{aa}	0.050	0.050	18.58	0.067	0.00	0.02	1.49
controller 3 ^{aa}	0.100	0.100	18.58	0.067	0.00	0.02	0.60
controller 4 ^{aa}	0.200	0.200	18.58	0.094	0.00	0.02	0.41
passive low			20.32	0.094	0.00	0.04	
passive medium			19.03	0.086	0.00	0.03	
passive high			18.58	0.094	0.00	0.02	

semi-active system with controller 4^{aa} is the same as for the 'best' passive system whereas the tire lift-off time of the semi-active system with controller 1^{aa}, 2^{aa} or 3^{aa} is 29 % lower than that of the 'best' passive system.

Tables 3.6 and 3.7 give the performance and the CR for the scraped road and the well. The suspension deflection remains within the available suspension working space but the tire loses contact with the road, so the controllers focus on a reduction of the tire lift-off time. For the scraped road, the tire lift-off time of the semi-active system with controller 1^{aa}, 2^{aa} or 3^{aa} is 9 % lower than that of the 'best' passive system on this road surface (passive medium), whereas the tire lift-off time of the semi-active system with controller 4^{aa} is equal to the tire lift-off time of the passive low system, which is the best passive system that can be realized with a constant setting of the two-level damper. For the well, the tire lift-off time of the semi-active system is for all controllers equal to that of the 'best' passive system on this road surface (passive high).

Table 3.6: Performance and CR for the scraped road of three passive systems and the DCC controlled semi-active system with different Δh_i and $s\Delta h_i = \Delta h_i$.

Scraped road	Δh_i [s]	$s\Delta h_i$ [s]	$\max \ddot{q}_{cr} $ [m/s ²]	tire lift-off [s]	$\max \delta^u$ [m]	$\max \delta^l$ [m]	CR [-]
controller 1 ^{aa}	0.025	0.025	8.51	0.043	0.00	0.00	13.74
controller 2 ^{aa}	0.050	0.050	8.51	0.043	0.00	0.00	1.57
controller 3 ^{aa}	0.100	0.100	8.51	0.043	0.00	0.00	0.61
controller 4 ^{aa}	0.200	0.200	8.51	0.050	0.00	0.00	0.41
passive low			8.51	0.050	0.00	0.00	
passive medium			9.48	0.047	0.00	0.00	
passive high			9.97	0.052	0.00	0.00	

Table 3.7: Performance and CR for the well of three passive systems and the DCC controlled semi-active system with different Δh_i and $s\Delta h_i = \Delta h_i$.

Well	Δh_i [s]	$s\Delta h_i$ [s]	$\max \ddot{q}_{cr} $ [m/s ²]	tire lift-off [s]	$\max \delta^u$ [m]	$\max \delta^l$ [m]	CR [-]
controller 1 ^{aa}	0.025	0.025	9.12	0.044	0.00	0.00	13.47
controller 2 ^{aa}	0.050	0.050	9.12	0.044	0.00	0.00	1.55
controller 3 ^{aa}	0.100	0.100	9.12	0.044	0.00	0.00	0.62
controller 4 ^{aa}	0.200	0.200	9.12	0.044	0.00	0.00	0.42
passive low			7.55	0.081	0.00	0.00	
passive medium			8.46	0.065	0.00	0.00	
passive high			9.12	0.044	0.00	0.00	

Table 3.8 gives the performance and the CR for the wave. The suspension deflection exceeds the available suspension working space, but tire lift-off does not occur, so the controllers focus on a reduction of the excesses of the bounds on the suspension deflection. The results are conspicuous. The performance of the best passive system that can be realized with a constant setting of the two-level damper (passive high) is better than the performance of the 'best' semi-active system for the wave. Furthermore, the controllers 1^{aa} and 2^{aa} not only have the same switching time points as controller 3^{aa} but they even have more switching opportunities in the preview interval than controller 3^{aa}. However, contrary to the expectation, the performance decreases by increasing the number of switching time points in the preview interval *i.e.* by using controller 1^{aa} or 2^{aa} instead of controller 3^{aa}. The cause of this unexpected behavior is further investigated. If controllers with different Δh_i and $s\Delta h_i = \Delta h_i$ start to control the semi-active vehicle model with velocity V and initial state $\underline{x}(0)$ at the same road position, then

Table 3.8: Performance and CR for the wave of three passive systems and the DCC controlled semi-active system with different Δh_i and $s\Delta h_i = \Delta h_i$.

Wave	Δh_i [s]	$s\Delta h_i$ [s]	$\max \ddot{q}_{cr} $ [m/s ²]	tire lift-off [s]	$\max \delta^u$ [m]	$\max \delta^l$ [m]	CR [-]
controller 1 ^{aa}	0.025	0.025	14.56	0.000	0.00	0.02	13.21
controller 2 ^{aa}	0.050	0.050	14.43	0.000	0.00	0.02	1.47
controller 3 ^{aa}	0.100	0.100	14.19	0.000	0.00	0.02	0.57
controller 4 ^{aa}	0.200	0.200	15.61	0.000	0.02	0.02	0.37
passive low			23.97	0.000	0.08	0.04	
passive medium			17.14	0.000	0.02	0.03	
passive high			13.65	0.000	0.00	0.02	

these controllers have the same initial state and the same preview information for the first preview interval only. Table 3.9 gives the performance for the wave of the semi-active vehicle model with $V = 63$ km/h over $[0 \text{ s}, 0.2 \text{ s}]$ for controllers with $s\Delta h_i = 0.2$ s and different Δh_i , where the vehicle is initially ($t' = 0$ s) in static equilibrium. This table shows that the performance over the first preview interval does not decrease if Δh_i decreases, *i.e.* if more switching time points are chosen in the preview interval. However, if parts of the vehicle model response which determine the performance of the

Table 3.9: Performance over $[0 \text{ s}, 0.2 \text{ s}]$ for the wave of the DCC controlled semi-active system with different Δh_i and $s\Delta h_i = 0.2$ s.

Wave	Δh_i [s]	$s\Delta h_i$ [s]	$\max \ddot{q}_{cr} $ [m/s ²]	tire lift-off [s]	$\max \delta^u$ [m]	$\max \delta^l$ [m]
controller 1 ^{da}	0.025	0.200	4.85	0.000	0.00	0.00
controller 2 ^{da}	0.050	0.200	4.98	0.000	0.00	0.02
controller 3 ^{da}	0.100	0.200	4.98	0.000	0.00	0.02
controller 4 ^{da}	0.200	0.200	5.24	0.000	0.02	0.02

controlled vehicle over the total simulation time are not captured in this first preview interval whereas the applied damper setting of this interval influences the performance in front of the first preview interval then this applied setting may be undesirable with respect to the response in front of the first preview interval. In other words, the optimal settings for the first 0.2 s may not be favorable for the vehicle performance over a larger time interval. This implies that the performance decrease for controllers with more switching time points in the preview interval may be caused by a too short time interval for which the controller internal model response can be determined. Implicitly, this performance decrease is then caused by a too short preview interval, as the controller

internal model response can only be determined over the preview interval. The fact that the performance of the 'best' semi-active system is worse than the performance of the best passive system that can be realized with a constant setting of the two-level damper may also be due to a too short preview interval. If the controllers would have the performance determining part of the vehicle response over the total simulation time to their disposal in each preview interval, then each of the controllers would have recognized that permanent application of the high damper setting gives a better performance than the currently applied damper setting sequence. Whether a too short preview interval is indeed the cause of the disappointing performance of the semi-active systems can be investigated by comparing the performances of the controllers with different Δh_i and $s\Delta h_i = \Delta h_i$ for an increased wheelbase length, *i.e.* a larger value of t_p . The computational burden of the controllers increases tremendously for large values of t_p . Therefore, this investigation is postponed to Section 3.7 where a more efficient version of the controller is established.

Summarizing, for the traffic hump, the scraped road and the wave, the performance of the semi-active system increases distinctly if Δh_i is reduced from 0.200 s to 0.100 s. For the well, the performance of the semi-active system is the same for all controllers and for the standard brick the performance increases slightly if Δh_i is reduced from 0.050 s to 0.025 s at the expense of a much higher value for CR.

A subinterval length of 0.100 s implies a 10 Hz switching frequency $f_s = 1/\Delta h_i$ of the controller. This frequency is close to the highest undamped natural frequency $f_n = 9.7$ Hz of the linearized two-DOF vehicle model (linearized with respect to the static equilibrium position). Some extra simulations are carried out to investigate whether or not the highest undamped natural frequency f_n of the linearized model indeed determines the required value for Δh_i . For this purpose, f_n is increased to 29.6 Hz by multiplying the original tire stiffness by a factor 10 and the responses are determined for all incidental road excitations for $V = 63$ km/h.

For the scraped road and the well, only an excess of the constraint on the tire force occurs for the 'best' passive vehicle model and the semi-active vehicle models, both for $f_n = 9.7$ Hz and for $f_n = 29.6$ Hz. Figure 3.6 shows for each of these road surfaces the percentage tire lift-off time of the semi-active system with respect to the tire lift-off time of the 'best' passive system for $f_n = 9.7$ Hz for controllers with different subinterval lengths Δh_i and $s\Delta h_i = \Delta h_i$. The same is shown for the systems with $f_n = 29.6$ Hz. Figure 3.6 shows that the allowable switching frequency f_s of the semi-active system controller is close to or higher than f_n if a shorter tire lift-off time than for the 'best' passive system is required. Semi-active systems with $f_s \ll f_n$ have the same performance as the 'best' passive system or worse. Also for the other incidental road excitations, an improved performance of the semi-active system with respect to

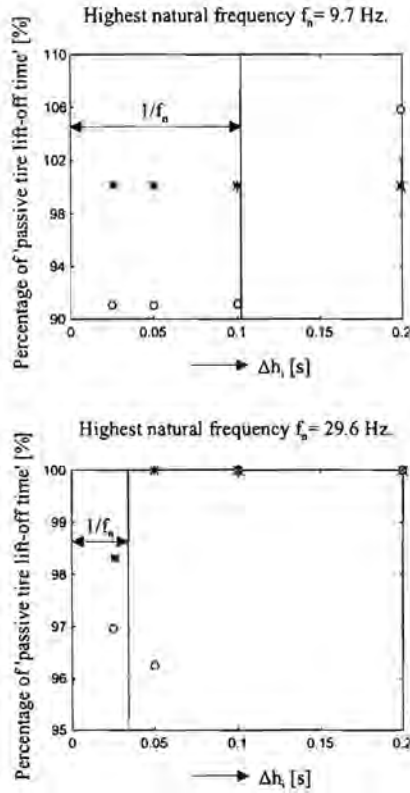


Figure 3.6: Percentage tire lift-off time of the semi-active system with respect to the tire lift-off time of the 'best' passive system for the scraped road and for the well. (*: semi-active system for the well; O: semi-active system for the scraped road)

the 'best' passive system is observed only for systems with f_s close to or higher than f_n . This is the case for the controllers 1^{aa} , 2^{aa} and 3^{aa} . However, CR is much higher for controller 1^{aa} than for the controllers 2^{aa} and 3^{aa} whereas f_s of controller 3^{aa} is only marginally higher than f_n . Therefore, controller 2^{aa} with $\Delta h_i = 0.050$ s, *i.e.* $f_s \approx 2f_n$, seems the most suitable one.

A smaller Δh_i might be desirable if the absolute locations of the switching time points with respect to the road excitation are important for a high performance of the system. A controller with a smaller Δh_i provides more switching time points and is in advantage then. It might be true that the absolute locations of the switching time points of controller 2^{aa} are fortunately chosen for the investigated road surfaces and that the performance of controller 2^{aa} decreases much if the position of the obstacles is slightly shifted. This means, for example, that the performance of the semi-active system with controller 2^{aa} at a forward velocity of 63 km/h might decrease much if at

$t' = 0$ s the obstacles are 0.025 s further away than in the previous simulations. This possible problem does not occur for the semi-active system with controller 1^{aa} because the state of this system after the application of one damper setting coincides with the original state (assuming static equilibrium for the system at $t' = 0$ s and a flat road surface for the first 0.025 s). The latter is shown in Figure 3.7. The performance of the semi-active system with controller 2^{aa} at a velocity of 63 km/h is therefore determined for all incidental road excitations, where the obstacles are at $t' = 0$ s, 0.025 s further away from the semi-active system than in the previous simulations. With respect to the original situation, the performance quantities remain unchanged for the scraped road, the well and the wave, whereas the performance increases with 2 % and decreases with 10 % for, respectively the standard brick and the traffic hump. So, using controller 1^{aa} instead of controller 2^{aa} to have more switching opportunities seems useful for some of the road excitations. However, the CR strongly increases while the performance for most of the road excitations remains unchanged by using $\Delta h_i = 0.025$ s instead of $\Delta h_i = 0.050$ s. Therefore, it is decided to use $\Delta h_i = 0.050$ s.

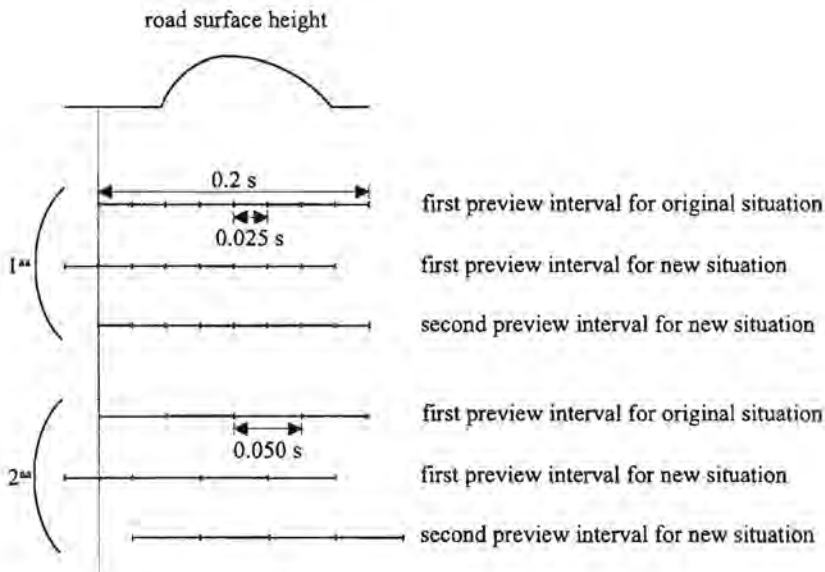


Figure 3.7: The original and the new situation for the semi-active system with controller 1^{aa} respectively controller 2^{aa}

3.5.2 Application interval length $s\Delta h_i$

In this section the influence of the application interval length $s\Delta h_i$ on the performance is investigated for $V = 63$ km/h ($t_p = 0.2$ s) and $\Delta h_i = 0.050$ s. The investigated values for $s\Delta h_i$ are 0.050 s, 0.100 s, 0.150 s and 0.200 s. The road surface is supposed to be known as a continuous function of time over the preview interval and the responses of the controller internal model are determined with a variable-order variable-step Adams method and a sample period $\Delta h_c = 0.0001$ s.

The semi-active system performance for the wave is given in Table 3.10 for controllers with different application times. The performance decreases considerably if $s\Delta h_i > 0.100$ s. For the standard brick, the scraped road, the well and the traffic

Table 3.10: Performance for the wave of the DCC controlled semi-active system with $\Delta h_i = 0.050$ s and different $s\Delta h_i$.

Wave	Δh_i [s]	$s\Delta h_i$ [s]	$\max \ddot{q}_{cr} $ [m/s ²]	tire lift-off [s]	$\max \delta^u$ [m]	$\max \delta^l$ [m]
controller 2 ^{aa}	0.050	0.050	14.43	0.000	0.00	0.02
controller 2 ^{ba}	0.050	0.100	14.48	0.000	0.00	0.02
controller 2 ^{ca}	0.050	0.150	15.72	0.000	0.01	0.02
controller 2 ^{da}	0.050	0.200	16.94	0.000	0.02	0.03

hump, the semi-active system performance remains unchanged if $s\Delta h_i$ increases from 0.050 s to 0.200 s. For the first three road surfaces, this might be due to the fact that the first preview interval is the same for the different application times and that in this preview interval the controller perceives all parts of the response which might influence the performance quantities.

To investigate the behavior for a less ideal situation, the simulation with a forward velocity of 63 km/h is repeated for the well, where at $t' = 0$ s the well is 0.095 s further away from the semi-active system than in the previous simulation. Now, the controller does not perceive the whole performance determining part of the response in the first preview interval. This is shown in Figure 3.8, which gives the simulation results of the semi-active system with controller 2^{ca} for two situations. The figures at the left and at the right side show the results for the original simulation, respectively for the situation where the well is 0.095 s shifted in time. The results of the semi-active system with different controllers for this shifted road surface are summarized in Table 3.11. This table shows that for the well the performance of the DCC controlled semi-active system may decrease considerably if $s\Delta h_i > 0.100$ s. The critical length for $s\Delta h_i$ in the range (0.100 s, 0.150 s] is unknown. Although, according to the previous results,

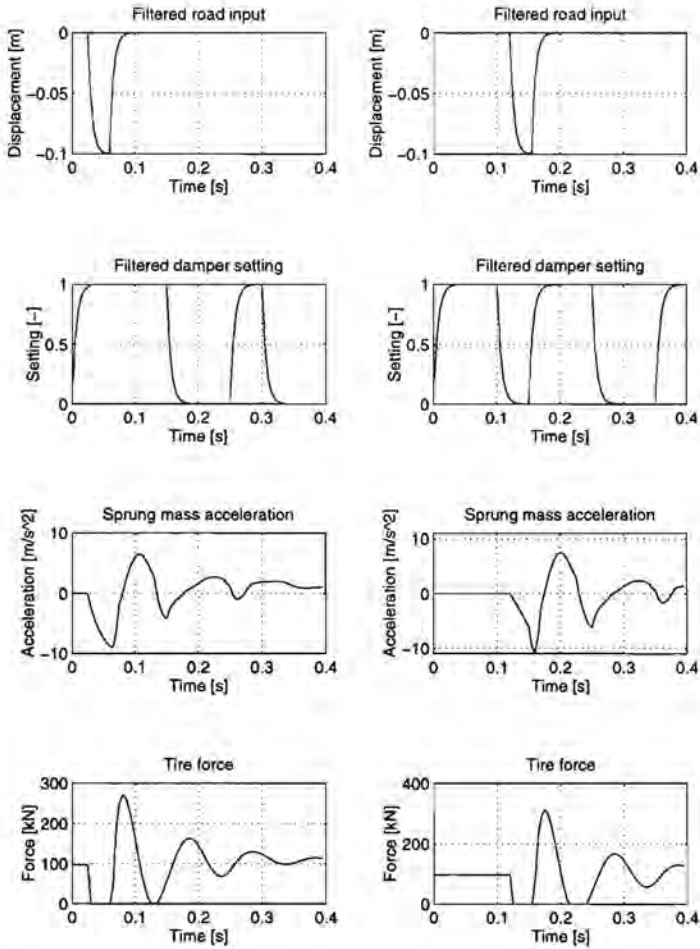


Figure 3.8: Simulation results of the semi-active system with controller 2^{ca} for the original situation (left figures) and the situation where at $t' = 0$ s the well is 0.095 s further away than in the original situation (right figures)

$s\Delta h_i = 0.100$ s might be acceptable, it is decided to use $s\Delta h_i = 0.050$ s in order to have a safety margin.

Table 3.11: Performance for the well of the DCC controlled semi-active system with $\Delta h_i = 0.050$ s and different $s\Delta h_i$, if the well is, at $t' = 0$ s, 0.095 s further away than in the original simulation ($V = 63$ km/h).

Well	Δh_i [s]	$s\Delta h_i$ [s]	$\max \ddot{q}_{cr} $ [m/s ²]	tire lift-off [s]	$\max \delta^u$ [m]	$\max \delta^l$ [m]
controller 2 ^{aa}	0.050	0.050	9.12	0.044	0.00	0.00
controller 2 ^{ba}	0.050	0.100	9.12	0.044	0.00	0.00
controller 2 ^{ca}	0.050	0.150	10.90	0.065	0.00	0.00
controller 2 ^{da}	0.050	0.200	7.74	0.079	0.00	0.00

3.5.3 Sample interval length Δh_c and integration routine

The value for CR reduces if the sample period Δh_c is increased and/or if a simpler integration routine is used. This section describes the determination of the maximum allowable Δh_c and the selection of a simple integration routine for which the performance of the controller with $\Delta h_i = 0.050$ s and $s\Delta h_i = \Delta h_i$ is maximum.

First the maximum allowable Δh_c for the evaluation of the performance index is determined. The road surface is supposed to be known as a continuous function of time over the preview interval and the controller internal model response is calculated with a variable-order variable-step Adams method at discrete times in the preview interval with a sample period 0.0001 s. The investigated values of Δh_c are in the range of 0.0001 s to 0.0500 s. The velocity V of the vehicle again is 63 km/h.

The semi-active system performance for the standard brick and for the wave is the same for all investigated Δh_c if $\Delta h_i = 0.050$ s and $s\Delta h_i = \Delta h_i$ whereas for the traffic hump only the performance for $\Delta h_c = 0.0500$ s differs from the performance for the other sample intervals Δh_c . For the scraped road and the well, the performance of the semi-active system decreases if $\Delta h_c > 0.0050$ s. For the well, this is shown in Table 3.12. According to these results, the maximum allowed length of Δh_c for the evaluation of the performance index seems to be 0.0050 s.

Next, the explicit Euler integration routine is used to determine the responses of the controller internal model for the controllers 2^{aa} to 2^{ad}. For each controller, the stepsize of the integration routine is taken equal to Δh_c . Again, $V = 63$ km/h and the simulation model responses are determined with a variable-order variable-step Adams method with a sample interval of 0.0001 s.

Table 3.12: Performance for the well of the DCC controlled semi-active system with $\Delta h_i = 0.050$ s, $s\Delta h_i = \Delta h_i$ and different Δh_c .

Well	Δh_i [s]	$s\Delta h_i$ [s]	Δh_c [s]	$\max \ddot{q}_{cr} $ [m/s ²]	tire lift-off [s]	$\max \delta^u$ [m]	$\max \delta^l$ [m]	CR [-]
controller 2 ^{aa}	0.050	0.050	0.0001	9.12	0.044	0.00	0.00	1.58
controller 2 ^{ab}	0.050	0.050	0.0005	9.12	0.044	0.00	0.00	0.47
controller 2 ^{ac}	0.050	0.050	0.0010	9.12	0.044	0.00	0.00	0.28
controller 2 ^{ad}	0.050	0.050	0.0050	9.12	0.044	0.00	0.00	0.11
controller 2 ^{ae}	0.050	0.050	0.0100	9.12	0.054	0.00	0.00	0.09
controller 2 ^{af}	0.050	0.050	0.0500	10.88	0.067	0.00	0.00	0.10

The semi-active system performance for the standard brick and for the well is the same for $\Delta h_c = 0.0001$ s through $\Delta h_c = 0.0050$ s whereas for the traffic hump, the scraped road and the wave only the performance for $\Delta h_c = 0.0050$ s differs from the performance for the other sample lengths Δh_c , if $\Delta h_i = 0.050$ s and $s\Delta h_i = \Delta h_i$. For the scraped road, this is shown in Table 3.13. Previously it is shown that the performance is independent of the sample interval length Δh_c if $\Delta h_c \leq 0.0050$ s and a comprehensive integration routine is used to determine the controller model response. This means that the performance decrease for $\Delta h_c = 0.0050$ s is caused by the integration routine. This is likely, as a stepsize of 0.0050 s is larger than the smallest time constant in the linearized two-DOF model (linearized with respect to the static equilibrium position), which is about 0.0045 s.

Table 3.13: Performance for the scraped road of the DCC controlled semi-active system with $\Delta h_i = 0.050$ s, $s\Delta h_i = \Delta h_i$, and different Δh_c , using the explicit Euler routine for the controller internal model.

Scraped road	Δh_i [s]	$s\Delta h_i$ [s]	Δh_c [s]	$\max \ddot{q}_{cr} $ [m/s ²]	tire lift-off [s]	$\max \delta^u$ [m]	$\max \delta^l$ [m]	CR [-]
controller 2 ^{aae}	0.050	0.050	0.0001	8.51	0.043	0.00	0.00	0.25
controller 2 ^{abe}	0.050	0.050	0.0005	8.51	0.043	0.00	0.00	0.07
controller 2 ^{ace}	0.050	0.050	0.0010	8.51	0.043	0.00	0.00	0.05
controller 2 ^{ade}	0.050	0.050	0.0050	11.23	0.045	0.00	0.00	0.03

The CR for the controller with the variable-order variable-step Adams algorithm and $\Delta h_c = 0.0050$ s is higher than the CR for the controller with the explicit Euler integration algorithm and $\Delta h_c = 0.0010$ s (= stepsize). The latter is therefore chosen for application in the following sections. However, also the explicit Euler integration algorithm with stepsize 0.0010 s and $\Delta h_c = 0.0050$ s might be allowed to evaluate the controller internal model response, as the system performance seems to be independent of Δh_c if $\Delta h_c \leq 0.0050$ s.

3.5.4 Conclusions

A two-DOF vehicle model with a DCC controlled two-level damper is used to determine suitable values for the subinterval length Δh_i , the application interval length $s\Delta h_i$ and the sample interval length Δh_c for the response of the controller internal model. Furthermore, an integration algorithm for the determination of the controller internal model response is established. The following conclusions can be drawn with respect to these aspects:

- A better performance for the semi-active system than for the 'best' passive system is only obtained for subinterval lengths smaller than or at least close to the smallest natural oscillation time of the linearized two-DOF model. Therefore, the length of the subintervals Δh_i is chosen equal to 0.050 s which is somewhat smaller than the smallest natural oscillation time of the linearized two-DOF model.
- The performance of the semi-active system decreases considerably if the optimum damper setting combination is applied for more than two subintervals. It is decided to apply only the first damper setting, *i.e.* $s\Delta h_i = \Delta h_i$, in order to be at the safe side.
- For determining the performance for a damper setting combination over the preview interval, it seems sufficient to evaluate the response of the two-DOF controller internal model at a sample interval length $\Delta h_c = 0.005$ s.
- The responses of the controller internal model are properly determined with an explicit Euler integration routine with a stepsize of 0.001 s. This algorithm with $\Delta h_c = 0.001$ s is about two times faster than a variable-order variable-step Adams routine with $\Delta h_c = 0.005$ s. Although even $\Delta h_c = 0.005$ s might be sufficient for the explicit Euler integration algorithm with stepsize 0.001 s, it has been decided to use the explicit Euler integration algorithm with $\Delta h_c = 0.001$ s.

3.6 Concept choice

In this section, the performances and the computational burden for the system with conventional passive damper, the semi-active system with the controlled two-level damper and the semi-active system with the controlled continuously variable damper are compared and one of the semi-active concepts is chosen for further investigation. The DCC is used to control the two-level damper and the SQPCO and SQPCE are used to control the continuously variable damper. The DCC uses the control objective of Section 3.2 whereas the SQPCO and SQPCE use the adapted versions of this objective that were discussed in Section 3.4. The subinterval length Δh_i , the application length $s\Delta h_i$, the sample interval length of the controller internal model response, Δh_c , and the integration algorithm are as proposed in the previous section, also for the controllers based on the SQP method.

Tables 3.14 to 3.18 show the performances on the incidental road surfaces of the mentioned semi-active two-DOF systems and the 'passive medium' two-DOF system (PASM). The latter represents the conventional passive vehicle with the best average performance for the road surfaces used by a tractor-semitrailer. As this is the only passive system used in this section, it is simply called passive system in the remainder of this section. For the semi-active systems, also the reduction of the performance values with respect to the performance values for the 'passive medium' system is given. On each of the road surfaces, the prescribed forward vehicle velocity according to Chapter 2 is used. The passive and the controlled vehicle responses are determined with a variable-order variable-step Adams method with a sample interval of 0.0001 s. These responses are used to determine a large number of the criterion values that are explained in Chapter 2. The weighted sprung mass acceleration $\ddot{q}_{cr,w}$ in Tables 3.14 to 3.18 is derived by weighting the sprung mass acceleration according to the ISO 2631 standard [20] for vertical accelerations. The sprung mass jerk, *i.e.* $\ddot{\ddot{q}}_{cr}$, is determined by numerical differentiation of the sprung mass acceleration using the following central difference scheme

$$\ddot{\ddot{q}}_{cr}(t) = \frac{1}{10\Delta h_c} (-2\ddot{q}_{cr}(t-2\Delta h_c) - \ddot{q}_{cr}(t-\Delta h_c) + \ddot{q}_{cr}(t+\Delta h_c) + 2\ddot{q}_{cr}(t+2\Delta h_c)). \quad (3.18)$$

General

Before discussing results for specific road excitations, some general remarks are given. First, the comfort criteria are considered.

For the road surfaces where the controllers focus entirely on a reduction of the maximum absolute sprung mass acceleration, *i.e.* for the road surfaces where no constraint violations (tend to) occur, the values of all comfort quantities except the jerk are lower

for the semi-active systems than for the passive system. The increased values for the jerk are often caused by the fact that a reduction of the maximum absolute sprung mass acceleration sometimes requires a switching of the damper for a non-zero relative velocity over the damper, which results in high values for the jerk. Therefore, it seems important to change the minimization of the maximum absolute sprung mass acceleration in the control objective into the minimization of the maximum absolute sprung mass jerk, if the jerk turns out to be the most important comfort criterion. It appears furthermore that the values for the quantitative comfort criteria which depend on the complete time response of the vehicle model (RMS and VD values) are lower for the systems with continuously variable damper than for the system with two-level damper, if the controllers focus entirely on a reduction of the maximum absolute sprung mass acceleration. Besides, in this case the continuously variable damper with SQPCE gives lower values for these quantities than the continuously variable damper with SQPCO. These differences in performance for the SQPCO system and the SQPCE system show that the chosen description of the control objective is indeed of importance for the performance of the SQP controlled semi-active vehicle. If the bounds on the suspension deflection are reached or if tire lift-off occurs and the controllers can not focus on a reduction of the maximum absolute sprung mass acceleration only, then most of the quantitative comfort criteria are still lower for the semi-active systems than for the passive system, even if the maximum absolute sprung mass acceleration over the total simulation time is not reduced. The damping of the sprung mass displacement is judged qualitatively from the time plots of this displacement. The damping behavior is better for the semi-active system with an SQPC controller than for the semi-active system with a DCC controller. For all road surfaces, the damping behavior of the DCC system is worse than that of the passive system whereas the damping behavior of the SQPCE system is equal to or better than that of the passive system. For the scraped road and the well, this is shown in Figure 3.9.

The maximum discrepancy in performance between the passive system and the semi-active systems is found for the fatigue load. The PM number, a measure for the fatigue damage, is much lower for the semi-active systems than for the passive system for all road surfaces. This is due to the strong influence of large sprung mass accelerations on the PM number. Some of the large sprung mass accelerations are considerably lower for the semi-active system than for the passive system and consequently also the PM number is considerably lower for the semi-active system than for the passive system. So, the lifespan of the vehicle for the same road excitations seems to increase by using one of the semi-active suspensions instead of the passive suspension.

The road damage for the semi-active systems varies within a range of -37 to +69 % compared to the road damage for the passive system. So, the influence of the semi-active

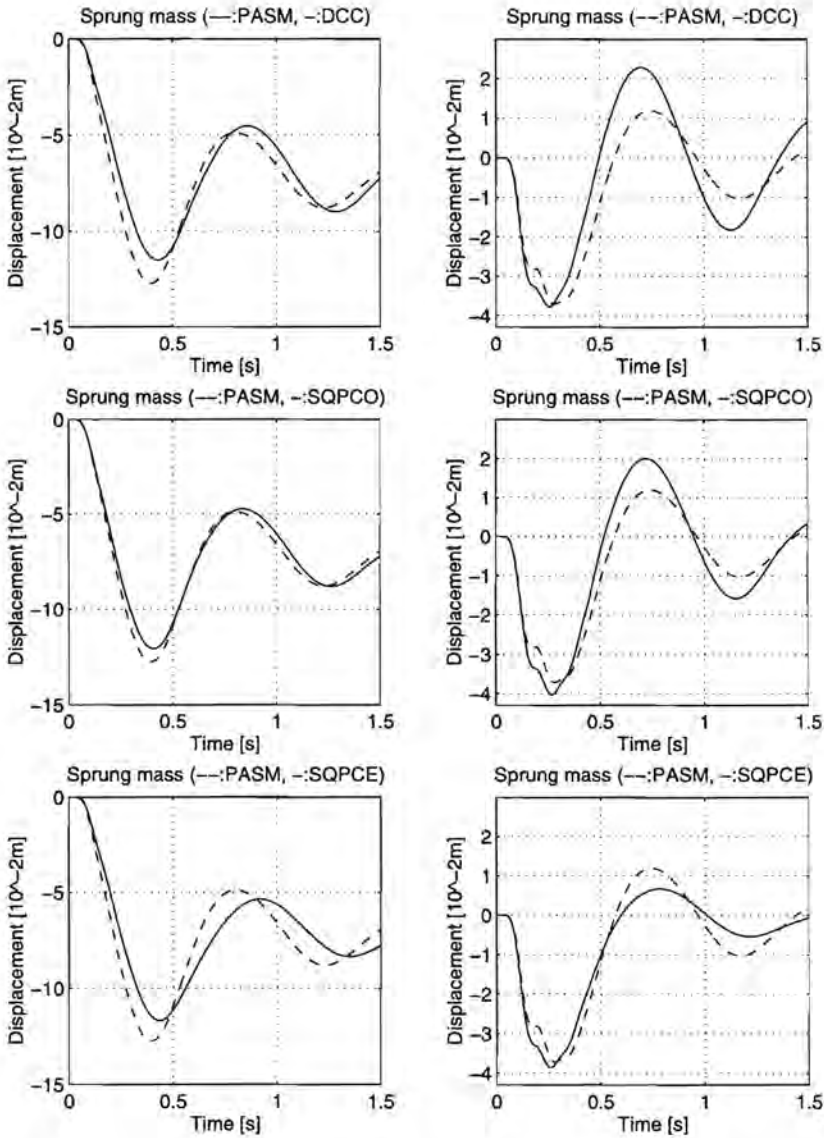


Figure 3.9: Sprung mass displacements of the passive system and the semi-active systems for the scraped road (left figures) and the well (right figures)

suspension on the road damage seems to be large.

The most conspicuous discrepancy between the DCC controlled system and the SQP controlled systems concerns the computational requirements. The computational requirements for the SQP controllers are more than 40 times higher than the computational requirement for the DCC controller.

Standard brick

For the standard brick, the bounds on the tire force and on the suspension deflection are not reached. Hence, the controllers focus on a reduction of the maximum absolute sprung mass acceleration. The DCC system gives the smallest reduction and the SQPCO system gives the largest reduction of this acceleration whereas the SQPCE system gives the largest reduction of all other comfort quantities, compared to the values for the passive system. All comfort quantities, except the jerk, are 18 to 32 % lower for the semi-active systems than for the passive system. The jerk is higher for some of the semi-active systems than for the passive system: 53 % for the DCC system and 32 % for the SQPCO system. Figure 3.10 shows the time plots of the sprung mass acceleration and the suspension deflection for the passive system and for the semi-active systems.

Table 3.14: Performance and CR for the standard brick of the vehicle suspension systems.

aspect	criterion	unit	PASM	DCC	SQPCO	SQPCE
comfort	max $ \ddot{q}_{cr} $	[m/s ²]	3.09	2.28 (-26%)	2.09 (-32%)	2.21 (-28%)
	max $ \ddot{q}_{cr,w} $	[m/s ²]	2.36	1.69 (-28%)	1.69 (-28%)	1.69 (-28%)
	RMS \ddot{q}_{cr}	[m/s ²]	0.51	0.42 (-18%)	0.41 (-20%)	0.40 (-22%)
	RMS $\ddot{q}_{cr,w}$	[m/s ²]	0.40	0.33 (-18%)	0.33 (-18%)	0.32 (-20%)
	VD \ddot{q}_{cr}	[m/s ^{1.75}]	1.18	0.91 (-23%)	0.88 (-25%)	0.85 (-28%)
	VD $\ddot{q}_{cr,w}$	[m/s ^{1.75}]	0.91	0.70 (-23%)	0.69 (-24%)	0.66 (-27%)
load	max $ \dot{q}_{cr} $	[m/s ³]	352	537 (+53%)	464 (+32%)	260 (-26%)
	max $ \ddot{q}_{cr} $	[m/s ²]	3.09	2.28 (-26%)	2.09 (-32%)	2.21 (-28%)
deflection	PM \ddot{q}_{cr}	[10 ⁻² -]	0.06	0.03 (-50%)	0.02 (-67%)	0.01 (-83%)
	nr bound excesses	[-]	0	0	0	0
handling	RMS $q_{cr} - q_{ar}$	[10 ⁻² m]	0.45	0.34 (-24%)	0.34 (-24%)	0.44 (-2%)
	tire lift-off	[s]	0.000	0.000 (0%)	0.000 (0%)	0.000 (0%)
damage	<75% stat tire force	[s]	0.038	0.054 (+42%)	0.058 (+53%)	0.066 (+74%)
	RMS dyn tire force	[10 ³ N]	14.58	15.27 (+5%)	15.41 (+6%)	16.75 (+15%)
comp time	η_{max}	[-]	85.40	85.57 (0%)	85.56 (0%)	85.54 (0%)
	CR	[-]		0.03	5.07	22.39

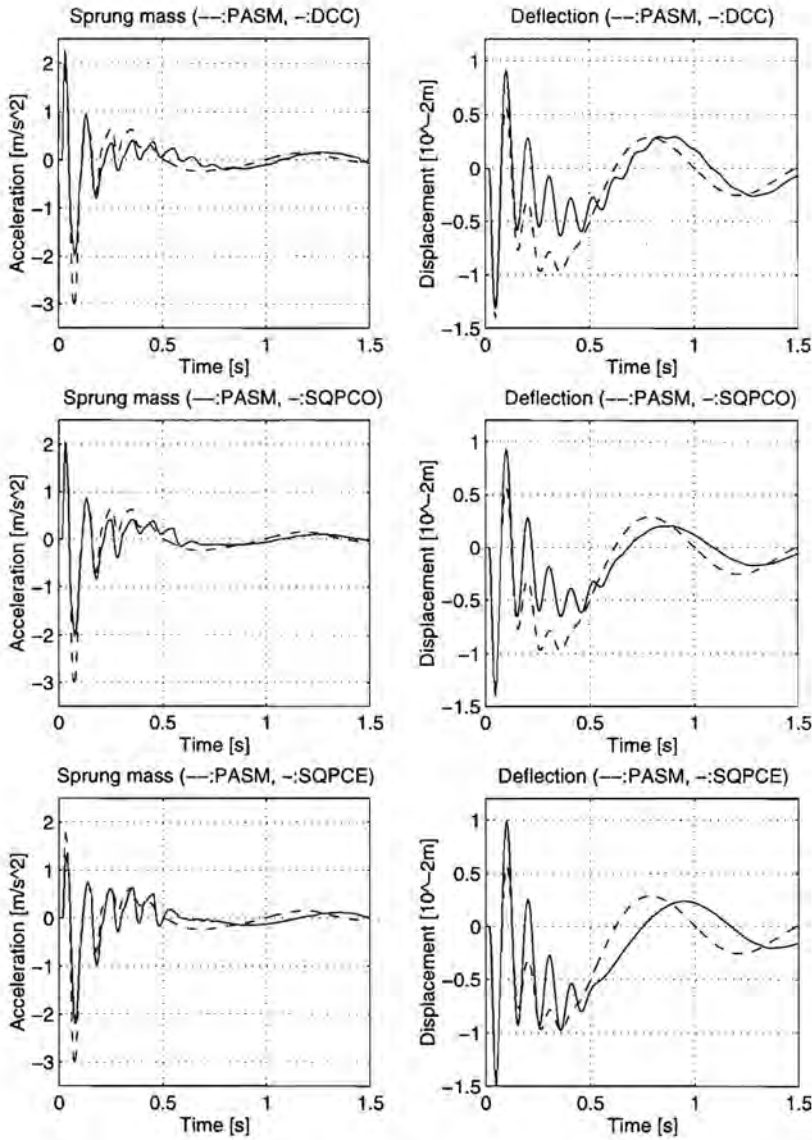


Figure 3.10: Sprung mass acceleration and suspension deflection of the passive system and the semi-active systems for the standard brick

This figure shows that the DCC and SQPCO systems reduce the maximum absolute acceleration at the expense of an increased other high acceleration peak whereas this is not the case for the SQPCE system.

Often, improved comfort is at the expense of an increased suspension working space. The RMS values of the suspension deflection suggest a reduced suspension working space for the systems with the best comfort, *i.e.* the semi-active systems. However, these RMS values of the suspension deflection are misleading. Figure 3.10 shows that indeed an increased suspension working space is required for the semi-active systems, compared to the passive system. The minimum increase in suspension working space is obtained for the DCC system (14 %) whereas the maximum increase in suspension working space is obtained for the SQPCE system (27 %).

The times for which less than 75 % of the static tire force is available and the RMS values of the dynamic tire force are higher for the semi-active systems than for the passive system. The semi-active system with the smallest values for most of the comfort quantities shows the largest values for the handling quantities and the other way round. Therefore, improved comfort seems to be at the expense of a reduced handling capability.

The road damage on an incidental road surface is determined by $\eta_{max} \cdot (F_{tire,stat})^4$ (see Section 2.4). However, the relative road damage of the passive vehicle model and the semi-active vehicle models is completely determined by the road damage factor η_{max} , because $F_{tire,stat}$ is the same for all models. Table 3.14 shows a slightly higher road damage for the semi-active systems than for the passive system, irrespective of the used controller.

Traffic hump

For the traffic hump, the bounds on the tire force and the suspension deflection are not reached, so the controllers focus on a reduction of the maximum absolute sprung mass acceleration. The DCC system gives the largest reduction and the SQPC systems give the smallest reduction of this acceleration, compared to the value for the passive system. The largest reduction of all other comfort quantities, except the jerk, is obtained for the SQPCE system. All comfort quantities, except the jerk, are 14 to 28 % lower for the semi-active systems than for the passive system. The jerk is higher for all semi-active systems than for the passive system: 140 % for the DCC system, 52 % for the SQPCO system and 57 % for the SQPCE system. Figure 3.11 shows the time plots of the sprung mass acceleration and the suspension deflection for the passive system and for the semi-active systems. This figure shows similar acceleration signals for the investigated semi-active systems. Not only the maximum absolute acceleration but also

Table 3.15: Performance and CR for the traffic hump of the vehicle suspension systems.

aspect	criterion	unit	PASM	DCC	SQPCO	SQPCE
comfort	max $ \ddot{q}_{cr} $	[m/s ²]	8.67	6.28 (-28%)	6.29 (-27%)	6.34 (-27%)
	max $ \ddot{q}_{cr,w} $	[m/s ²]	5.57	4.71 (-15%)	4.71 (-15%)	4.56 (-18%)
	RMS \ddot{q}_{cr}	[m/s ²]	3.62	3.03 (-16%)	2.96 (-18%)	2.86 (-21%)
	RMS $\ddot{q}_{cr,w}$	[m/s ²]	2.29	1.95 (-15%)	1.93 (-16%)	1.86 (-19%)
	VD \ddot{q}_{cr}	[m/s ^{1.75}]	5.14	4.15 (-19%)	4.13 (-20%)	4.04 (-21%)
	VD $ \ddot{q}_{cr,w} $	[m/s ^{1.75}]	3.20	2.74 (-14%)	2.73 (-15%)	2.64 (-18%)
	max $ \ddot{q}_{cr} $	[m/s ³]	153	367 (+140%)	232 (+52%)	240 (+57%)
load	max $ \ddot{q}_{cr} $	[m/s ²]	8.67	6.28 (-28%)	6.29 (-27%)	6.34 (-27%)
	PM \ddot{q}_{cr}	[10 ⁻² -]	27.51	8.19 (-70%)	8.11 (-71%)	8.62 (-69%)
deflection	nr bound excesses	[-]	0	0	0	0
	RMS $q_{cr} - q_{ar}$	[10 ⁻² m]	4.76	4.34 (-9%)	4.27 (-10%)	4.25 (-11%)
handling	tire lift-off	[s]	0.000	0.000 (0%)	0.000 (0%)	0.000 (0%)
	<75% stat tire force	[s]	0.280	0.284 (+1%)	0.256 (-9%)	0.247 (-12%)
	RMS dyn tire force	[10 ³ N]	33.03	27.49 (-17%)	26.80 (-19%)	26.06 (-21%)
damage	η_{max}	[-]	7.99	7.22 (-10%)	7.22 (-10%)	7.21 (-10%)
comp time	CR	[-]		7.37	319.09	988.40

other high acceleration peaks are lower for the semi-active systems than for the passive system.

For the traffic hump, the reduced values for the comfort quantities (except for the jerk) are not at the expense of an increased suspension working space: the RMS values of the suspension deflection are lower for the semi-active systems than for the passive system and, as the time plots of the suspension deflection in Figure 3.11 show, also the suspension working space for the semi-active systems is smaller than for the passive system. The required suspension working space is the same for all semi-active systems.

Of the semi-active systems, the DCC system gives the smallest reduction of the RMS value for the dynamic tire force and a slight increase of the time for which less than 75 % of the static tire force is available, compared to the passive system. The SQPC systems give larger reductions of the RMS value for the dynamic tire force and reductions of the time for which less than 75 % of the static tire force is available, compared to the passive system. So, the handling capability is certainly improved for the SQPC systems and perhaps improved for the DCC system.

The expected road damage, expressed by the road damage factor η_{max} , is about 10 % lower for the semi-active systems than for the passive system.

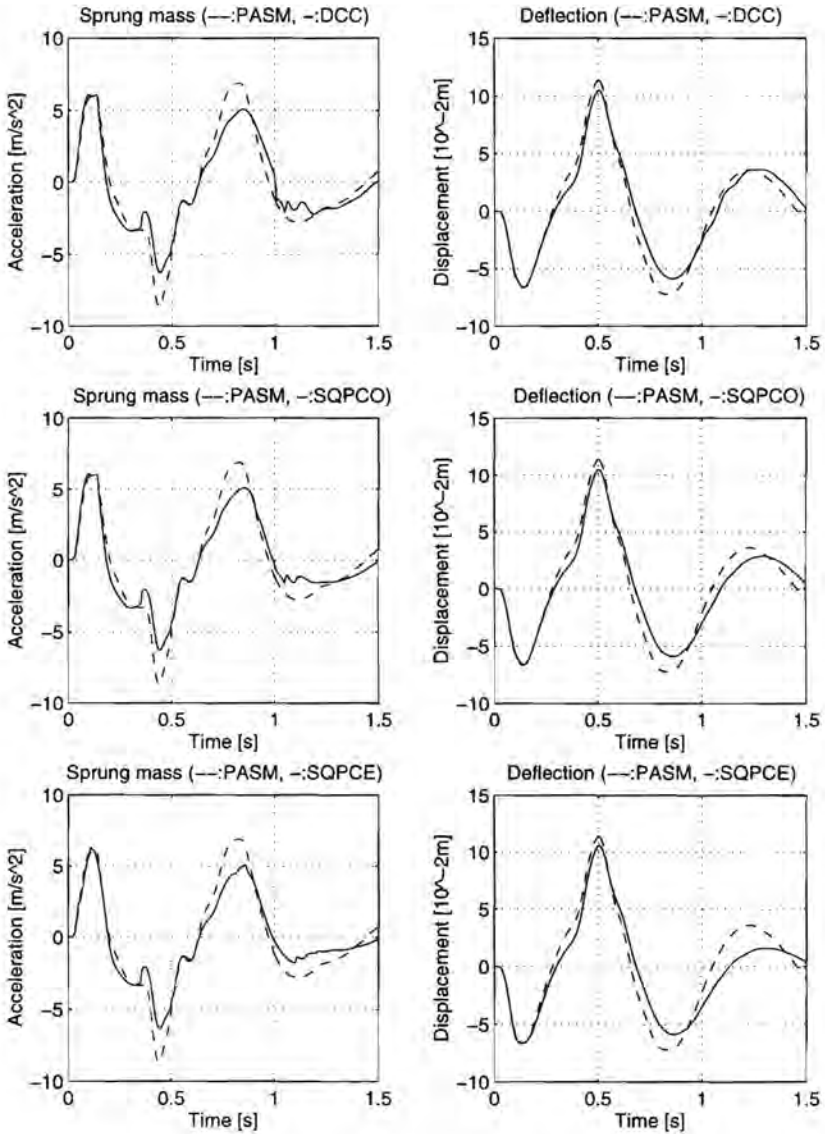


Figure 3.11: Sprung mass acceleration and suspension deflection of the passive system and the semi-active systems for the traffic hump.

Scraped road

For the scraped road, there is an excess of the bound on the tire force, whereas the bounds on the suspension deflection are not reached. Hence, the controllers of the semi-active systems focus on a reduction of the tire lift-off time. The tire lift-off times for the DCC system and the SQPCE system are smaller whereas the tire lift-off time of the SQPCO system is somewhat larger than that of the passive system (see also Figure 3.12). This larger tire lift-off time for the SQPCO system is probably caused by the fact that the SQP algorithm searches an optimum which is not necessarily the global optimum for the stated problem. The time for which less than 75 % of the static tire force is available and the RMS value of the dynamic tire force, give the same indication of the handling capability as the tire lift-off time, *i.e.* these quantities increase (decrease) if the tire lift-off time increases (decreases).

Table 3.16: Performance and CR for the scraped road of the vehicle suspension systems.

aspect	criterion	unit	PASM	DCC	SQPCO	SQPCE
comfort	max $ \ddot{q}_{cr} $	[m/s ²]	9.48	8.51 (-10%)	8.01 (-16%)	8.51 (-10%)
	max $ \ddot{q}_{cr,w} $	[m/s ²]	7.36	6.48 (-12%)	6.02 (-18%)	6.48 (-12%)
	RMS \ddot{q}_{cr}	[m/s ²]	2.18	1.87 (-14%)	1.97 (-10%)	1.76 (-19%)
	RMS $\ddot{q}_{cr,w}$	[m/s ²]	1.59	1.37 (-14%)	1.43 (-10%)	1.32 (-17%)
	VD \ddot{q}_{cr}	[m/s ^{1.75}]	4.03	3.47 (-14%)	3.47 (-14%)	3.46 (-14%)
	VD $\ddot{q}_{cr,w}$	[m/s ^{1.75}]	3.10	2.68 (-14%)	2.65 (-15%)	2.68 (-14%)
	max $ \dot{q}_{cr} $	[m/s ³]	499	384 (-23%)	605 (+21%)	384 (-23%)
load	max $ \ddot{q}_{cr} $	[m/s ²]	9.48	8.51 (-10%)	8.01 (-16%)	8.51 (-10%)
	PM \ddot{q}_{cr}	[10 ⁻² -]	9.45	3.99 (-58%)	3.93 (-58%)	4.42 (-53%)
deflection	nr bound excesses	[-]	0	0	0	0
	RMS $q_{cr} - q_{ar}$	[10 ⁻² m]	2.45	2.37 (-3%)	2.35 (-4%)	2.32 (-5%)
handling	tire lift-off	[s]	0.047	0.043 (-8%)	0.048 (+2%)	0.043 (-8%)
	<75% stat tire force	[s]	0.098	0.097 (-1%)	0.101 (+3%)	0.097 (-1%)
	RMS dyn tire force	[10 ³ N]	44.20	43.12 (-2%)	46.01 (+4%)	42.79 (-3%)
damage	η_{max}	[-]	9.12	15.37 (+69%)	15.06 (+65%)	15.37 (+69%)
comp time	CR	[-]		0.07	11.30	47.60

With respect to the comfort criteria, the SQPCO system shows the smallest values for the maximum absolute non-weighted and weighted acceleration and for the VD value of the weighted acceleration. The SQPCE system shows the smallest values for the other comfort quantities whereas, of the investigated semi-active systems, the SQPCO system shows the largest values for these other quantities. Figure 3.12 shows the time plots of

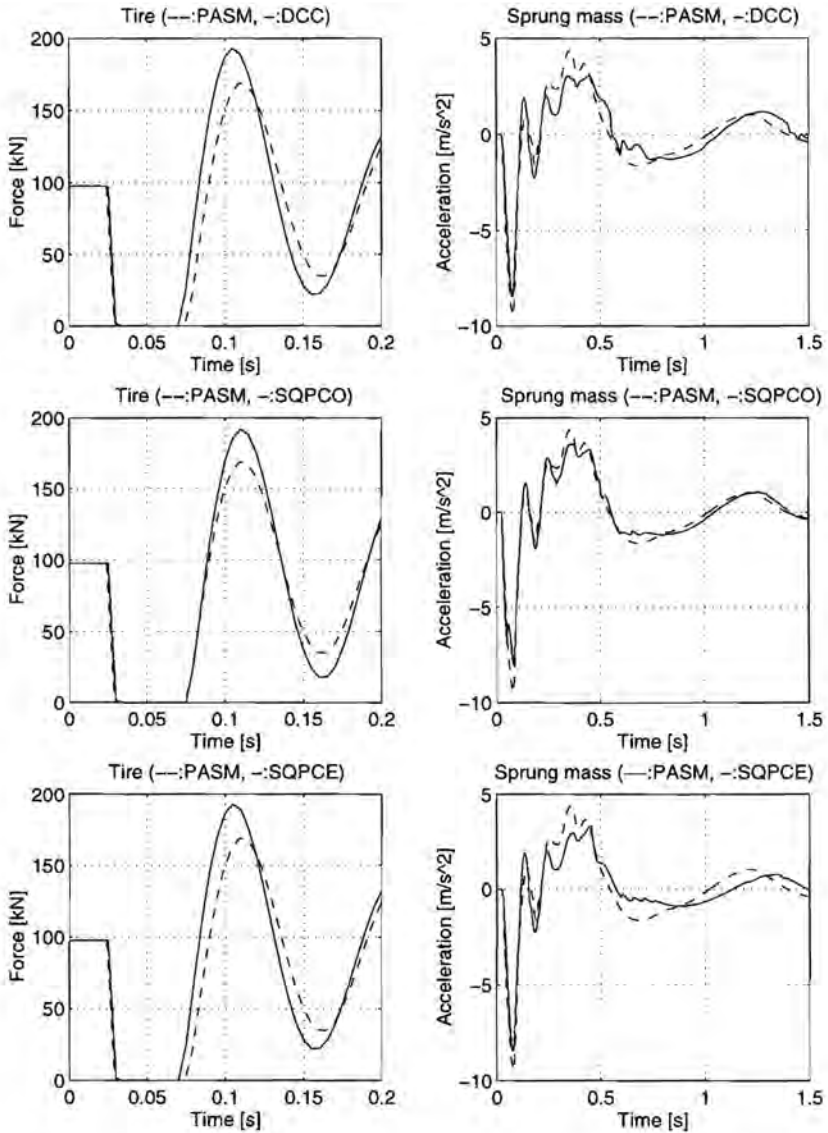


Figure 3.12: Tire force and sprung mass acceleration of the passive system and the semi-active systems for the scraped road

the sprung mass acceleration for the passive system and for the semi-active systems. This figure shows that not only the maximum absolute acceleration is lower for the semi-active systems than for the passive system but that also the other acceleration peaks at $t' = 0.35$ s and $t' = 0.65$ s are lower. The SQPCO system shows the smallest maximum absolute sprung mass acceleration. However, the peak at $t' = 0.35$ s is smallest for the DCC system whereas the peak at $t' = 0.65$ s is smallest for the SQPCE system.

The required suspension working space is not to the disadvantage of the improved comfort and the improved handling capability for the DCC system and SQPCE system. The RMS value of the suspension deflection is reduced whereas the differences between the maximum and the minimum suspension deflections are the same for the passive system and the semi-active systems.

Only the road damage is worse for all semi-active systems than for the passive system: the road damage factor η_{max} is more than 65 % higher for all semi-active systems than for the passive system.

Well

For the well, there are excesses of the bound on the tire force whereas the bounds on the suspension deflection are not reached, so the controllers for the semi-active system focus on a reduction of the tire lift-off time. The tire lift-off time is smaller for all semi-active systems than for the passive system. The time for which less than 75 % of the static tire force is available and the RMS value of the dynamic tire force for the SQPCE system and the RMS value of the dynamic tire force for the DCC system are lower whereas the remaining handling quantities are higher than for the passive system. So, compared to the passive system, the road-holding on the well is improved for the SQPCE system whereas the improvement of the road-holding on the well for the DCC and the SQPCO system is doubtful.

The SQPCO system, *i.e.* the semi-active system with the largest tire lift-off time, gives 2 to 15 % lower values for the comfort quantities than the passive system. For the other semi-active systems, most of the values for the comfort quantities which depend on the complete time response of the vehicle model (RMS and VD values) are lower whereas most of the values for the other comfort quantities are larger than for the passive system. Figure 3.13 shows the time plots for the tire force and the sprung mass acceleration of the passive system and the semi-active systems for the well. This figure shows for all systems a nearly equal first negative peak in the sprung mass acceleration. The first positive acceleration peak, which determines the maximum absolute sprung mass acceleration of the passive system, is reduced only for the SQPCO system whereas this peak is increased for the DCC system and the SQPCE system. However, these

Table 3.17: Performance and CR for the well of the vehicle suspension systems.

aspect	criterion	unit	PASM	DCC	SQPCO	SQPCE
comfort	max $ \ddot{q}_{cr} $	[m/s ²]	10.19	10.62 (+4%)	9.87 (-3%)	10.35 (+2%)
	max $ \ddot{q}_{cr,w} $	[m/s ²]	10.47	10.59 (+1%)	9.88 (-6%)	10.39 (-1%)
	RMS \ddot{q}_{cr}	[m/s ²]	2.53	2.49 (-2%)	2.49 (-2%)	2.41 (-5%)
	RMS $\ddot{q}_{cr,w}$	[m/s ²]	2.27	2.18 (-4%)	2.19 (-4%)	2.16 (-5%)
	VD \ddot{q}_{cr}	[m/s ^{1.75}]	4.95	4.96 (0%)	4.76 (-4%)	4.91 (-1%)
	VD $\ddot{q}_{cr,w}$	[m/s ^{1.75}]	4.62	4.58 (-1%)	4.42 (-4%)	4.54 (-2%)
load	max $ \ddot{q}_{cr} $	[m/s ³]	1300	1586 (+22%)	1099 (-15%)	1510 (+16%)
	max $ \ddot{q}_{cr} $	[m/s ²]	10.19	10.62 (+4%)	9.87 (-3%)	10.35 (+2%)
deflection	PM \ddot{q}_{cr}	[10 ⁻² -]	81.14	69.06 (-14%)	55.01 (-32%)	65.07 (-20%)
	nr bound excesses	[-]	0	0	0	0
	RMS $q_{cr} - q_{ar}$	[10 ⁻² m]	2.08	2.00 (-4%)	2.20 (+6%)	1.85 (-11%)
handling	tire lift-off	[s]	0.101	0.087 (-14%)	0.099 (-2%)	0.088 (-13%)
	<75% stat tire force	[s]	0.144	0.156 (+8%)	0.166 (+15%)	0.140 (-3%)
	RMS dyn tire force	[10 ³ N]	78.41	74.72 (-5%)	80.04 (+2%)	74.62 (-5%)
damage	η_{max}	[-]	253.75	169.10 (-33%)	204.54 (-19%)	171.18 (-33%)
comp time	CR	[-]		0.13	39.48	166.99

increased peak values are acceptable as Figure 3.13 shows that the systems are focusing on a reduction of the tire lift-off time at the time the peak occurs. The second negative acceleration peak is lower for the DCC system and the SQPCE system than for the SQPCO system.

For the DCC system and the SQPCE system, not only the RMS value of the suspension deflection is lower but also the difference between the maximum and the minimum suspension deflection is lower than for the passive system. For the SQPCO system, the RMS value of the suspension deflection is higher than for the passive system whereas the distance between the maximum and the minimum suspension deflection is the same as for the passive system. So, the required suspension working space for each semi-active system is equal to or lower than that for the passive system.

For all semi-active systems, the road damage is considerably lower than for the passive system.

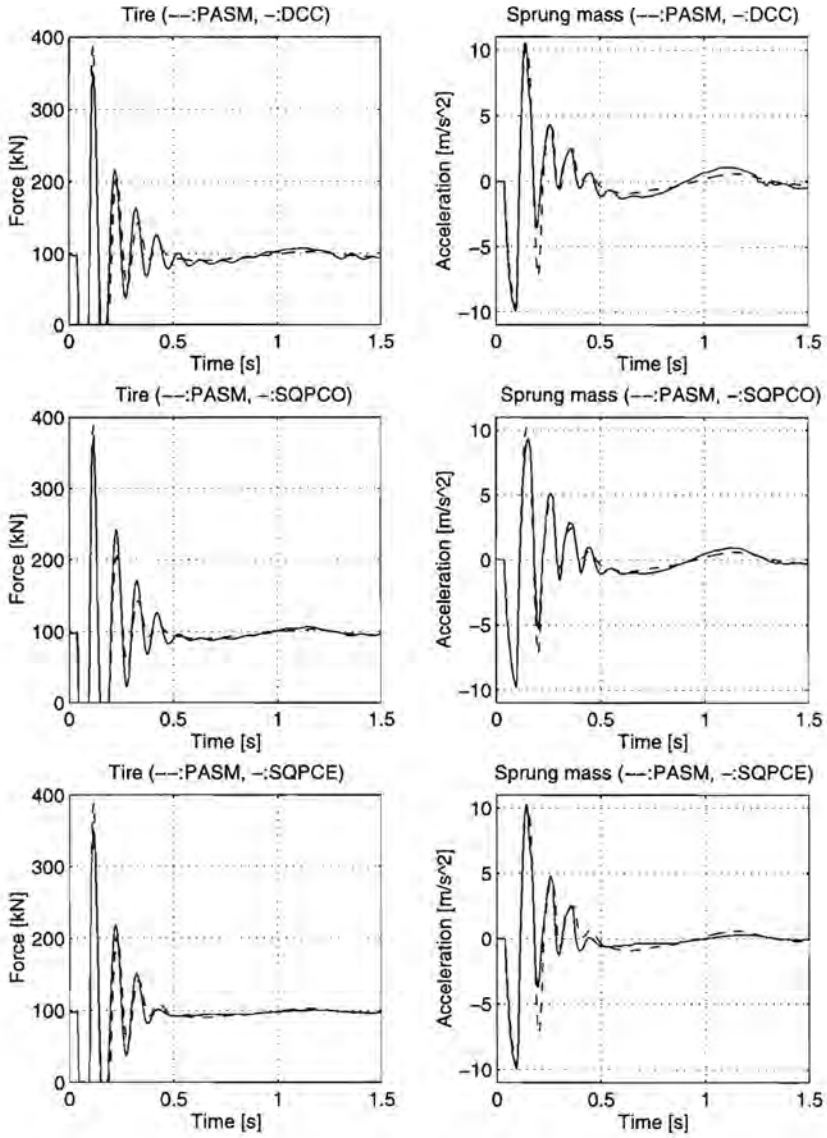


Figure 3.13: Tire force and sprung mass acceleration of the passive system and the semi-active systems for the well

Wave

For the wave, excesses of the bounds on the suspension deflection and the bound on the tire force occur for both the passive system and the semi-active systems. The semi-active systems therefore focus on a reduction of these excesses, however without great success: not even the number of excesses of the bounds on the suspension deflection is lower for one of these systems than for the passive system. The excesses of the bound

Table 3.18: Performance and CR for the wave of the vehicle suspension systems.

aspect	criterion	unit	PASM	DCC	SQPCO	SQPCE
comfort	$\max \ddot{q}_{cr} $	[m/s ²]	29.78	28.95 (-3%)	28.71 (-4%)	25.92 (-13%)
	$\max \ddot{q}_{cr,w} $	[m/s ²]	18.36	17.50 (-5%)	18.23 (-1%)	15.88 (-14%)
	RMS \ddot{q}_{cr}	[m/s ²]	8.31	8.31 (0%)	8.39 (+1%)	7.55 (-9%)
	RMS $\ddot{q}_{cr,w}$	[m/s ²]	5.17	5.08 (-2%)	5.14 (-1%)	4.50 (-13%)
	VD \ddot{q}_{cr}	[m/s ^{1.75}]	15.74	15.34 (-2%)	15.78 (0%)	13.93 (-12%)
	VD $\ddot{q}_{cr,w}$	[m/s ^{1.75}]	10.04	9.55 (-5%)	9.85 (-2%)	8.48 (-16%)
	$\max \ddot{q}_{cr} $	[m/s ³]	356	598 (+68%)	719 (+102%)	693 (+95%)
load	$\max \ddot{q}_{cr} $	[m/s ²]	29.78	28.95 (-3%)	28.71 (-4%)	25.92 (-13%)
	PM \ddot{q}_{cr}	[10 ⁻² -]	3103.20	2911.34 (-6%)	2980.49 (-4%)	1986.91 (-36%)
deflection	nr bound excesses	[-]	4	4	4	4
	$\max \delta^u$	[10 ⁻² m]	15	14 (-7%)	14 (-7%)	21 (+40%)
	$\max \delta^l$	[10 ⁻² m]	5	5 (0%)	5 (0%)	5 (0%)
	$\max \Delta \dot{q} $ at ¹ $\Delta q = l^u$	[m/s]	0.97	0.94 (-3%)	0.67 (-31%)	1.16 (+20%)
	$\max \Delta \dot{q} $ at $\Delta q = l^l$	[m/s]	1.58	1.60 (+1%)	1.60 (+1%)	1.29 (-18%)
	RMS $q_{cr} - q_{ar}$	[10 ⁻² m]	12.52	12.70 (+1%)	11.47 (-8%)	14.39 (+15%)
handling	tire lift-off	[s]	0.077	0.013 (-83%)	0.345 (+348%)	0.127 (+65%)
	<75% stat tire force	[s]	0.957	1.176 (+23%)	0.915 (-4%)	1.009 (+5%)
	RMS dyn tire force	[10 ³ N]	75.51	75.36 (0%)	119.08 (+58%)	72.99 (-3%)
damage	η_{max}	[-]	216.04	187.02 (-13%)	237.59 (+10%)	136.09 (-37%)
comp time	CR	[-]		0.03	4.71	17.73

$$^1 \Delta q = q_{cr} - q_{ar}$$

on the negative suspension deflection are the same for all systems. The DCC system is the only semi-active system with both a lower maximum suspension deflection and a lower tire lift-off time than the passive system. The SQPCO system shows a lower maximum excess of the bound on the positive suspension deflection, but a higher tire lift-off time than the passive system whereas the SQPCE system shows both a higher maximum excess of the bound on the positive suspension deflection and a higher tire

lift-off time than the passive system. The disappointing performance of the SQPCE system is probably caused by a too short preview interval. This may mislead the controller as will be explained in Section 3.7.

A reduction of the tire lift-off time does not automatically imply improved road-holding as the system with the smallest tire lift-off time, the DCC system, shows the largest time for which less than 75 % of the static tire force is available. Furthermore, the semi-active systems with a much larger tire lift-off time than the passive system show either a smaller time for which less than 75 % of the static tire force is available or a smaller RMS value of the dynamic tire force than the passive system.

Although there is not an unambiguous relation between $\max(\delta^l)$, $\max(\delta^u)$ and $\max(|\Delta\dot{q}|)$ at the lower and upper bound of the suspension deflection, a higher value of $\max(\delta^u)$ corresponds to a higher value for $\max(|\Delta\dot{q}|)$. This implies that the impact force is indeed higher if $\max(\delta^u)$ is higher, as assumed in Section 3.2 for the establishment of the control objective.

For the DCC system and the SQPCE system, the values of the comfort quantities except the jerk are 0 to 5 %, respectively 9 to 16 % lower than for the passive system. The jerk is much higher for these systems than for the passive system. For the SQPCO system, the values of the comfort quantities are 0 to 4 % lower than for the passive system, except the RMS value of the sprung mass acceleration and the value of the jerk.

The SQPCE system shows the minimum road damage. The value of the road damage factor η_{max} is 37 % lower for this system than for the passive system. For the DCC system and the SQPCO system, the road damage factor is 13 % lower, respectively 10 % higher than for the passive system.

Conclusions

The large number of criteria makes it difficult to choose one of the semi-active systems for further development. Each semi-active system is preferable for some of the criteria. To facilitate the choice, only the CR and the criteria which correspond best to the control objective are used. These criteria are: $\max(|\ddot{q}_{cr}|)$, $\max(\delta^u)$, $\max(\delta^l)$ and the tire lift-off time. The values for these criteria in Tables 3.14 to 3.18 have a bold typeface. For the traffic hump, the scraped road, the well and the wave, the DCC system shows the best values for these criteria in combination with the minimum CR. For the standard brick, the bounds on the suspension deflection and the bound on the tire force are not reached. Therefore, only the value for $\max(|\ddot{q}_{cr}|)$ and CR are important on this road surface. The DCC system shows a somewhat higher value for $\max(|\ddot{q}_{cr}|)$, but a much lower value for CR than the SQPC systems. Therefore, the

DCC system is chosen for further development.

3.7 Applicable direct calculation controller

3.7.1 Concept

The direct calculation controller with $\Delta h_i = 0.050$ s, $s\Delta h_i = \Delta h_i$ and $\Delta h_c = 0.001$ s, as presented in Section 3.5, supposes that the optimum damper setting for the interval $(t, t + \Delta h_i]$ is available at time t whereas the required preview information, *i.e.* the height of the road surface for $(t, t + I\Delta h_i]$, becomes available at time t . Hence, the time to calculate the optimum control sequence over the preview interval $(t, t + I\Delta h_i]$ is neglected. To take this time into account, a slightly modified controller, the so-called applicable direct calculation controller (ADCC), is presented in this section. The principle of this controller is shown in Figure 3.14. The DCC determines the optimum

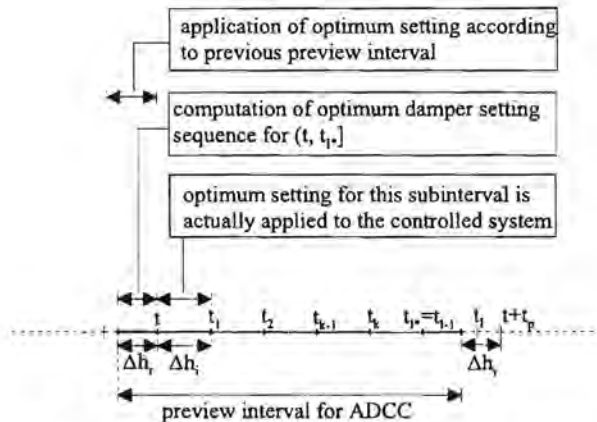


Figure 3.14: Principle of the applicable direct calculation controller.

damper setting for subinterval $(t, t + \Delta h_i]$ by using the road height over the preview interval $(t, t + t_p]$, whereas the ADCC determines the optimum damper setting for this subinterval by using the road height over the preview interval $(t - \Delta h_r, t + t_p - \Delta h_r]$. The applicable controller uses the time interval $(t - \Delta h_r, t]$ of the available preview interval to determine the optimum damper setting sequence for $(t, t + I^*\Delta h_i]$, where $I^* = I$ if $\Delta h_r \leq t_p - I\Delta h_i$ and $I^* < I$ otherwise. Meanwhile, for $(t - \Delta h_i, t]$, the optimum setting according to the calculations in the previous preview interval is applied. Only the very first damper setting to be applied by the ADCC, *e.g.* when the vehicle starts driving, can not be determined with this procedure and has to be chosen in a different way.

The required Δh_r will be smaller and $(t, t + I^* \Delta h_i]$ may be larger if the computing speed of the controller increases whereas both the required Δh_r and $(t, t + I^* \Delta h_i]$ may increase if the forward vehicle velocity decreases. Therefore, an appropriate Δh_r depends both on the controller hardware and the forward vehicle velocity. As more preview information is captured in a unit of time for large vehicle velocities than for low vehicle velocities, it is more important to use the smallest possible Δh_r for large vehicle velocities than for low vehicle velocities. In this thesis the controller hardware for the ADCC is not established. This makes a suitable choice for Δh_r rather difficult. Therefore, Δh_r is chosen equal to Δh_i and as a result, the ADCC determines the optimum damper setting sequence over $(t, t + (I - 1)\Delta h_i]$ by using the preview information over $(t - \Delta h_i, t + t_p - \Delta h_i]$. It is assumed that Δh_i is sufficient for the controller hardware to determine the optimum control sequence over $(t, t + (I - 1)\Delta h_i]$, irrespective of the forward vehicle velocity. Due to the fact that the ADCC determines the optimum control sequence over the interval $(t, t + (I - 1)\Delta h_i]$, the performance of this controller will coincide with the performance of a DCC for which the length of the preview interval is shortened with Δh_i .

Simulations with the laden two-DOF model have been carried out to compare the performance of the ADCC controlled system with the DCC controlled system. To facilitate a comparison of the ADCC system and the DCC system, only the performance criteria that are strongly related to the control objective, *i.e.* $\max(|\ddot{q}_{cr}|)$, $\max(\delta^u)$, $\max(\delta^l)$ and the tire lift-off time, are used. Table 3.19 shows the relevant values for the incidental road excitations of both the DCC and the ADCC system. The forward velocity of the systems for each of the road surfaces is equal to the prescribed forward velocity in Chapter 2. For the standard brick, the scraped road and the well, the values

Table 3.19: Performance and controller requirements of the DCC and ADCC controlled vehicle systems.

		standard brick		traffic hump		scraped road		well		wave	
critereon	unit	DCC	ADCC	DCC	ADCC	DCC	ADCC	DCC	ADCC	DCC	ADCC
$\max \ddot{q}_{cr} $	$[\text{m/s}^2]$	2.28	2.28	6.28	6.26	8.51	8.51	10.62	10.62	28.95	36.89
$\max \delta^u$	$[10^{-2} \text{ m}]$	0.00	0.00	0.00	0.00	0.00	0.00	0.00	0.00	14.00	25.29
$\max \delta^l$	$[10^{-2} \text{ m}]$	0.00	0.00	0.00	0.00	0.00	0.00	0.00	0.00	5.00	6.32
tire lift-off	$[\text{s}]$	0.000	0.000	0.000	0.000	0.043	0.043	0.087	0.087	0.013	0.000

of the criteria for the DCC and the ADCC system are equal. For the traffic hump, the value of the $\max(|\ddot{q}_{cr}|)$ is, in contrast to the expectation, somewhat lower for the ADCC system than for the DCC system. This is due to the fact that the simulation

with the DCC system starts just before the traffic hump whereas the simulation with the ADCC starts somewhat further before the obstacle to be sure that the arbitrarily chosen first damper setting for the ADCC system has no influence on the performance. These different starting points cause slightly different switching time points for the DCC and the ADCC system and this results in the slightly better performance of the ADCC system for the traffic hump. For the wave, the tire lift-off time is slightly smaller and the values of $\max(|\ddot{q}_{cr}|)$, $\max(\delta^u)$ and $\max(\delta^l)$ are much higher for the ADCC system than for the DCC system. Hence, for the wave, the overall performance of the ADCC system is worse than that of the DCC system. This is due to the reduction of the effective preview interval for the ADCC system.

3.7.2 Reduction of computation time

The CR for the ADCC system is approximately half the CR for the DCC system due to the a priori choice of the first damper setting in each preview interval for the ADCC system. However, in practical situations the CPU time of the ADCC might still be too long, *i.e.* larger than 0.050 s. Therefore, a possibility for further reduction of the CR is considered in this section.

The original ADCC chooses a 'low' or 'high' damper setting for each of the subintervals 2 to I in the preview interval. The choice of the damper setting in subinterval I at the end of the preview interval is likely to be less important than the choice in subinterval 2 at the beginning of a preview interval. Here, the effect on the performance is investigated if only the damper settings for the subintervals 2, 3, \dots , i can be chosen while the settings for the subintervals $i + 1, \dots, I - 1, I$ are chosen to be the same as the damper setting for subinterval i . So, instead of determining the responses for all damper setting combinations represented in the tree diagram of Figure 3.15 (dashed lines), only the responses for the damper setting combinations represented by the solid lines are determined. This is done for several values of i . Hopefully, this will result in a value $i < I$ for which the performance does not decrease too much in comparison to the performance of the original ADCC. A value $i < I$ will certainly reduce the CR because less damper setting sequences have to be evaluated.

The CR for the original ADCC controller increases if the number of subintervals I increases. Therefore, in order to reduce the maximum CR of the ADCC controller it is especially important to reduce the number of subintervals with an independent damper setting if I is large. This situation occurs, for instance, for small forward vehicle velocities. Consequently, first a possible reduction of the number of subintervals with an independent damper setting is investigated for a low forward vehicle velocity, *i.e.* $V = 20$ km/h. Next, a reduction of the number of subintervals with an independent

upper branch originating from branch point: low damper setting
 lower branch originating from branch point: high damper setting

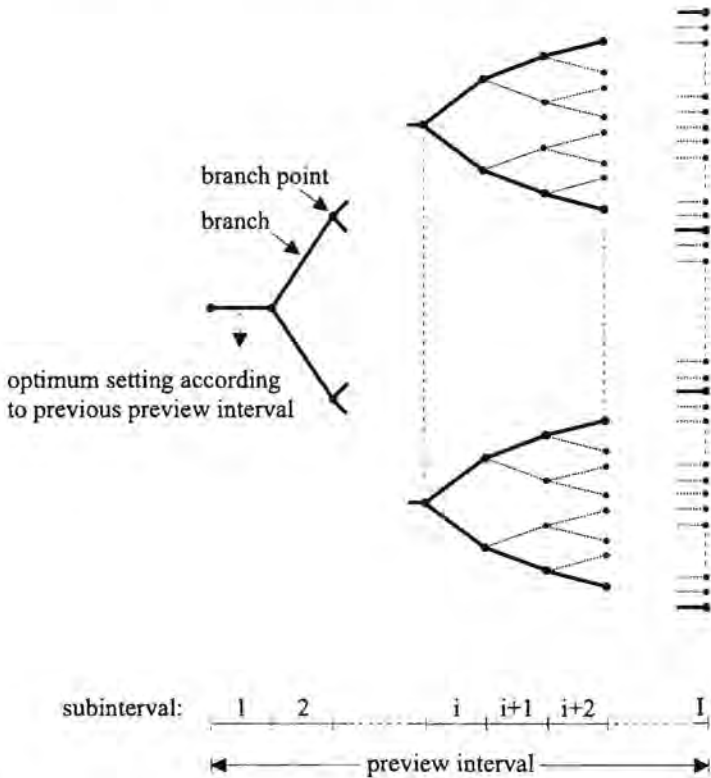


Figure 3.15: Tree diagram, representing all possible damper setting combinations (dashed lines) and the investigated damper setting combinations (solid lines).

damper setting is investigated for higher velocities.

The performance of the original ADCC system with a forward velocity $V = 20$ km/h is shown in Table 3.20 for five incidental road excitations. For this case $I = 12$. Next to the performance of the original ADCC system, *i.e.* the ADCC system with $i = I$, the performance of the ADCC systems with $i = 2, 3, \dots, 11$ is given in Table 3.20. For the standard brick, the scraped road and the wave, the performances for the ADCC systems with $i = 2, 3, \dots, 11$ are equal to the performance for the original ADCC system whereas for the well the performances of the ADCC systems with $i = 3, \dots, 11$ are equal to the performance for the original ADCC system and only the performance of the ADCC system with $i = 2$ is worse than that of the original ADCC system. For the traffic hump, the ADCC systems with $i = 6, 7, \dots, 11$ and also the ADCC systems

Table 3.20: Performance and controller requirements of the original ADCC system and the ADCC systems with $i = 2, 3, \dots, 11$ for $V = 20$ km/h.

		standard brick	traffic hump			scraped road	well		wave
criterion	unit	$2 \leq i \leq 12$	$i = 2$	$3 \leq i \leq 5$	$6 \leq i \leq 12$	$2 \leq i \leq 12$	$i = 2$	$3 \leq i \leq 12$	$2 \leq i \leq 12$
$\max \ddot{q}_{cr} $	$[\text{m/s}^2]$	5.90	7.86	6.67	6.26	8.25	15.83	12.82	0.87
$\max \delta^u$	$[10^{-2} \text{ m}]$	0.00	0.00	0.00	0.00	0.00	0.00	0.00	0.00
$\max \delta^l$	$[10^{-2} \text{ m}]$	0.00	0.00	0.00	0.00	0.00	0.01	0.00	0.00
tire lift-off	[s]	0.033	0.000	0.000	0.000	0.037	0.090	0.083	0.000
CR	[-]	0.04 - 3.53	0.04	0.06 - 0.16	0.21 - 3.58	0.04 - 4.22	0.04	0.06 - 3.55	0.06 - 3.61

Table 3.21: Performance and controller requirements of the original ADCC system and the ADCC systems with $i = 2, 3, \dots, 7$ for $V = 30$ km/h.

		standard brick	traffic hump				scraped road			
criterion	unit	$2 \leq i \leq 8$	$i = 2$	$3 \leq i \leq 4$	$i = 5$	$6 \leq i \leq 8$	$i = 2$	$i = 3$	$i = 4$	$5 \leq i \leq 8$
$\max \ddot{q}_{cr} $	$[\text{m/s}^2]$	4.65	13.05	10.46	10.57	10.54	9.61	8.42	8.45	8.42
$\max \delta^u$	$[10^{-2} \text{ m}]$	0.00	0.00	0.00	0.00	0.00	0.00	0.00	0.00	0.00
$\max \delta^l$	$[10^{-2} \text{ m}]$	0.00	0.00	0.00	0.00	0.00	0.00	0.00	0.00	0.00
tire lift-off	[s]	0.026	0.062	0.050	0.051	0.051	0.050	0.041	0.041	0.041
CR	[-]	0.04 - 0.25	0.05	0.07 - 0.08	0.09	0.12 - 0.32	0.04	0.05	0.07	0.14 - 0.25

		well	wave
criterion	unit	$2 \leq i \leq 8$	$2 \leq i \leq 8$
$\max \ddot{q}_{cr} $	$[\text{m/s}^2]$	14.28	1.92
$\max \delta^u$	$[10^{-2} \text{ m}]$	0.00	0.00
$\max \delta^l$	$[10^{-2} \text{ m}]$	0.00	0.00
tire lift-off	[s]	0.108	0.000
CR	[-]	0.05 - 0.28	0.09 - 0.25

with $i = 3, 4, 5$ show the same performance. The first mentioned systems show the same performance and the second mentioned systems show a worse performance than the original ADCC system. However, the ADCC system with $i = 2$ shows by far the worst performance for the traffic hump. Hence, the simulations with $V = 20$ km/h show the same performance for the ADCC system with $i = 6$ as for the original ADCC system. The CR for the ADCC system with $i = 6$ is a factor 15 lower than for the original ADCC system. So, a large reduction of the CR is possible without performance deterioration for $V = 20$ km/h.

A restriction of the subintervals with an independent damper setting to the subintervals 2 to 6 is only sensible if this restriction is also suitable for other vehicle velocities with $I > 6$. Therefore, the performances for the original ADCC system and the ADCC systems with $i = 2, 3, \dots, I - 1$ are also determined for the velocity $V = 30$ km/h. The results in Table 3.21 show that for this velocity the performance for the ADCC system with $i = 6$ is equal to that for the original ADCC system for all investigated incidental road excitations.

Using the ADCC system with $i = 6$ instead of the original ADCC system is thus possible without any performance deterioration, according to the results for $V = 20$ km/h and $V = 30$ km/h. The same results show that for the standard brick, the scraped road, the well and the wave even the ADCC system with $i = 3$ shows nearly the same performance as the original ADCC system. Therefore, if a performance deterioration of 7 % is acceptable for the traffic hump then even the ADCC system with $i = 3$ can be used instead of the original ADCC system. The performances for the incidental road surfaces of the ADCC systems with $i = 2, 3, \dots, I$ are also determined for $V = 40$ km/h and $V = 60$ km/h. The results for these velocities confirm the assumption that the ADCC system with a small value for i instead of the original ADCC system can be used with only a small performance deterioration. After all, for these velocities only the performance of the ADCC system with $i = 2$ deviates sometimes from the performance of the original ADCC system whereas the performance of the ADCC system with $i > 2$ is always equal to that of the original ADCC system.

3.7.3 Required preview information for the wave

Until now, it is assumed that the disappointing performance for the wave of the semi-active systems is caused by a too short preview interval. It is not shown that more preview information indeed improves the performance of the semi-active systems for this road excitation, because the required controller computation time of an original DCC or ADCC is extremely large for long preview intervals. However, the much smaller controller computation time and the equal performance for an ADCC system with $i =$

6 with respect to the original ADCC system gives the opportunity to determine the necessity of more preview information for the wave without extreme large computation times. Therefore, the performance for the wave of an ADCC system with $i = 6$ is determined for different wheelbase lengths L and for both the vehicle velocity $V = 63$ km/h, used in Section 3.5, and the 'prescribed' vehicle velocity for the wave, *i.e.* $V = 80$ km/h. The results in Tables 3.22 and 3.23 show that a wheelbase length of more than 10.5 m is required to improve the performance of the semi-active system for $V = 63$ km/h and $V = 80$ km/h with respect to the performance of the system with a wheelbase length of 3.5 m. So, a longer preview interval and the controller internal model response over a larger time interval indeed improves the performance of the semi-active systems. Furthermore, comparison of the results in Table 3.22 with the results in Table 3.8 shows that the performance of the semi-active system with a wheelbase length of more than 10.5 m is better than that of the 'best' passive system (passive high) for the wave at $V = 63$ km/h.

Table 3.22: Performance for the wave of the ADCC controlled semi-active system with $V = 63$ km/h, $\Delta h_i = s\Delta h_i = 0.050$ s, $\Delta h_c = 0.001$ s, explicit Euler integration and $i = 6$.

Wave	L [m]	t_p [s]	$\max \ddot{q}_{cr} $ [m/s ²]	tire lift-off [s]	$\max \delta^u$ [m]	$\max \delta^l$ [m]
	3.5	0.2	14.45	0.000	0.00	0.02
	7.0	0.4	15.37	0.000	0.00	0.02
	10.5	0.6	15.08	0.000	0.00	0.02
	14.0	0.8	13.44	0.000	0.00	0.01
	17.5	1.0	13.44	0.000	0.00	0.01
	21.0	1.2	13.43	0.000	0.00	0.01
	24.5	1.4	13.43	0.000	0.00	0.01
	28.0	1.6	13.43	0.000	0.00	0.01
	31.5	1.8	13.43	0.000	0.00	0.01
	35.0	2.0	13.43	0.000	0.00	0.01

Table 3.23: Performance for the wave of the ADCC controlled semi-active system with $V = 80$ km/h, $\Delta h_i = s\Delta h_i = 0.050$ s, $\Delta h_c = 0.001$ s, explicit Euler integration and $i = 6$.

Wave	L [m]	t_p [s]	$\max \ddot{q}_{cr} $ [m/s ²]	tire lift-off [s]	$\max \delta^u$ [m]	$\max \delta^t$ [m]
	3.5	0.1575	36.88	0.000	0.25	0.06
	7.0	0.3150	26.63	0.036	0.14	0.05
	10.5	0.4725	26.47	0.000	0.14	0.05
	14.0	0.6300	26.49	0.000	0.14	0.05
	17.5	0.7875	26.49	0.000	0.14	0.05
	21.0	0.9450	26.49	0.000	0.14	0.05
	24.5	1.1025	26.49	0.000	0.14	0.05
	28.0	1.2600	26.49	0.000	0.14	0.05
	31.5	1.4175	26.49	0.000	0.14	0.05
	35.0	1.5750	26.49	0.000	0.14	0.05

3.7.4 Conclusions

The ADCC is presented as an adapted version of the DCC which can take into account the computation time of the controller for determining the optimum damper setting sequence over a preview interval. It is shown that the performance of the ADCC system does not deteriorate whereas the computation time reduces significantly if only the damper settings for the subintervals 2 to 6 can be chosen while the settings for subsequent subintervals are chosen to be the same as the setting for subinterval 6. A further reduction of the controller computation time with only a small performance deterioration is possible if only the damper settings for the subintervals 2 and 3 can be chosen while the settings for the subsequent subintervals are chosen to be the same as the setting for subinterval 3. Finally, it is shown that the disappointing performance of the semi-active system for the wave indeed is caused by a too short preview interval.

It is decided to use the ADCC with $\Delta h_r = \Delta h_i = 0.050$ s, $s\Delta h_i = \Delta h_i$, $\Delta h_c = 0.001$ s, explicit Euler integration for determining the internal model responses and with only independent damper settings for the subintervals 2 to 6, *i.e.* $i = 6$, for the simulations with the 3D vehicle model in Chapter 4.

Performance of the passive and the semi-active 3D vehicle model

This chapter discusses the performance of the passive and the semi-active 3D vehicle model. The behavior of the passive 3D vehicle model is compared to the behavior of a real tractor-semitrailer, to get an idea about the quality of the vehicle model. The configuration of the semi-active system is described and the performance of the semi-active system is compared to the performance of the passive system for both the laden and the un-laden vehicle.

4.1 Verification of the vehicle model

The 3D vehicle model developed by Bekkers [3] is used for the evaluation of the passive and the semi-active vehicle behavior. As a first verification, Bekkers compared the responses of the 3D vehicle model with available measurements on a tractor without semitrailer for a bump-hill and a railway crossing. Bekkers concluded that the behavior of the tractor model is rather similar to the behavior of the real tractor. However, some aspects of the model and the vehicle were different. The wheelbase of the tractor was 3.50 m for the model and 3.25 m for the real vehicle. Furthermore, the springs in the model were air springs whereas the real vehicle was equipped with leaf springs in the rear axle suspension of the tractor. The influence of the difference in wheelbase on the vehicle behavior is difficult to predict. However, the influence of the different spring types will be large due to the fact that the stiffnesses of the leaf springs are much higher than those of the air springs. This is caused by the fact that the measurements are done on a tractor without semitrailer and that the stiffnesses of the air springs are 'adjusted' to the cargo load whereas the stiffnesses of the leaf springs are fixed and based on the maximum cargo load.

To judge the quality of the vehicle model with air springs in the rear axle suspension, an extra comparison is made between the 3D model and available measurements on a

vehicle where both the vehicle and the model have air springs in the rear axle suspension of the tractor, a laden semitrailer and a wheelbase length of 3.80 m. The behavior of the model with respect to the behavior of the real vehicle is investigated for a severe railway crossing and a common forward velocity. The results are shown in Figures 4.1 to 4.3.

The responses of the real vehicle in Figure 4.1 and Figure 4.2 are the original measured signals. The large amplitudes of the high frequency components (> 15 Hz) in many of the acceleration signals for the real vehicle are surprising. However, for a harmonic component with frequency f , the amplitude of the corresponding displacement is a factor $4\pi^2 f^2$ smaller than that of the acceleration signal. This results in amplitudes of less than 1 mm for the displacement signals corresponding to the given acceleration signals, which is plausible. Although the components in the acceleration signals with a frequency higher than 15 Hz may influence the comfort of the occupants (due to noise) and the fatigue load on the chassis components, large performance improvements of the semi-active suspension with respect to the passive suspension can not be expected for these higher frequencies, because the low order controller model does not predict these components. If the measured signals are used to determine the actual state for the controller internal model then the controller might try to influence the high frequency behavior of the vehicle while it is not able to do this. Therefore, it will probably be necessary to filter the measured signals with a low-pass filter with low phase distortion before passing these signals to the controller of the real semi-active vehicle. The components with frequencies higher than 15 Hz are of less importance for this investigation. Therefore, the 3D model describes the behavior of the real vehicle only for frequencies between 0 and 15 Hz.

To compare the behavior of the 3D model and of the real vehicle for this frequency range, Figure 4.3 gives the accelerations according to the 3D model and the output of a 15 Hz low-pass filter without phase distortion, with the real vehicle accelerations as input. The 0 to 15 Hz frequency components of the cabin vertical acceleration, the kingpin vertical acceleration and the suspension deflections at the right front and the right rear side of the tractor show rather similar shapes for the model and the real vehicle. This especially is the case for the first part of these responses. Frequency domain analysis shows relatively high power for the 5.5, 7.5, 8.5, 10 and 11.5 Hz frequency components in the filtered cabin longitudinal acceleration compared to this acceleration for the 3D model. Furthermore, a relatively high power for the 14 Hz frequency component shows up in the filtered tractor chassis vertical acceleration with respect to this acceleration for the 3D model. These differences between the 3D model and the actual vehicle are probably due to un-modeled dynamics, like the chassis and (some of the) semitrailer flexibilities. The influence of the excitation of the semitrailer axles

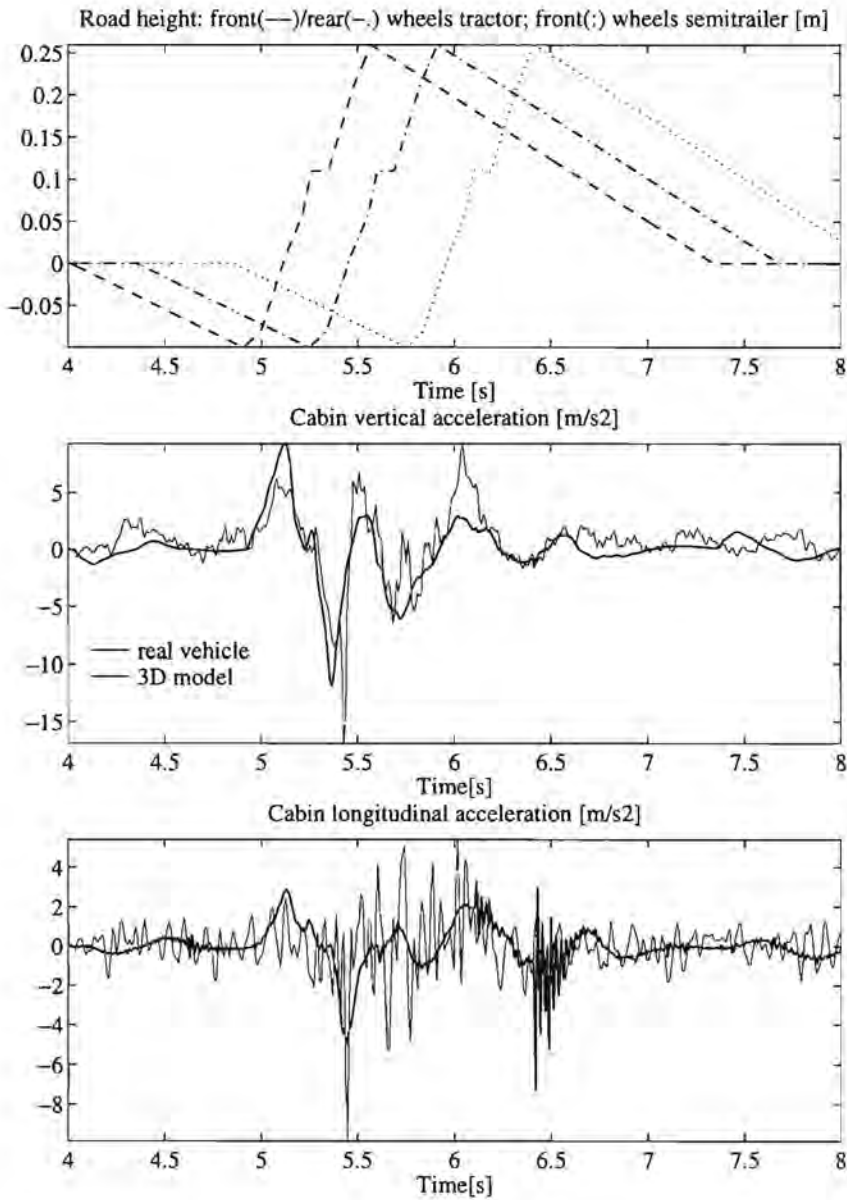


Figure 4.1: Road height and comparison of cabin accelerations for the 3D vehicle model and the real vehicle for a severe railway crossing

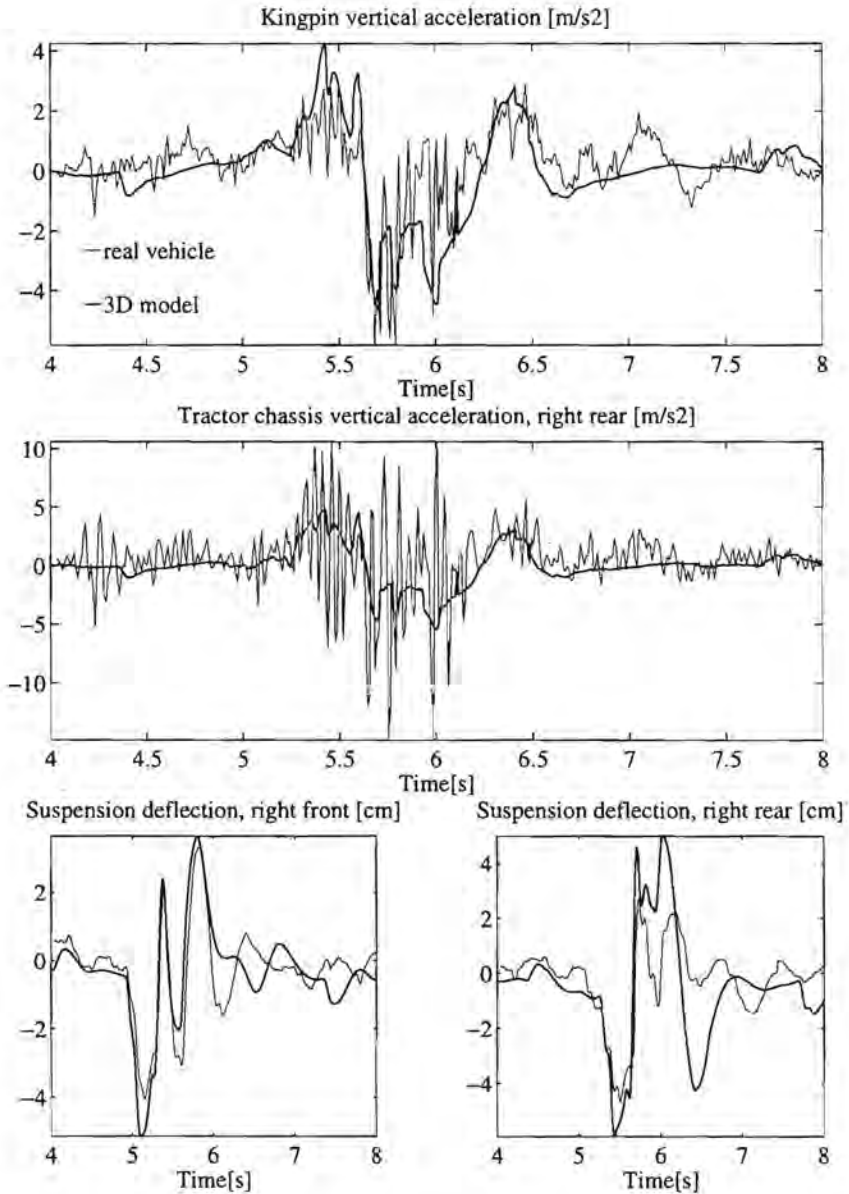


Figure 4.2: Comparison of kingpin accelerations, tractor chassis accelerations and suspension deflections for the 3D vehicle model and the real vehicle for a severe railway crossing

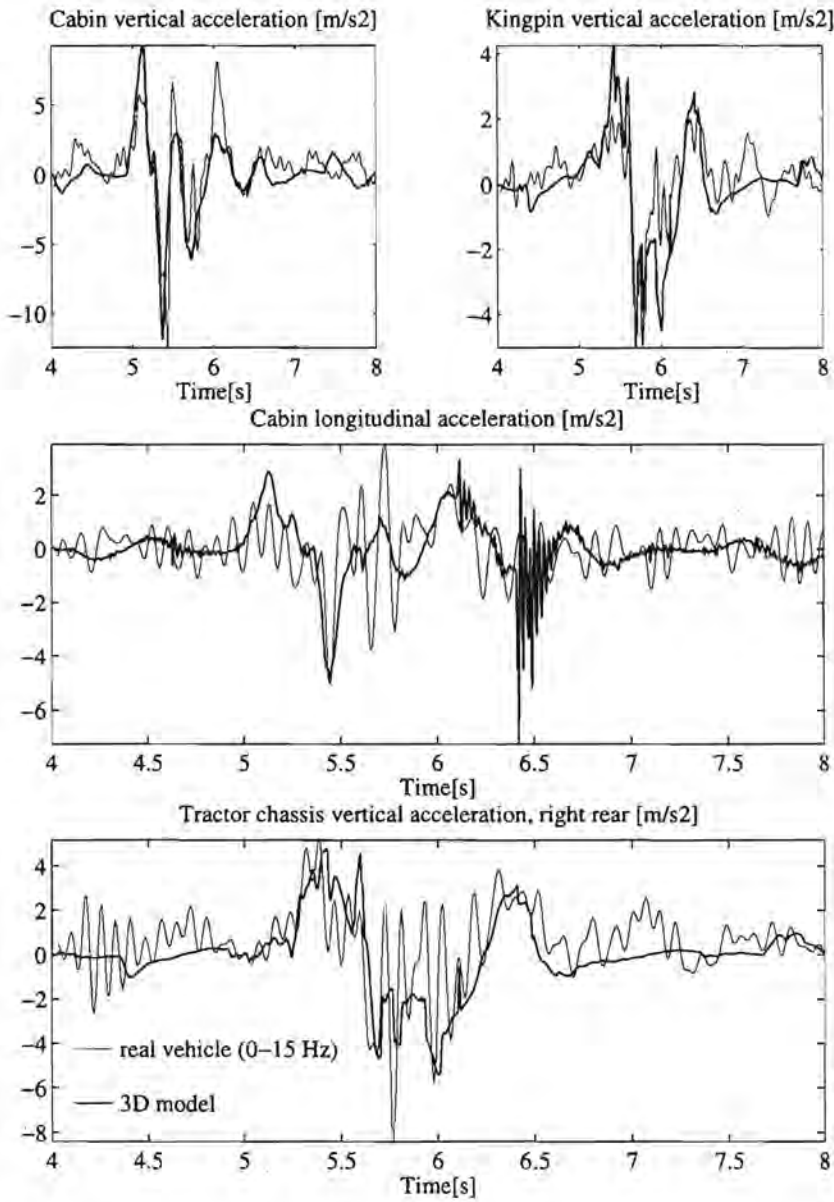


Figure 4.3: Comparison of cabin accelerations, kingpin accelerations and tractor chassis accelerations for a severe railway crossing; the signals are unmodified for the 3D vehicle model and 15 Hz low-pass filtered for the real vehicle

on the cabin longitudinal acceleration is much larger for the model than for the real vehicle. This might also be due to the used rigid model of the tractor chassis and the rather rigid model of the semitrailer.

The 3D model describes fairly well the dynamics of the real vehicle for the frequency range 0 to 15 Hz. However, the results in this section show that it is desirable to incorporate a realistic, practical description of the chassis and the semitrailer flexibilities into the 3D model in order to get more realistic simulation results for this frequency range. Unfortunately, this extension of the model was not possible in this investigation because no validated flexible body models of these components were available. However, even without this extension the given 3D model is useful, because it can give more insight in the influence of un-modeled dynamics (for the frequency range 0 to 15 Hz) in the controller model on the performance of the semi-active system.

4.2 Configuration of the semi-active system

The semi-active system for the 3D model contains a damper of the type described in Section 2.2, both at the left and the right side in the tractor rear axle suspension. Each damper is controlled by a separate applicable direct calculation controller (ADCC), which treats the damper as a two-state damper. The controllers use a two-DOF internal model (representing one half of the rear side of the tractor) and the control objective of Section 3.2. The subinterval length Δh_i , the application length $s\Delta h_i$, the sample interval length of the controller model response Δh_c , the integration algorithm and the number of subintervals i with an independent choice of the damper setting are chosen as proposed in Section 3.7.4.

Each controller determines the state for the internal model at the start of a preview interval from the vertical displacements and the vertical velocities of the points to which the controlled damper is connected. These displacements and velocities are not only affected by the excitation of the tractor rear wheels but, due to the coupling between the axles of the vehicle, also by the excitations at the tractor front wheels and the semitrailer wheels. This is an important difference between the 3D simulation model and the two-DOF simulation model. Due to the influence of the excitations at the tractor front wheels on the state of the tractor rear side, the semi-active suspension at the rear side of the tractor in the 3D simulation model can, in contrast to the semi-active suspension in the two-DOF simulation model, react before the obstacle has reached the rear side of the tractor if the road surface before the obstacle is flat.

The controller for the damper at the left (right) side supposes that the road surface under the left (right) front wheel of the tractor passes a preview time later the left (right) rear wheels. As mentioned before, the road surface under the front wheels of

the tractor is assumed to be known exactly by the controller. Possible errors due to reconstruction of the road surface by an observer are not taken into account.

4.3 Performance for the passive and the semi-active 3D vehicle model

This section compares the behavior of the passive and the semi-active 3D vehicle model for the road surfaces mentioned in Section 2.3, using the prescribed forward velocity for these road surfaces. All responses are determined with an explicit Adams-Bashforth-Moulton predictor-corrector method at a sample interval of 0.001 s. The accelerations are weighted according to ISO 2631 and the jerk is estimated with the central difference scheme (3.18) in Chapter 3.

4.3.1 Performance for the laden vehicle

Tables 4.1 and 4.2 show the performance improvements (white blocks) and performance deteriorations (black blocks) of the laden semi-active system (ADCC) with respect to the laden passive system (PASM). The area of each block is proportional to the percentage value of performance improvement/deterioration. The actual values of the performance criteria for both systems are given in Appendix B.

For the wave, the performance for the semi-active system is much worse than for the passive system. The disappointing behavior of the semi-active system for this road excitation is probably caused by a too short preview interval, which, as already concluded in Chapter 3, will mislead the controller.

Before discussing specific results for the other road excitations, some general remarks are given. First the performance criteria closely related to the control objective are considered¹, *i.e.* $\max |\ddot{q}_{cvl'r}|$, $\max |\ddot{q}_{cvr'r}|$, the tire lift-off times, the number of times a bound on the suspension deflection is hit and $\max |\Delta \dot{q}_{l'r}|$ and $\max |\Delta \dot{q}_{r'r}|$ at the bounds of the suspension deflection. The controller puts the highest priority on the requirements with respect to the suspension deflection and the tire force. The constraints on the suspension deflection are not reached for the considered road surfaces whereas the constraint on the tire force is reached for the scraped road and the well. The semi-active system does not prevent tire lift-off. However, the tire lift-off time of the tractor rear tires is reduced with 8 to 20 % with respect to the passive system for these roads. The $\max |\ddot{q}_{cvl'r}|$ and the $\max |\ddot{q}_{cvr'r}|$ are 3 to 11 % lower for the semi-active system than for the passive system for the considered road excitations except for the well. For the latter, $\max |\ddot{q}_{cvl'r}|$ is 2 % higher for the semi-active system. This is due to the fact that

¹See for an explanation of the following symbols the legends in Tables 4.1 and 4.2.

Table 4.1: Percentage of performance improvement (white blocks) or performance deterioration (black blocks) of the laden 3D model with semi-active tractor rear axle suspension with respect to the laden 3D vehicle model with passive tractor rear axle suspension: comfort

aspect	criterion	standard brick	traffic hump	scraped road	well	wave	legend [%]
comfort	$\max \ddot{q}_{sv} $	■	•	•	□	■	
	$\max \ddot{q}_{slo} $	■	■	•	□	■	
	$\max \ddot{q}_{sla} $	■	■	■	□	■	
	$\max \ddot{q}_{sv,w} $	■	•	•	□	■	
	$\max \ddot{q}_{slo,w} $	■		•	□	■	
	$\max \ddot{q}_{sla,w} $	□	□	•	□	■	■ 50
	RMS \ddot{q}_{sv}	■	•	•	□	■	■ 40
	RMS \ddot{q}_{slo}	■	•	■	□	■	■ 30
	RMS \ddot{q}_{sla}	■	•	•	□	■	□ 20
	RMS $\ddot{q}_{sv,w}$	■	□	•	□	■	□ 10
	RMS $\ddot{q}_{slo,w}$	■	□	■	□	■	□ 5
	RMS $\ddot{q}_{sla,w}$	■	□	•	□	■	□ 1
	VD \ddot{q}_{sv}	■	□	□	□	■	• 1
	VD \ddot{q}_{slo}	■	•	•	□	■	■ 5
	VD \ddot{q}_{sla}	■	■	□	□	■	■ 10
	VD $\ddot{q}_{sv,w}$	■	□	•	□	■	■ 20
	VD $\ddot{q}_{slo,w}$	■	•	•	□	■	■ 30
	VD $\ddot{q}_{sla,w}$	■	□	•	□	■	■ 40
	$\max \dot{q}_{sv} $	•	□	•	□	■	■ 50
	$\max \dot{q}_{slo} $	•	■	□	□	■	
	$\max \dot{q}_{sla} $	■	■	□	□	■	
	RMS $ \dot{q}_{sv} $	•	□	•	□	■	
RMS $ \dot{q}_{slo} $	■	■	■	□	■		
RMS $ \dot{q}_{sla} $	■	■	□	□	■		

$q_{..}$: displacement, specified by ..
w: weighted *s*: driver seat *v*: vertical *lo*: longitudinal *la*: lateral

Table 4.2: Percentage of performance improvement (white blocks) or performance deterioration (black blocks) of the laden 3D model with semi-active tractor rear axle suspension with respect to the laden 3D vehicle model with passive tractor rear axle suspension: load, deflection, handling and damage

aspect	criterion	standard	traffic	scraped	well	wave	legend [%]
		brick	hump	road			
load	$\max \ddot{q}_{kv} $		○	□	•	■	
	$\max \ddot{q}_{cvlr} $	○	○	□	-	■	
	$\max \ddot{q}_{cvrr} $	○	○	□	□	■	
	PM \ddot{q}_{cvlf}	□	□	-	□	■	□ 50
	PM \ddot{q}_{cvrf}	□	□		□	■	□ 40
	PM \ddot{q}_{cvlr}	□	□	□	□	■	□ 30
	PM \ddot{q}_{cvrr}	□	□	□	□	■	□ 20
deflection	nr bound hits $\dot{l}r$					■	□ 10
	nr bound hits $\dot{r}r$					■	○ 5
	$\max \Delta \dot{q}_{lr} $ at bounds					■	• 1
	$\max \Delta \dot{q}_{rr} $ at bounds					□	• 1
	RMS Δq_{lr}	■	○	•	□	•	• 5
	RMS Δq_{rr}	□	○	•	□	•	■ 10
handling	tire lift-off $\dot{l}r$			□	□	■	■ 20
	tire lift-off $\dot{r}r$			□		■	■ 30
	<75% stat tire force $\dot{l}r$		■	•	□	■	■ 40
	<75% stat tire force $\dot{r}r$		■	•		•	■ 50
	RMS dyn tire force $\dot{l}r$	•	□	•	□	•	
	RMS dyn tire force $\dot{r}r$	■	□	•	•	•	
damage	road damage all tires	-	•	•	□	•	
	road damage rear tires	-	○	■	□	■	

$q_{..}$: displacement, specified by ..

$$\Delta q_{..} = q_{c..} - q_{a..}$$

a : tractor axle c : tractor chassis k : kingpin v : vertical f : front r : rear l : left r' : right

the semi-active system is focusing on a reduction of the tire lift-off time at the same time the peak in $\ddot{q}_{cvl'r}$ occurs. For the evaluation of the performance, $\max |\ddot{q}_{cvl'r}|$ and $\max |\ddot{q}_{cvr'r}|$ over the total simulation time are considered. However, at time t the controller only considers the maximum absolute values over the preview interval $[t, t + t_p]$. This results in a reduction of other high peaks in the signals $\ddot{q}_{cvl'r}$ and $\ddot{q}_{cvr'r}$ next to the reduction of the maximum peaks in these signals. The latter is shown in Figure 4.4 which gives the values for $\ddot{q}_{cvl'r}$ and $\ddot{q}_{cvr'r}$ as a function of time for the considered road surfaces. This figure shows that the reduction of the other high acceleration peaks is sometimes larger than the reduction of the maximum peaks for the semi-active system compared to the passive system.

Considering the performance criteria which are not directly related to the control objective, Table 4.1 shows a deterioration of comfort for the standard brick and an improvement of comfort for the well for the semi-active system with respect to the passive system. For the traffic hump and the scraped road, the values of some comfort criteria increase whereas the values of other comfort criteria decrease. The relative longitudinal displacement with respect to the nominal longitudinal displacement, the lateral displacement and the vertical displacement of the seat as a function of time are rather similar for the passive and the semi-active vehicle. For the scraped road, this is shown in Figure 4.5. So, there is no significant difference in damping behavior of these movements for the passive and the semi-active vehicle. Finally, it can be concluded that a reduction of the maximum absolute chassis accelerations at the rear side of the tractor not automatically leads to an improvement of comfort.

The maximum absolute acceleration at the kingpin is used as a measure for the incidental load on the cargo. For the semi-active system, this incidental load is lower for the symmetric road excitations (traffic hump, scraped road) and higher for the asymmetric road excitations (standard brick, well) compared to the incidental load on the cargo for the passive system. The value of the chassis acceleration at the kingpin, which is at the mid rear side of the tractor chassis, will have approximately the mean value of the chassis acceleration at respectively the left and the right rear side of the tractor. For symmetric road excitations, the maximum absolute chassis accelerations at the left and the right rear side of the tractor will generally occur at the same time point whereas this is not the case for asymmetric road excitations. This might explain why only for the symmetric road excitations an independent reduction of the maximum absolute chassis accelerations at the left and the right rear side of the tractor results in a reduction of the maximum absolute acceleration at the kingpin. The fatigue loads on the chassis components are judged by the PM numbers. For the considered road excitations, the fatigue loads for the semi-active system are nearly equal to or lower than those for the passive system. So, the lifespan of the vehicle for the same road

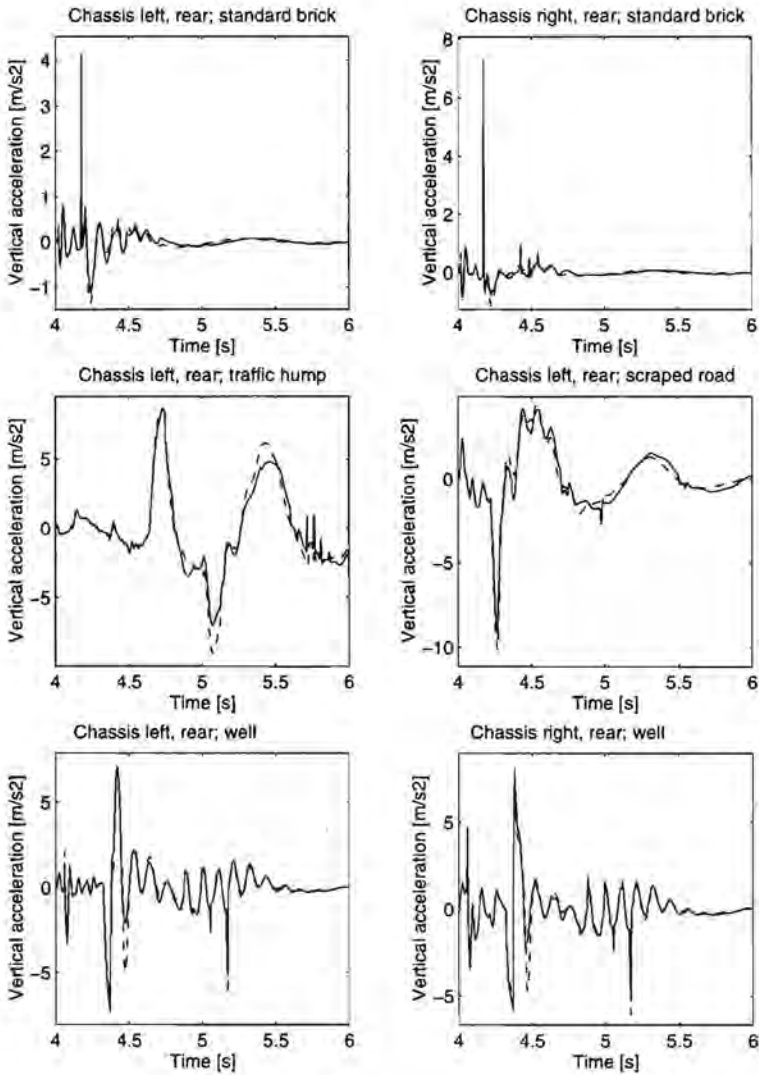


Figure 4.4: Vertical accelerations as a function of time at the rear side of the tractor for the laden vehicle; — : semi-active; - - : passive

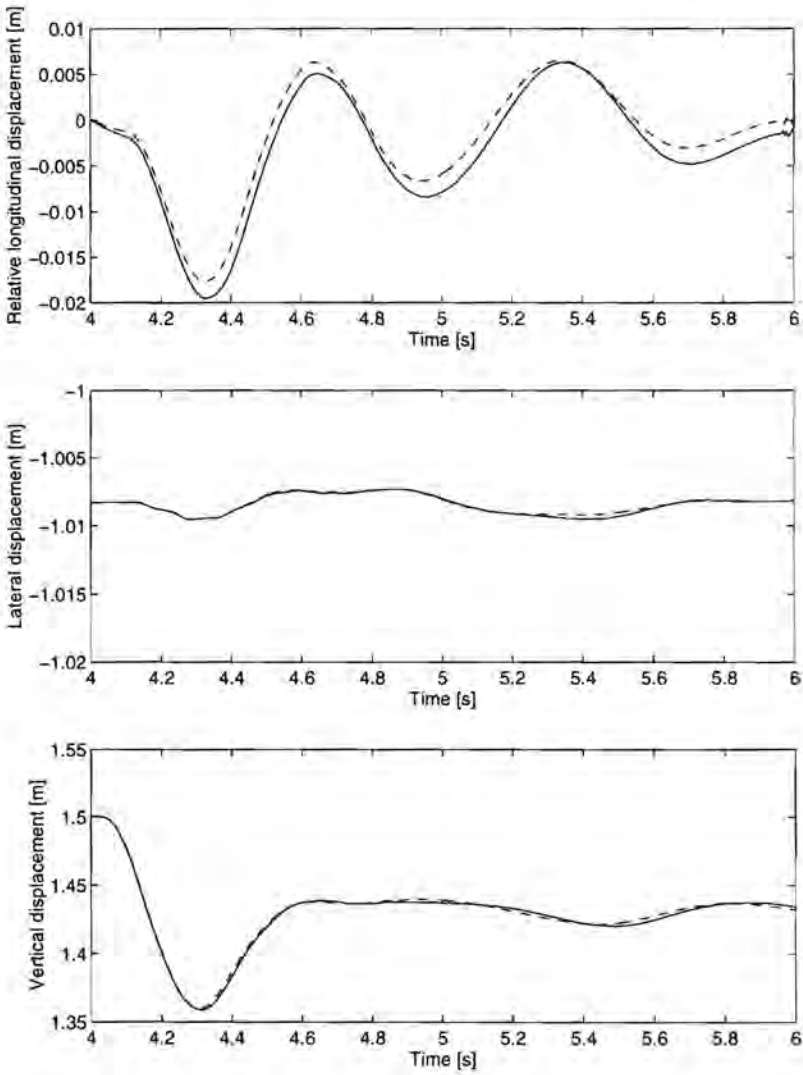


Figure 4.5: Relative longitudinal displacement, lateral displacement and vertical displacement of the seat as a function of time for the scraped road; — : semi-active; - - : passive

excitations increases. However, the allowed increase of stress amplitude in elements which connect vehicle components to the chassis, without reducing the lifespan of these connections is still small due to the rather small increase of allowed stress amplitude with a reduction of the number of load cycles for the same fatigue damage in the SN curve [35] (also termed Wöhler curve). An increase of the allowed stress amplitude can imply a decrease of the needed un-laden vehicle mass and thus an increase of the allowed payload. Unfortunately, this is not noticeably possible with the semi-active suspension.

The road damage caused by the rear wheels of the tractor for the semi-active system varies from -55 to +22 % with respect to the road damage of these wheels for the passive system. This results in a variation of -6 to +7 % of the total road damage caused by the wheels of the tractor and the semitrailer of the semi-active system with respect to the total road damage for the passive system. So, the influence of the semi-active tractor rear axle suspension on the road damage is considerable.

For the standard brick, the bound on the tire force and the bounds on the suspension deflection are not reached. The rather high values for the maximum absolute chassis accelerations at the rear side of the tractor for both the passive and the semi-active 3D vehicle model compared to the values calculated with the two-DOF vehicle model in Chapter 3 for this road are striking. The time plots, given in Figure 4.6, show that these high maximum absolute accelerations are due to a high peak in the chassis accelerations at the rear side of the tractor. These peaks occur at the same time as the peak in the tire force of the left rear tire of the tractor. Peaks are not present in the time signals of the damper forces and the air spring forces transmitted between the rear axle of the tractor and the chassis. However, peaks similar to the peaks in the mentioned chassis accelerations are present in the time signals of the forces transmitted by the links which connect the rear axle to the tractor chassis. The largest components of these peak forces are transmitted in longitudinal direction between the axle and the tractor chassis. However, smaller peak forces, with a significant value compared to the forces by the air spring and the damper in the tractor rear axle suspension, are transmitted in vertical direction between the axle and the tractor chassis. Therefore, the maximum absolute accelerations at the rear side of the tractor are strongly influenced by the link mechanism between the rear axle and the tractor chassis. The use of longer links with the connection points to the chassis at the same height as the connection points to the rear axle might reduce the influence of the link mechanism on the vertical accelerations at the rear side of the tractor chassis. The higher chassis acceleration at the right rear side than at the left rear side of the tractor while the standard brick excites the vehicle model at the left side is striking and the cause is not clear at this moment.

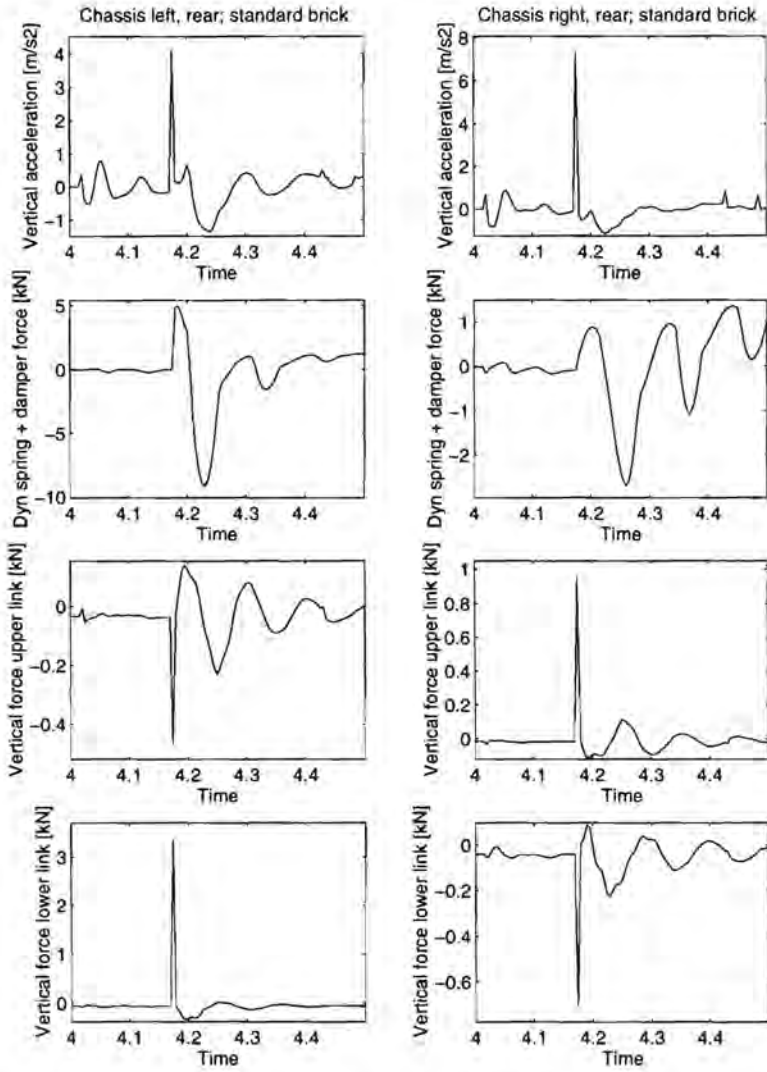


Figure 4.6: Accelerations of and forces on the rear side of the tractor chassis for the standard brick

4.3.2 Performance for the un-laden vehicle

Tables 4.3 and 4.4 show the performance improvements (white blocks) and performance deteriorations (black blocks) of the un-laden semi-active system (ADCC) with respect to the un-laden passive system (PASM). Again, the area of each block is proportional to the percentage value of performance improvement/deterioration. The actual values of the performance criteria for both systems are given in Appendix B.








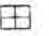
First, the laden passive vehicle model and the un-laden passive vehicle model are compared (see Appendix B). The comfort for the traffic hump and the scraped road is better for the laden passive vehicle and the comfort for the well is better for the un-laden passive vehicle. The average fatigue load and the average incidental load on the chassis components at the rear side of the tractor are higher for the un-laden vehicle than for the laden vehicle for all road excitations, except for the wave, whereas the fatigue load at the front side of the tractor is lower for the un-laden vehicle than for the laden vehicle for all road excitations. For the un-laden vehicle, the RMS values of the suspension deflection are lower than for the laden vehicle, except for the standard brick. The tire lift-off time and time for which less than 75 % of the static tire force is available, are higher, whereas the RMS values for the dynamic tire force are lower for the un-laden than for the laden vehicle for most of the road excitations. The increase of the tire lift-off time and of the time for which less than 75 % of the static tire force is available and the decrease of the RMS values for the dynamic tire force may be explained by the lower static tire force for the un-laden vehicle with respect to the laden vehicle. This lower static force causes a higher tire lift-off time and a higher time for which less than 75 % of the static tire force is available for the same dynamic tire force. The road damage is, as may be expected, lower for the un-laden vehicle than for the laden vehicle.

Next, a comparison is made between the passive system and the semi-active system for the un-laden situation. First, the values for the criteria closely related to the control objective are considered. The bounds on the suspension deflection are not reached whereas tire lift-off occurs for both the passive system and the semi-active system for all incidental road excitations, except for the wave. The average tire lift-off time is 3 to 17 % lower for the semi-active system than for the passive system.

For the standard brick, the accelerations² $\max |\ddot{q}_{cvl'r}|$ and $\max |\ddot{q}_{cvt'r}|$ are 15 % respectively 3 % lower whereas for the other incidental road excitations the average value of $\max |\ddot{q}_{cvl'r}|$ and $\max |\ddot{q}_{cvt'r}|$ is 2 to 22 % higher for the semi-active system than for the passive system. Besides, as for the laden vehicle, the maximum absolute chassis accelerations for the standard brick are strongly influenced by forces transmitted through

²See for an explanation of the following symbols the legends in Tables 4.3 and 4.4.

Table 4.3: Percentage of performance improvement (white blocks) or performance deterioration (black blocks) of the un-laden 3D model with semi-active tractor rear axle suspension with respect to the un-laden 3D vehicle model with passive tractor rear axle suspension: comfort

aspect	criterion	standard brick	traffic hump	scraped road	well	wave	legend [%]
comfort	max $ \ddot{q}_{sv} $	■	■	□	■	□	
	max $ \ddot{q}_{slo} $	■	□	□	□	■	
	max $ \ddot{q}_{sla} $	□	□	■	■	·	
	max $ \ddot{q}_{sv,w} $	■	■	·	·	□	
	max $ \ddot{q}_{slo,w} $	■	·	□	□	■	
	max $ \ddot{q}_{sla,w} $	□	□	·	·	■	 50
	RMS \ddot{q}_{sv}	■	·	□	□	·	 40
	RMS \ddot{q}_{slo}	■	□	□	□	·	 30
	RMS \ddot{q}_{sla}	■	■	·	·	■	 20
	RMS $\ddot{q}_{sv,w}$	■	·	□	□	·	 10
	RMS $\ddot{q}_{slo,w}$	·	·	□	□	·	 5
	RMS $\ddot{q}_{sla,w}$	□	■	□	□	■	 1
	VD \ddot{q}_{sv}	■	·	□	·	□	· 1
	VD \ddot{q}_{slo}	·	□	□	□	■	■ 5
	VD \ddot{q}_{sla}	■	■	■	·	■	■ 10
	VD $\ddot{q}_{sv,w}$	■	·	□	□	□	■ 20
	VD $\ddot{q}_{slo,w}$	·	·	□	□	·	■ 30
	VD $\ddot{q}_{sla,w}$	·	·	□	□	■	■ 40
	max $ \ddot{q}_{sv} $	□	■	□	□	□	■ 50
	max $ \ddot{q}_{slo} $	·	□	 40	·	■	
	max $ \ddot{q}_{sla} $	■	■	■	■	■	
	RMS $ \ddot{q}_{sv} $	■	■	□	□	□	
	RMS $ \ddot{q}_{slo} $	■	□	□	□	·	
	RMS $ \ddot{q}_{sla} $	■	■	■	·	·	

$q_{..}$: displacement, specified by ..

w : weighted

s : driver seat

v : vertical

lo : longitudinal

la : lateral

Table 4.4: Percentage of performance improvement (white blocks) or performance deterioration (black blocks) of the un-laden 3D model with semi-active tractor rear axle suspension with respect to the un-laden 3D vehicle model with passive tractor rear axle suspension: load, deflection, handling and damage

aspect	criterion	standard	traffic	scraped	well	wave	legend [%]
		brick	hump	road			
load	$\max \ddot{q}_{kv} $	□	•	■	•		
	$\max \ddot{q}_{cvlr} $	□	•	■	•	•	
	$\max \ddot{q}_{cvr'r} $	□	•	■		•	
	PM \ddot{q}_{cvlf}	■		□	■	•	□ 50
	PM $\ddot{q}_{cvr'f}$	■	•	□	■	•	□ 40
	PM \ddot{q}_{cvlr}	□	□	■	□	■	□ 30
	PM $\ddot{q}_{cvr'r}$	□	□	■	□	•	□ 20
deflection	nr bound hits $\dot{l}r$						□ 10
	nr bound hits $\dot{r}r$						• 5
	$\max \Delta \dot{q}_{lr} $ at bounds						• 1
	$\max \Delta \dot{q}_{r'r} $ at bounds						• 1
	RMS Δq_{lr}	□	•	□	□	■	• 5
	RMS $\Delta q_{r'r}$	□	•	□	□	■	• 10
handling	tire lift-off $\dot{l}r$	□		□	□		■ 20
	tire lift-off $\dot{r}r$		□	□			■ 30
	<75% stat tire force $\dot{l}r$	■	•	■	□	•	■ 40
	<75% stat tire force $\dot{r}r$	■	•	■	•	□	■ 50
	RMS dyn tire force $\dot{l}r$	•		□	□	•	
	RMS dyn tire force $\dot{r}r$	■		□	•	•	
damage	road damage all tires	•	□		□	•	
	road damage rear tires	■	□	□	□	•	

$q_{..}$: displacement, specified by ..

$$\Delta q_{..} = q_{c..} - q_{a..}$$

a : tractor axle c : tractor chassis k : kingpin v : vertical f : front r : rear l' : left r' : right

the links which connect the tractor chassis and the rear axle. For the traffic hump, the scraped road and the well, these higher maximum absolute acceleration values are explicable because for these roads the controller focuses on a reduction of the tire lift-off time at the moments these maximum absolute accelerations occur. Furthermore, Figure 4.7 shows that for the scraped road and the well, the high acceleration peaks in the signals $\ddot{q}_{cvl'r}$ and $\ddot{q}_{cvt'r}$ after the danger for tire lift-off has disappeared, are lower for the semi-active system than for the passive system. For the wave, the controller of the semi-active system focuses at time t on a reduction of the values for $\max|\ddot{q}_{cvl'r}|$ and $\max|\ddot{q}_{cvt'r}|$ over the preview interval $[t, t + t_p]$. However, as for the laden situation, this does not result in a reduction of the average value for $\max|\ddot{q}_{cvl'r}|$ and $\max|\ddot{q}_{cvt'r}|$ over the total simulation time. This is probably caused by a too short preview interval for this road.

Now, the values for the criteria that are not directly related to the control objective are studied. Table 4.3 shows decreased values for some comfort criteria and increased values for other comfort criteria for the semi-active system with respect to the passive system. For the standard brick, the traffic hump and the wave, the values of most comfort criteria are higher for the semi-active system than for the passive system whereas for the scraped road and the well, the values of most comfort criteria are lower for the semi-active system than for the passive system. Furthermore, the damping behavior of the relative longitudinal displacement with respect to the nominal longitudinal displacement, the lateral displacement and the vertical displacement of the seat is, as for the laden vehicle, rather similar for the passive and the semi-active vehicle. The results for the standard brick show that a reduction of the maximum absolute chassis accelerations at the rear side of the tractor not automatically results in an improvement of comfort, which is the same conclusion as drawn for the laden situation.

As seen before, only for the standard brick the incidental loads on the chassis components, *i.e.* $\max|\ddot{q}_{cvl'r}|$ and $\max|\ddot{q}_{cvt'r}|$, are lower for the semi-active system than for the passive system. Contrary to the results for the laden vehicle, this leads to a reduction of the incidental load on the semitrailer for the semi-active system with respect to the passive system. For the standard brick, the traffic hump and the wave, the average fatigue load is lower whereas for the scraped road and the well, it is higher for the semi-active system than for the passive system. The large reduction of the PM numbers for the semi-active system with respect to the passive system, shown for the laden vehicle for the incidental road excitations, except for the wave, are certainly not valid for the un-laden vehicle. It is remarkable that often a decrease (increase) of the PM numbers for the front side of the tractor goes together with an increase (decrease) of these numbers for the rear side of the tractor for the semi-active system with respect to the passive system.

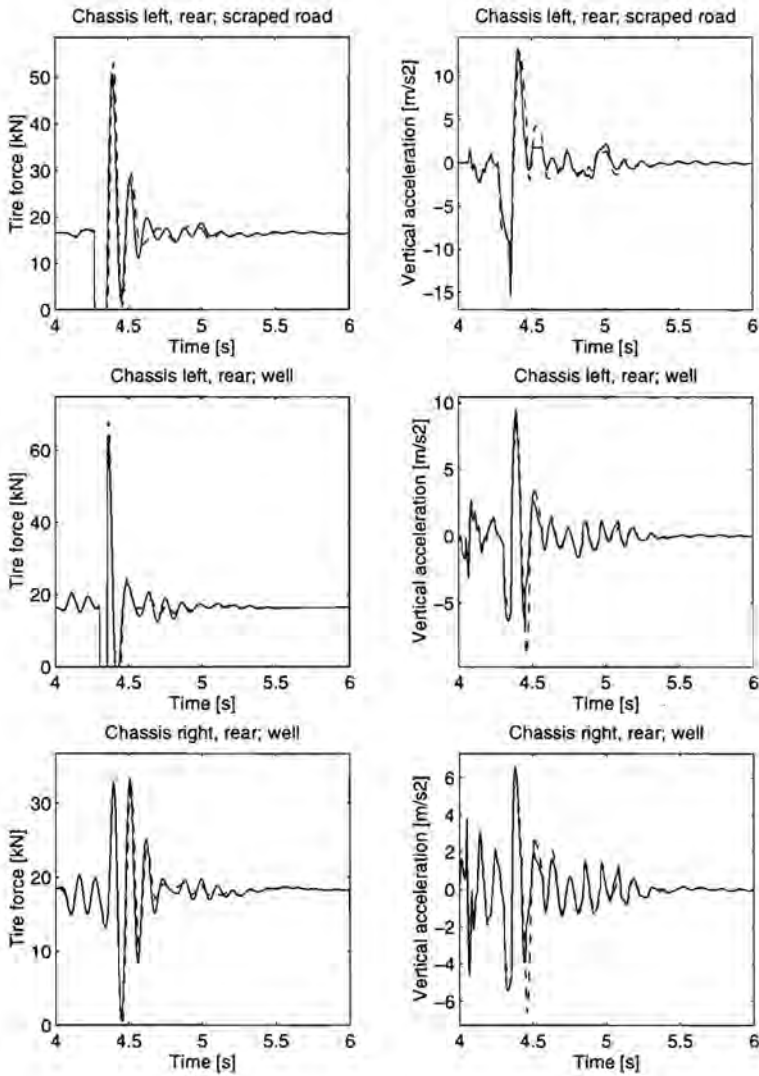


Figure 4.7: Tire forces and vertical accelerations as a function of time at the rear side of the tractor for the un-laden vehicle; — : semi-active; - - : passive

The handling capabilities of the vehicle model are judged with the tire lift-off time, the time for which less than 75 % of the static tire force is available and the RMS value of the dynamic tire force. The results show that a reduction of the tire lift-off time does not automatically lead to a reduction of the values for the other handling criteria. These differences in the assessment of the handling capabilities of the vehicle by the different handling criteria makes the choice of an appropriate handling criterion in the control objective of the semi-active system to an important issue.

The road damage for the laden vehicle is much higher than for the un-laden vehicle and therefore more important. Nevertheless, the total road damage for the un-laden semi-active system is 1 to 4 % lower than the total road damage for the un-laden passive system for all incidental road excitations except for the wave.

4.3.3 Conclusions

In this chapter, the simulation results for the 3D vehicle model with a passive tractor rear axle suspension are compared to the simulation results for the 3D vehicle model with a semi-active tractor rear axle suspension. The 3D vehicle model approximates the behavior of a real tractor-semitrailer for the frequency range of 0 to 15 Hz. Unfortunately, the influence of chassis flexibilities and some of the semitrailer flexibilities on the vehicle response in this frequency range could not be incorporated.

Some conclusions can be drawn from the comparisons between the vehicle with a passive tractor rear axle suspension and the vehicle with an ADCC controlled semi-active tractor rear axle suspension that uses the nonlinear two-DOF model of Section 3.1 as controller internal model and the control objective of Section 3.2.:

- The performance of the semi-active system with respect to that of the passive system is disappointing for the wave. As explained in Chapter 3, this is probably due to a too short preview interval for this road surface.
- The semi-active system shows 3 to 20 % lower average tire lift-off times than the passive system for the considered payload/road excitation combinations where tire lift-off occurs, except for the wave.
- The maximum absolute accelerations at the rear side of the tractor are 3 to 5 % lower for the semi-active system than for the passive system for situations where tire lift-off and hits of the bounds on the suspension deflection do not (tend to) occur, except for the wave. Sometimes even larger reductions of these maximum absolute accelerations occur for the semi-active system with respect to the maximum absolute accelerations for the passive system for situations where tire lift-off does occur. Often a reduction of other high peaks in the chassis accelerations at the rear side of the tractor is obtained for the semi-active system,

even if tire lift-off occurs. The reduction of these peaks is sometimes larger than the reduction of the maximum absolute chassis accelerations.

- A reduction of the maximum absolute chassis accelerations at the rear side of the tractor leads to a reduction of the peak load on the cargo of the laden vehicle for symmetric road excitations, a reduction of the fatigue load on the chassis components at the rear side of the tractor, but not automatically to an improved comfort and to a reduction of the peak load on the cargo of the laden vehicle for asymmetric road excitations.
- The total road damage caused by the wheels of the tractor and the semitrailer of the semi-active system varies from -6 to +7 % with respect to the total road damage for the passive system.
- The results show that not only the air springs and the dampers but also the axle guidance may influence the performance of the suspension.

Review, conclusions and recommendations

5.1 Review

This section gives an overview of the research described in this thesis, together with the results.

The objective is to develop a controller for a semi-active suspension with an adjustable damper for the tractor rear axle suspension of a tractor-semitrailer combination, using wheelbase preview of the road. The system has to improve the dynamic behavior of the vehicle compared to that of the passive vehicle for incidental road excitations.

The requirements with respect to the dynamic behavior, like comfort of the occupants, load on the chassis components and on the cargo, handling and road damage, are subjective. A suitable representation of these requirements in a simple mathematical form is not available at this moment. This makes the development of such a semi-active system rather difficult. Together with the switching dynamics and the nonlinear force-relative velocity characteristics of the adjustable damper, this makes it impossible to use the classical linear optimal control theory, using quadratic performance criteria. Therefore, in Chapter 3 model-based control methods for the semi-active suspension are proposed which can take the nonlinear behavior of the dampers and other elements into account and can handle a broad class of control objectives. All methods are based on knowledge of the road surface between the front and the rear wheels of the tractor. This so-called preview information may be obtained by reconstruction from measurements at the vehicle. The controllers split the time interval for which the oncoming road surface is known, the preview interval, in subintervals of equal length and determine an optimal, constant damper setting for each of these subintervals.

The developed control methods use the damper either as a continuously variable damper or as a multi-level damper. In a continuously variable damper an infinite

number of force-relative velocity characteristics can be realized whereas this number is finite for a multi-level damper. For the multi-level damper, the direct calculation controller (DCC) and the branch-and-bound controller (BBC) are presented. The DCC is applicable for a broad class of control objectives whereas the BBC is applicable for control objectives with a monotonously non-decreasing objective function over the preview interval for each damper setting combination. For these objectives, the BBC is preferable to the DCC because it requires at the utmost the same but in general much less CPU time to determine the optimum control sequence over a preview interval. Furthermore, if the allowed controller computation time is too small to determine this sequence then it is likely that the optimum of the BBC is the optimum over a larger part of the preview interval. So in real time applications, a less powerful computation device may be used for the BBC than for the DCC for nearly the same performance. Both the DCC and the BBC determine the global optimum for the stated control objective if enough time is available for the computation of the optimum control sequence over the complete preview interval. However, for cases with a huge number of possible control sequences over the preview interval or for multi-level dampers with many levels, an alternative controller based on dynamic programming may be more suitable (see Muijderman et al. [29]). For the continuously variable damper, so-called SQPC controllers are presented. These controllers are based on sequential quadratic programming and can handle control objectives with constraints. A drawback is that these SQPC controllers may converge to a local optimum for the stated control problem.

For further development of the control concepts and to make comparison of the different suspension types possible, a specific internal vehicle model and a specific objective are chosen. The order of the internal vehicle model is restricted in practice due to the enormous increase of controller CPU time for increasing order. Here, a two-DOF model is used because this is the simplest model that shows the conflict between comfort, suspension deflection and tire force. The minimization of the maximum absolute acceleration of the sprung mass, without tire lift-off and without reaching the bounds on the suspension deflection, is chosen as the control objective. If tire lift-off is inevitable then the lift-off time must be as small as possible. If reaching the bounds on the suspension deflection is inevitable then the impact forces, *i.e.* the relative velocities between the sprung mass and the unsprung mass just before the bounds are reached, must be as small as possible.

To facilitate the choice of the control parameters and to select a damper type and a control method for the tractor rear axle suspension of an extensive 3D tractor-semitrailer model, a two-DOF simulation model is used. This model describes the behavior of half the rear side of the tractor for the laden situation.

The control parameters are established by using a two-level damper with a DCC.

The optimum parameters for the BBC strategy will be the same and it is expected that the optimum parameters for the DCC will result in the best possible performance of the systems with continuously variable damper. With respect to the control parameters, it is shown that:

- A better performance of the semi-active system than that of a good passive system is only obtained for subinterval lengths smaller than or at least close to the smallest natural oscillation time of the linearized two-DOF model. Therefore, the length of the subintervals is chosen equal to 0.050 s, which is somewhat smaller than the mentioned natural oscillation time. A smaller subinterval length is not chosen as the computation time of the controller increases enormously if the length of the subintervals decreases.
- The performance of the semi-active system decreases considerably if the optimum damper setting combination for a preview interval is applied for more than two subintervals with length 0.050 s. It is decided to apply only the optimum damper setting for the first subinterval, in order to be at the safe side.
- Responses of the controller internal model are required to determine the performance for a given damper setting sequence. These responses are properly determined by an explicit Euler integration routine with a stepsize of 0.001 s. This algorithm is about two times faster than a variable-order variable-step Adams routine which evaluates the responses at a sample interval of 0.005 s. It is therefore chosen for application in the controller.

For the incidental road excitations, the performance of the 'laden' two-DOF simulation model with the passive suspension and the performances of this model with the different semi-active suspensions are compared for a large number of performance criteria, using the earlier determined control parameters. This provides insight in the performance of the different suspension types and in the performance criteria. First, only the criteria closely related to the control objective are considered. With respect to these criteria, the following conclusions can be drawn:

- The performance of the semi-active systems for one of the incidental road excitations, *i.e.* the wave, is disappointing. This is probably caused by a too short preview interval for this road surface. The performances of the semi-active systems for the other road excitations are very promising. Reductions of more than 25 % of the maximum absolute sprung mass acceleration are obtained for road excitations where the bounds on the suspension deflection and the tire force are not reached whereas reductions of about 10 % of the tire lift-off time are possible if the semi-active system can focus entirely on a reduction of the tire lift-off time. Furthermore, for the road excitations where tire lift-off occurs, at least some of the high sprung mass acceleration peaks are lower for the semi-active systems

than for the passive system,

- The controlled two-level damper is preferable to the controlled continuously variable damper, as the performance is nearly equal and the computational burden is much lower.

With respect to the other criteria, the following conclusions can be drawn:

- All evaluated quantitative comfort criteria, except the maximum absolute jerk, are lower for the semi-active systems than for the passive system if the controllers focus entirely on a reduction of the maximum absolute sprung mass acceleration.
- The quantitative comfort criteria which depend on the complete time response of the vehicle model (RMS and VD values) are lower for the systems with continuously variable damper than for the system with two-level damper if the controllers focus entirely on a reduction of the maximum absolute sprung mass acceleration.
- If the bounds on the suspension deflection are reached or if tire lift-off occurs and the controllers can not focus on a reduction of the maximum absolute sprung mass acceleration only, then most of the quantitative comfort criteria are still lower for the semi-active systems than for the passive system, even if the maximum of the absolute sprung mass acceleration over the total simulation time is not reduced.
- The damping behavior of the semi-active system with DCC controlled two-level damper is worse whereas the damping behavior of the semi-active system with SQPC controlled continuously variable damper can be equal to or better than that for the passive system.
- The fatigue damage for the semi-active systems is much lower than for the passive system.
- The road damage varies considerably between the different suspension types. For example, the road damage for the semi-active systems varies between -37 to +69 % compared to the road damage for the passive system.

The two-level damper with DCC is chosen for further development, because the performance with respect to the criteria closely related to the control objective is nearly equal for the two-level damper and the continuously variable damper whereas the computational burden is much lower for the controller of the two-level damper than for the controllers of the continuously variable damper.

The DCC strategy has to be adapted in order to obtain an applicable strategy, *i.e.* a strategy which takes into account the required CPU time for determining the optimum control sequence over the preview interval. The time of the first subinterval is used to determine the best control input for the remaining subintervals, given the current state of the controlled system and the preview information. During the first subinterval, the optimum damper setting for this interval according to the previous preview interval is applied to the controlled system. For this applicable direct calculation controller

(ADCC), it is shown that the system performance does not deteriorate if the controller is forced to choose the damper settings in the 7th and subsequent subintervals equal to the damper setting in the 6th subinterval. This knowledge can be used to limit the increase of computational burden for the controller at low vehicle velocities. A further reduction of the number of subintervals with independent damper settings seems to be possible with only a small performance deterioration.

Unfortunately, it was not possible to use a real tractor-semitrailer for the evaluation of the performance of the proposed semi-active rear axle suspension. Instead, an elaborated 3D model of the tractor-semitrailer is used. The model reasonably approximates the behavior of a real tractor-semitrailer. Differences are mainly due to the assumed rigidity of the tractor chassis and the assumed high stiffness of the semitrailer frame. The semi-active 3D model contains a tractor rear axle suspension with a two-level damper at both the left and the right side. Each damper is controlled by its own ADCC. Each controller uses a two-DOF internal vehicle model and is provided with the preview information on the road surface between the front and the rear wheels of the tractor at the side of the controlled damper. The earlier chosen control parameters are used and eventually present 7th and subsequent subintervals are forced to choose the same damper setting as the 6th subinterval. The performance of this semi-active system is compared to the performance of a 3D model with conventional passive dampers in the tractor rear axle suspension for a number of incidental road excitations and for both the laden and the un-laden vehicle. The conclusions that can be drawn from this comparison are:

- For the wave, the performance of the semi-active system is disappointing in comparison to the performance of the passive system. This was also the case for the two-DOF simulation model and is probably due to a too short preview interval for this road surface.
- The performance improvement of the semi-active system compared to the performance of the passive system with respect to the quantities closely related to the control objective is sometimes less than predicted with the two-DOF simulation model, but there is still some improvement. The reduction of the maximum absolute accelerations at the rear side of the tractor chassis for road excitations where the bounds on the suspension deflection and the tire force are not reached is less than 5 % and the tire lift-off times of the semi-active system are 3 to 20 % lower than those for the passive system. Furthermore, often a reduction of other high peaks in the chassis accelerations at the rear side of the tractor is obtained for the semi-active system with respect to the passive system. The reduction of these peaks is sometimes larger than the reduction of the maximum absolute acceleration.

- A reduction of the maximum absolute chassis accelerations at the rear side of the tractor leads to a reduction of the peak load on the cargo of the laden vehicle for symmetric road excitations, a reduction of the fatigue load on the chassis components at the rear side of the tractor, but not automatically to improved comfort for the occupants of the vehicle and not automatically to a reduction of the peak load on the cargo of the laden vehicle for asymmetric road excitations.
- The total road damage of the wheels of the tractor and the wheels of the semitrailer for the semi-active 3D model varies considerably, *i.e.* within a range of -6 % to +7 %, with respect to the road damage of the passive 3D model.
- The results for the standard brick show that not only the air springs and the dampers but also the axle guidance influences the performance of the suspension.

5.2 Conclusions

Model-based control methods which use wheelbase preview of the road are proposed for a multi-level damper and for a continuously variable damper. All methods can handle a broad class of control objectives and can take into account the nonlinear characteristics of air springs, dampers and tires. From simulations with a nonlinear two-DOF vehicle model it can be concluded that:

- The length of the subintervals in the preview interval has to be close to or smaller than the smallest natural oscillation time of the linearized two-DOF model in order to obtain a better performance for the semi-active system than for a system with a good passive suspension.
- The performance of the semi-active system decreases strongly if the application interval of the optimum damper setting combination over a preview interval is longer than the smallest natural oscillation time of the linearized two-DOF model.
- The performances of the semi-active systems compared to the performance of a representative passive system are promising for most of the evaluated incidental road excitations. Reductions of more than 25 % of the maximum absolute sprung mass acceleration are obtained for road excitations where the bounds on the suspension deflection and the bound on the tire force are not reached whereas reductions of about 10 % of the tire lift-off time are possible if the semi-active system can focus entirely on a reduction of the tire lift-off time.
- The system with two-level damper and the system with continuously variable damper show comparable reductions of the maximum absolute sprung mass acceleration and the excesses of the bounds on the suspension deflection and the bound on the tire force. The values for those evaluated quantitative comfort criteria which depend on the complete time response of the vehicle model (RMS

values etc.) are higher and the damping behavior is worse for the semi-active system with two-level damper than for the semi-active system with continuously variable damper. However, the required computation time of the control methods for the two-level damper is less than 2.5 % of the required computation time of the control methods for the continuously variable damper for the same number of subintervals in the preview interval.

From simulations with a 3D tractor-semitrailer model with controlled two-level dampers in the tractor rear axle suspension and a 3D model with conventional passive suspension it can be concluded that:

- The performance improvement of the semi-active system compared to the performance of the passive system with respect to the quantities closely related to the control objective is sometimes less than predicted with the two-DOF simulation model, but there is still some improvement. The reduction of the maximum absolute accelerations at the rear side of the tractor chassis for road excitations where the bounds on the suspension deflection and the tire force are not reached is maximum 5 % and the tire lift-off times of the semi-active system are 3 to 20 % lower than those for the passive system. Furthermore, often a reduction of other high peaks in the chassis accelerations at the rear side of the tractor is obtained for the semi-active system with respect to the passive system. The reduction of these peaks is sometimes larger than the reduction of the maximum absolute acceleration.
- A reduction of the maximum absolute chassis accelerations at the rear side of the tractor leads to a reduction of the peak load on the cargo of the laden vehicle for symmetric road excitations, a reduction of the fatigue load on the chassis components at the rear side of the tractor, but not automatically to an improved comfort for the occupants of the vehicle and not automatically to a reduction of the peak load on the cargo of the laden vehicle for asymmetric road excitations.
- The total road damage caused by the wheels of the tractor and the semitrailer of the semi-active 3D model varies considerably, *i.e.* within a range of -6 to +7 %, with respect to the road damage of the passive 3D model.
- The results show that not only the air springs and the dampers but also the axle guidance may influence the performance of the suspension.

5.3 Recommendations

Based on the results, the following recommendations and considerations concerning future investigations can be given:

- A very important subject for future research is the translation of subjective notions, like comfort and handling, into mathematical terms. A prototype vehicle with the proposed semi-active system might be useful with regard to this aspect. Subjective occupant opinions about comfort and handling of this vehicle for different control objectives may be used for establishing mathematical descriptions for comfort and handling.
- The reduction of the maximum absolute accelerations at the rear side of the tractor chassis does not lead to improved comfort for the occupants of the vehicle. If both the load on the chassis components and on the cargo has to be reduced and the comfort of the occupants has to be improved and only two semi-active dampers can be applied, then it is recommendable to use a higher order controller internal vehicle model which incorporates a suspended cabin, to use cabin related quantities as comfort criterion in the control objective and to put the dampers in the tractor rear axle suspension. Depending on whether the longitudinal movements or the lateral movements of the cabin are the most annoying, a front-rear half vehicle model or a left-right half vehicle model has to be used. For determining the responses of a front-rear half vehicle model over the preview interval, not only the road height between the front and the rear wheels of the tractor is required but also the road height before the front wheels of the tractor. This implies that a controller with a front-rear half vehicle model either has to make assumptions about the road height in front of the vehicle or requires look-ahead sensors which 'measure' the road height in front of the vehicle for the controller. Further investigation has to show then whether or not a controlled adjustable damper at the rear side of the tractor indeed can simultaneously improve the load on the chassis components/cargo and the comfort of the occupants. There is a large number of dynamic elements between the adjustable damper and the cabin or seat. Therefore, if the improvement of comfort is much more important than the reduction of the load on the chassis components/cargo or if more than two semi-active dampers can be used then it is recommendable to put adjustable dampers in the cabin suspension and/or in the seat suspension for the improvement of occupants comfort.
- The results show that for some road excitations the preview information is not enough for a suitable choice of the optimum control sequence. Therefore, weighting the terminal state of the preview interval in the performance index is recommended. This gives the controller the opportunity to put emphasis on a suitable system state at the end of the preview interval for unforeseen future obstacles. For example, a static equilibrium state can be preferred to a state with large suspension compression in combination with a high inward suspension velocity for

the end of a preview interval.

- Preliminary, not reported, simulation results show potential for the semi-active system to improve the performance for stochastic road excitations, like brick paved roads and motor-ways, compared to the performance of a passive system for these roads. Further investigating the possible performance improvement of the semi-active system compared to the performance of a passive system on these road surfaces is recommended. After all, it would be advantageous if the switching possibility of the damper is useful for all road excitations and not only at incidents.
- A number of the natural frequencies of the chassis and the semitrailer in the frequency range 0 to 15 Hz are not taken into account by the 3D vehicle model. They might deteriorate the performance of the semi-active system. Investigation of the influence of these un-modeled dynamics on the performance of the semi-active system is therefore useful.
- Further development of the proposed semi-active suspension system requires building and testing of a prototype vehicle with this system. It is recommended to build a prototype where the controller uses an analog electronic circuit (representing a time scaled equivalent of the controller internal model) for determining the responses for the possible damper setting combinations (see de Jager [21]) and a digital device for the evaluation and comparison of the performances for the damper setting combinations. Such a configuration is fast and relatively cheap whereas the flexibility of the controller with respect to the control objective is maintained. Assuming that the accuracy of the reconstructor, used to estimate the current state of the vehicle and the preview information, is already optimized in tests, actual driving tests with the complete prototype vehicle will show the effectiveness of the controlled suspension system. Furthermore, the robustness of the control loop for measurement noise, for parameter errors (*e.g.* differences in the actual and the estimated vehicle velocity for the oncoming preview interval), for disturbances and for un-modeled dynamics will reveal.
- To avoid running in all practical problems related to an implementation at the same time, hardware-in-the-loop (HWIL) simulations may be useful as an intermediate step (see Vissers [41]). For example, a HWIL set up where the damper in the simulation model is replaced by a real semi-active damper may reveal unforeseen time delays and time lags in the control loop and the suitability of the damper model in the controller internal model.
- It might be possible to determine switching rules for the adjustable damper by comparison of the calculated optimal damper settings and the responses of the semi-active system. These rules might be used to establish a knowledge based controller with a small computation time. A first attempt to establish such a

controller is described by Soede [34].

- The results show that it is important to take the axle guidance into account for the improvement of the suspension performance. Reconsideration of the air springs is recommended. The forces transmitted by these springs are often larger than the forces transmitted by the dampers. Some research on adjustable spring stiffnesses is carried out by Benschop [5]. His simulation results show relatively large performance improvements for a system with an adjustable spring compared to a passive system.

Appendix A

Determination of the penalty factors in the control objective criterion

The choice of values for penalty factors in a criterion function is often rather difficult. Scaling is often used to facilitate this choice. This appendix shows how the penalty factors in the criterion function of Section 3.2 can be scaled and how the scaled factors can be determined.

The mentioned criterion (without the term J_{ext}) can be written as

$$J = \max_{j \in \{1, 2, \dots, C\}} [a(j) + V_1 \cdot b(j) + V_2 \cdot c(j) + W \cdot d], \quad (\text{A.1})$$

where

$$a(j) = |\dot{x}_3(t + j\Delta h_c)| \quad (\text{A.2})$$

$$b(j) = \delta^l(t + j\Delta h_c) \quad (\text{A.3})$$

$$c(j) = \delta^u(t + j\Delta h_c) \quad (\text{A.4})$$

$$d = \Delta h_c \sum_{j=1}^{C-1} \varepsilon(F_l(t + j\Delta h_c)) + \frac{1}{2} \Delta h_c \varepsilon(F_l(t + C\Delta h_c)). \quad (\text{A.5})$$

The weighting factors V_1 , V_2 and W can be scaled by writing them as

$$V_1 = \frac{V_1^* \cdot a_{max}}{b_{max}}, \quad V_2 = \frac{V_2^* \cdot a_{max}}{c_{max}}, \quad W = \frac{W^* \cdot a_{max}}{d_{max}}, \quad (\text{A.6})$$

where a_{max} , b_{max} , c_{max} and d_{max} are estimates for the maxima of respectively a , b , c and d and V_1^* , V_2^* and W^* are factors determining the importance of the corresponding penalized quantity with respect to quantity a . The latter is easily seen by writing the criterion function as

$$J = \max_{j \in \{1, 2, \dots, C\}} \left(a_{max} \left[\left(\frac{a(j)}{a_{max}} \right) + V_1^* \cdot \left(\frac{b(j)}{b_{max}} \right) + V_2^* \cdot \left(\frac{c(j)}{c_{max}} \right) + W^* \cdot \left(\frac{d}{d_{max}} \right) \right] \right). \quad (\text{A.7})$$

Hence, V_1 , V_2 and W can be determined if a_{max} , b_{max} , c_{max} , d_{max} , V_1^* , V_2^* and W^* are known. It is possible to determine estimates for a_{max} , b_{max} , c_{max} and d_{max} from simulations with a two-DOF vehicle model with a passive suspension. Furthermore, V_1^* , V_2^* and W^* can be determined by looking at the importance of the penalized quantities with respect to quantity a .

Appendix B

**Performance of the 3D vehicle
model**

Table B.1: Performance of the laden 3D vehicle model with passive (PASM) and semi-active (ADCC) tractor rear axle suspension.

			standard brick		traffic hump		scraped road		well		wave	
aspect	criterion	unit	PASM	ADCC	PASM	ADCC	PASM	ADCC	PASM	ADCC	PASM	ADCC
comfort	max $ \ddot{q}_{sv} $	[m/s ²]	8.37	9.36	16.49	16.36	10.20	10.17	20.08	18.40	41.35	55.19
	max $ \ddot{q}_{sto} $	[m/s ²]	4.34	5.35	5.11	5.47	2.11	2.13	18.00	15.69	22.73	32.75
	max $ \ddot{q}_{sla} $	[m/s ²]	12.14	12.96	0.33	0.40	0.61	0.65	31.45	28.32	2.77	2.93
	max $ \ddot{q}_{sv,w} $	[m/s ²]	2.11	2.27	10.40	10.33	8.23	8.31	12.42	11.57	28.33	43.03
	max $ \ddot{q}_{sto,w} $	[m/s ²]	0.66	0.74	3.58	3.59	1.90	1.91	4.36	3.98	6.32	6.73
	max $ \ddot{q}_{sla,w} $	[m/s ²]	1.23	1.16	0.32	0.30	0.25	0.25	3.30	2.92	1.86	1.14
	RMS \ddot{q}_{sv}	[m/s ²]	0.86	0.90	4.64	4.54	2.50	2.48	3.10	2.91	10.80	13.02
	RMS \ddot{q}_{sto}	[m/s ²]	0.65	0.68	0.89	0.88	0.54	0.55	1.95	1.79	3.34	4.18
	RMS \ddot{q}_{sla}	[m/s ²]	1.23	1.27	0.10	0.10	0.12	0.12	2.73	2.57	0.64	0.67
	RMS $\ddot{q}_{sv,w}$	[m/s ²]	0.40	0.43	3.26	3.17	1.92	1.90	2.62	2.45	8.08	10.43
	RMS $\ddot{q}_{sto,w}$	[m/s ²]	0.10	0.10	0.89	0.86	0.62	0.64	0.53	0.50	2.06	2.39
	RMS $\ddot{q}_{sla,w}$	[m/s ²]	0.16	0.17	0.11	0.10	0.06	0.07	0.78	0.75	0.54	0.36
	VD \ddot{q}_{sv}	[m/s ^{1.75}]	2.75	2.83	8.74	8.53	5.51	5.42	7.40	6.87	20.05	26.94
	VD \ddot{q}_{sto}	[m/s ^{1.75}]	1.81	1.90	2.03	2.05	1.04	1.07	5.76	5.14	7.90	10.81
	VD \ddot{q}_{sla}	[m/s ^{1.75}]	4.06	4.22	0.18	0.18	0.27	0.26	8.90	8.09	1.31	1.37
	VD $\ddot{q}_{sv,w}$	[m/s ^{1.75}]	0.89	0.93	5.86	5.69	4.10	4.08	5.64	5.26	15.62	22.26
	VD $\ddot{q}_{sto,w}$	[m/s ^{1.75}]	0.24	0.25	1.76	1.77	1.13	1.14	1.58	1.44	3.56	3.99
	VD $\ddot{q}_{sla,w}$	[m/s ^{1.75}]	0.40	0.41	0.18	0.17	0.12	0.12	1.56	1.49	1.07	0.66
	max $ \ddot{\ddot{q}}_{sv} $	[m/s ³]	588	585	532	514	370	376	1558	1421	1797	2480
	max $ \ddot{\ddot{q}}_{sto} $	[m/s ³]	494	489	274	307	93	77	1264	1129	1307	2183
	max $ \ddot{\ddot{q}}_{sla} $	[m/s ³]	881	934	14	17	35	32	1726	1606	146	251
	RMS $ \ddot{\ddot{q}}_{sv} $	[m/s ³]	61	63	84	81	56	56	164	154	310	416
RMS $ \ddot{\ddot{q}}_{sto} $	[m/s ³]	62	64	41	42	15	16	178	162	240	305	
RMS $ \ddot{\ddot{q}}_{sla} $	[m/s ³]	89	91	4	4	7	7	199	185	30	42	

Table B.2: Performance of the laden 3D vehicle model with passive (PASM) and semi-active (ADCC) tractor rear axle suspension.

			standard brick		traffic hump		scraped road		well		wave	
aspect	criterion	unit	PASM	ADCC	PASM	ADCC	PASM	ADCC	PASM	ADCC	PASM	ADCC
load	max $ \ddot{q}_{kv} $	$[\text{m/s}^2]$	2.36	2.38	8.23	7.92	8.07	7.14	5.24	5.55	40.63	44.49
	max $ \ddot{q}_{cvlr} $	$[\text{m/s}^2]$	4.10	3.99	9.05	8.57	10.14	9.05	7.17	7.29	48.01	53.82
	max $ \ddot{q}_{cvt\dot{r}} $	$[\text{m/s}^2]$	7.34	7.14	8.98	8.50	10.25	9.18	8.17	7.54	47.70	54.12
	PM \ddot{q}_{cvtf}	$[-]$	2.52	2.04	1.51	1.23	1.31	1.33	74.04	45.65	165.29	378.01
	PM $\ddot{q}_{cvt\dot{r}f}$	$[-]$	0.91	0.73	1.45	1.19	1.28	1.28	30.98	17.98	158.43	374.74
	PM \ddot{q}_{cvtlr}	$[-]$	0.00	0.00	0.43	0.21	0.16	0.10	0.18	0.16	1603.32	2519.76
	PM $\ddot{q}_{cvt\dot{r}r}$	$[-]$	0.01	0.01	0.41	0.20	0.16	0.10	0.19	0.13	1396.73	2190.23
deflection	nr bound hits $\dot{l}r$	$[-]$	0	0	0	0	0	0	0	0	2	5
	nr bound hits $\dot{r}r$	$[-]$	0	0	0	0	0	0	0	0	1	4
	max $ \Delta\dot{q}_{lr} $ at bounds	$[\text{m/s}]$	0.00	0.00	0.00	0.00	0.00	0.00	0.00	0.00	0.96	1.35
	max $ \Delta\dot{q}_{r\dot{r}} $ at bounds	$[\text{m/s}]$	0.00	0.00	0.00	0.00	0.00	0.00	0.00	0.00	1.09	0.79
	RMS Δq_{lr}	$[10^{-2} \text{ m}]$	0.17	0.18	3.67	3.53	1.75	1.86	1.02	0.93	7.89	8.36
	RMS $\Delta q_{r\dot{r}}$	$[10^{-2} \text{ m}]$	0.29	0.26	3.65	3.50	1.79	1.87	0.61	0.58	7.88	8.41
handling	tire lift-off $\dot{l}r$	$[\text{s}]$	0.000	0.000	0.000	0.000	0.038	0.035	0.075	0.060	0.337	0.514
	tire lift-off $\dot{r}r$	$[\text{s}]$	0.000	0.000	0.000	0.000	0.036	0.033	0.000	0.000	0.341	0.388
	<75% stat tire force $\dot{l}r$	$[\text{s}]$	0.033	0.033	0.232	0.295	0.082	0.086	0.108	0.100	0.819	0.884
	<75% stat tire force $\dot{r}r$	$[\text{s}]$	0.000	0.000	0.214	0.289	0.076	0.082	0.035	0.035	0.816	0.850
	RMS dyn tire force $\dot{l}r$	$[10^3 \text{ N}]$	5.85	5.98	15.06	13.19	10.22	11.01	18.48	17.24	47.76	52.25
	RMS dyn tire force $\dot{r}r$	$[10^3 \text{ N}]$	1.11	1.46	14.96	13.10	10.32	11.01	5.08	5.30	48.07	53.02
damage	road damage all tires	$[10^{20} \text{ -}]$	4.72	4.71	1.13	1.12	1.37	1.43	23.65	22.08	67.06	71.11
	road damage rear tires	$[10^{20} \text{ -}]$	1.11	1.08	0.24	0.22	0.12	0.18	2.70	2.10	8.40	13.02

Table B.3: Performance of the un-laden 3D vehicle model with passive (PASM) and semi-active (ADCC) tractor rear axle suspension.

			standard brick		traffic hump		scraped road		well		wave		
aspect	criterion	unit	PASM	ADCC	PASM	ADCC	PASM	ADCC	PASM	ADCC	PASM	ADCC	
comfort	max $ \ddot{q}_{sv} $	$[\text{m}/\text{s}^2]$	5.88	6.15	17.34	17.89	10.56	9.89	12.20	12.76	47.35	46.09	
	max $ \ddot{q}_{slo} $	$[\text{m}/\text{s}^2]$	7.13	7.36	14.90	14.14	2.84	2.74	6.70	5.78	10.10	10.83	
	max $ \ddot{q}_{sla} $	$[\text{m}/\text{s}^2]$	9.85	9.67	1.51	1.47	1.31	1.41	9.28	9.48	4.89	4.93	
	max $ \ddot{q}_{sv,w} $	$[\text{m}/\text{s}^2]$	1.76	1.86	11.16	11.49	7.56	7.58	8.12	8.19	32.51	31.29	
	max $ \ddot{q}_{slo,w} $	$[\text{m}/\text{s}^2]$	0.78	0.85	4.10	4.13	2.42	2.06	1.83	1.61	3.80	4.12	
	max $ \ddot{q}_{sla,w} $	$[\text{m}/\text{s}^2]$	0.91	0.86	0.92	0.90	0.44	0.45	1.98	1.99	3.56	3.71	
	RMS \ddot{q}_{sv}	$[\text{m}/\text{s}^2]$	0.72	0.74	4.65	4.67	2.60	2.53	1.77	1.72	11.46	11.44	
	RMS \ddot{q}_{slo}	$[\text{m}/\text{s}^2]$	0.99	1.02	2.03	1.92	0.60	0.54	0.95	0.89	1.45	1.47	
	RMS \ddot{q}_{sla}	$[\text{m}/\text{s}^2]$	0.92	0.95	0.31	0.34	0.28	0.29	1.30	1.29	1.09	1.11	
	RMS $\ddot{q}_{sv,w}$	$[\text{m}/\text{s}^2]$	0.40	0.42	3.27	3.30	1.95	1.89	1.56	1.51	7.33	7.32	
	RMS $\ddot{q}_{slo,w}$	$[\text{m}/\text{s}^2]$	0.26	0.26	1.20	1.17	0.56	0.53	0.26	0.25	1.34	1.33	
	RMS $\ddot{q}_{sla,w}$	$[\text{m}/\text{s}^2]$	0.13	0.13	0.27	0.27	0.13	0.12	0.42	0.42	0.85	0.88	
	VD \ddot{q}_{sv}	$[\text{m}/\text{s}^{1.75}]$	1.95	2.01	8.96	9.10	5.66	5.46	4.42	4.43	22.05	21.81	
	VD \ddot{q}_{slo}	$[\text{m}/\text{s}^{1.75}]$	2.63	2.68	5.12	4.87	1.28	1.16	2.45	2.26	3.49	3.78	
	VD \ddot{q}_{sla}	$[\text{m}/\text{s}^{1.75}]$	3.00	3.11	0.65	0.68	0.53	0.55	3.44	3.45	2.43	2.49	
	VD $\ddot{q}_{sv,w}$	$[\text{m}/\text{s}^{1.75}]$	0.86	0.89	5.92	6.00	4.05	3.96	3.53	3.50	14.63	14.34	
	VD $\ddot{q}_{slo,w}$	$[\text{m}/\text{s}^{1.75}]$	0.39	0.40	2.19	2.17	1.21	1.08	0.69	0.63	2.39	2.44	
	VD $\ddot{q}_{sla,w}$	$[\text{m}/\text{s}^{1.75}]$	0.30	0.29	0.51	0.51	0.23	0.22	0.93	0.93	1.87	1.94	
	max $ \ddot{q}_{sv} $	$[\text{m}/\text{s}^3]$		425	388	449	493	344	324	827	812	1613	1485
	max $ \ddot{q}_{slo} $	$[\text{m}/\text{s}^3]$		680	690	1210	1132	124	96	583	585	439	475
	max $ \ddot{q}_{sla} $	$[\text{m}/\text{s}^3]$		601	667	84	89	68	106	690	703	200	227
	RMS $ \ddot{q}_{sv} $	$[\text{m}/\text{s}^3]$		48	49	83	86	58	54	84	82	224	220
	RMS $ \ddot{q}_{slo} $	$[\text{m}/\text{s}^3]$		94	97	149	141	28	23	85	79	70	72
	RMS $ \ddot{q}_{sla} $	$[\text{m}/\text{s}^3]$		67	69	16	18	18	19	87	87	36	36

Table B.4: Performance of the un-laden 3D vehicle model with passive (PASM) and semi-active (ADCC) tractor rear axle suspension.

			standard brick		traffic hump		scraped road		well		wave	
aspect	critereon	unit	PASM	ADCC	PASM	ADCC	PASM	ADCC	PASM	ADCC	PASM	ADCC
load	max $ \ddot{q}_{kv} $	[m/s ²]	8.83	7.78	16.45	16.18	11.65	12.73	6.55	6.76	12.08	12.11
	max $ \ddot{q}_{culr} $	[m/s ²]	9.98	8.47	18.20	18.93	12.79	15.48	9.13	9.49	11.61	12.32
	max $ \ddot{q}_{cufrr} $	[m/s ²]	13.03	12.59	18.29	18.84	12.81	15.69	6.61	6.63	12.56	12.47
	PM \ddot{q}_{culf}	[-]	0.14	0.25	1.16	1.16	0.50	0.48	0.91	1.73	63.11	62.08
	PM $\ddot{q}_{cuf f}$	[-]	0.02	0.02	1.01	1.01	0.46	0.44	0.37	0.55	59.62	58.01
	PM \ddot{q}_{culr}	[-]	0.18	0.07	11.26	9.38	0.96	3.37	0.48	0.34	1.21	1.50
	PM \ddot{q}_{cufrr}	[-]	0.35	0.24	11.06	9.39	0.97	3.72	0.10	0.08	1.51	1.57
deflection	nr bound hits $\dot{l}r$	[-]	0	0	0	0	0	0	0	0	0	0
	nr bound hits $\dot{r}r$	[-]	0	0	0	0	0	0	0	0	0	0
	max $ \Delta\dot{q}_{lr} $ at bounds	[m/s]	0.00	0.00	0.00	0.00	0.00	0.00	0.00	0.00	0.00	0.00
	max $ \Delta\dot{q}_{rr} $ at bounds	[m/s]	0.00	0.00	0.00	0.00	0.00	0.00	0.00	0.00	0.00	0.00
	RMS Δq_{lr}	[10 ⁻² m]	0.25	0.22	1.87	2.02	0.92	0.75	0.49	0.46	2.39	3.02
	RMS Δq_{rr}	[10 ⁻² m]	0.38	0.29	1.94	2.02	1.02	0.74	0.44	0.34	2.68	3.24
handling	tire lift-off $\dot{l}r$	[s]	0.034	0.029	0.270	0.272	0.091	0.084	0.096	0.080	0.000	0.000
	tire lift-off $\dot{r}r$	[s]	0.000	0.000	0.222	0.207	0.084	0.077	0.000	0.000	0.000	0.000
	<75% stat tire force $\dot{l}r$	[s]	0.060	0.088	0.379	0.401	0.140	0.159	0.117	0.110	0.536	0.528
	<75% stat tire force $\dot{r}r$	[s]	0.065	0.090	0.317	0.323	0.124	0.135	0.098	0.101	0.511	0.484
	RMS dyn tire force $\dot{l}r$	[10 ³ N]	5.56	5.81	9.87	9.89	5.73	5.46	6.02	5.52	6.39	6.66
	RMS dyn tire force $\dot{r}r$	[10 ³ N]	1.71	2.09	9.29	9.32	5.33	5.15	3.29	3.34	7.73	8.02
damage	road damage all tires	[10 ²⁰ -]	1.76	1.74	0.20	0.19	0.10	0.09	0.84	0.82	2.09	2.13
	road damage rear tires	[10 ²⁰ -]	0.33	0.37	0.04	0.03	0.02	0.01	0.03	0.02	0.00	0.00

References

- [1] Aa, M.A.H. van der, *Optimal control of semi-active suspension systems with preview*, Master thesis, Eindhoven University of Technology, Dept. of Mechanical Engineering, Report No. WFW 94.100, 1994.
- [2] Bellman, R., *Dynamic Programming*, Princeton University Press, Princeton, N.J., 1957.
- [3] Bekkers, F.P.J., *Modular based vehicle modelling. 3D modular based tractor-semitrailer models to predict the dynamic behaviour on handling and deterministic road irregularities*, Master thesis, Eindhoven University of Technology, Dept. of Mechanical Engineering, Report No. WFW 95.078, 1995.
- [4] Bender, E.K., *Optimum linear preview control with application to vehicle suspension*, Trans. ASME Journal of Basic Engineering, 213-221, June 1968.
- [5] Benschop, P.B., *The optimal control of an adjustable spring stiffness in a semi-active suspension system with preview*, Eindhoven University of Technology, Dept. of Mechanical Engineering, Report No. WFW 95.14, 1995.
- [6] Butsuen, T., Hedrick, J.K., *Optimal semi-active suspensions for automotive vehicles: the 1/4 car model*, Advanced Automotive Technologies - 1989, A.M. Karmel, E.H. Law, and S.R. Velinsky, eds., 305-319, ASME Winter Annual Meeting, San Francisco, CA., Dec 10-15, 1989.
- [7] CADSi, *DADS reference manual*, revision 7.5, Vol. 1-2, Computer Aided Design Software Inc., Coralville, 1993.
- [8] Clocquet, R.C., *A semi-active damper with DC controller in a 3D DAF95 model*, Master thesis, Eindhoven University of Technology, Dept. of Mechanical Engineering, Report No. WFW 96.022, 1996.
- [9] Foag, W., *Regelungstechnische Konzeption einer Aktiven PKW-Federung mit 'Preview'*, VDI-Verlag, 1990. Fortschr.-Ber. VDI Reihe 12 Nr. 139, ISBN 3-18-143912-6.
- [10] Gökten, A., Mitschke, M., *Road damage caused by heavy duty vehicles*, International Journal of Vehicle Design, 16(1):54-70, 1995.
- [11] Griffin, M.J., Whitham, E.M., *Discomfort produced by impulsive whole-body vibration*, Journal of the Acoustical Society of America, 68(5):1277-1284, 1980.
- [12] Griffin, M.J., *Evaluation of vibration with respect to human response*, SAE paper

- 860047, Institute of Sound and Vibration Research, University of Southampton, England, 1986.
- [13] Hać, A., Youn, I., *Optimal semi-active suspension with preview based on a quarter car model*, Trans. ASME Journal of Vibration and Acoustics, 114:84-92, 1992.
- [14] Haftka, R.T., and Gürdal, Z., *Elements of structural optimization*, Kluwer, 1992.
- [15] Haug, E.J., and Arora, J.S., *Applied optimal design*, John Wiley & Sons, 1979.
- [16] Hoberock, L.L., *A survey of longitudinal acceleration comfort studies in ground transportation vehicles*, Trans. ASME Journal of Dynamic Systems, Measurement, and Control, 99(2):76-84, 1977.
- [17] Howarth, H.V.C., Griffin, M.J., *Subjective reaction to vertical mechanical shocks of various waveforms*, Journal of Sound and Vibration, 147(3):395-408, 1991.
- [18] Hrovat, D., *Applications of optimal control to advanced automotive suspension design*, Trans. ASME Journal of Dynamic Systems, Measurement, and Control, 115:328-342, 1993.
- [19] Huisman, R.G.M., *A controller and observer for active suspensions with preview*, Ph.D. thesis, Eindhoven University of Technology, 1994, ISBN 90-386-0274-X.
- [20] ISO 2631/1-1985(E), *Evaluation of human exposure to whole-body vibration - part 1: general requirements*, International Organization for Standardization, 1985.
- [21] Jager, R.R.W. de, *Simulation of quarter-car model by analogue electronics*, Master thesis, Eindhoven University of Technology, 1997.
- [22] Karnopp, D., Crosby, M.J., Harwood, R.A., *Vibration control using semi-active force generators*, Trans. ASME Journal of Engineering for Industry, 619-626, May 1974.
- [23] Karnopp, D., *Active damping in road vehicle suspension systems*, Vehicle System Dynamics, 12:291-316, 1983.
- [24] Kjellberg, A., Wikström, B.-O., *Subjective reactions to whole-body vibration of short duration*, Journal of Sound and Vibration, 99(3):415-424, 1985.
- [25] Land, A.H., Doig, A.G., *An automatic method for solving discrete programming problems*, Econometrica, 28:497-520, 1960.
- [26] Margolis, D.L., *The response of active and semi-active suspensions to realistic feedback signals*, Vehicle System Dynamics, 11:267-282, 1982.
- [27] Mitschke, M., *Dynamik der Kraftfahrzeuge (Band B: Schwingungen)*, Springer Verlag, Berlin, 1997.
- [28] Miwa, T., *Evaluation methods for vibration effect, Part 7: The vibration greatness of pulses*, Industrial health, 6:143-164, 1967.
- [29] Muijderland, J.H.E.A., Veldpaus, F.E., Kok, J.J., *A semi-active suspension system based on dynamic programming*, Proc. of the Int. Symp. on Advanced Vehicle Control 1994 (AVEC'94), 177-182, Tsukuba City, 1994.

- [30] Muijderman, J.H.E.A., Veldpaus, F.E., Kok, J.J., Heck, J.G.A.M. van, *A general criterion controller with preview for a semi-active truck suspension*, Proc. of the Int. Symp. on Advanced Vehicle Control 1996 (AVEC'96), 63-75, Aachen, 1996.
- [31] Newland, D.E., *An introduction to random vibrations and spectral analysis*, Longman, 1975.
- [32] Segel, L., Ervin, R., Fancher, P., *The mechanics of heavy-duty trucks and truck combinations*, Proc. of the Int. Assoc. for Vehicle Design, course notes. Aston Clinton, UK, September 1981.
- [33] Snowdon, J.C., *Vibration and shock in damped mechanical systems*, John Wiley & Sons, Inc., 1968.
- [34] Soede, M.J., *A semi-active suspension of a tractor-semitrailer combination with preview*, Master thesis, Eindhoven University of Technology, Dept. of Mechanical Engineering, Report No. WFW 95.171, 1995.
- [35] Suresh, S., *Fatigue of materials*, Cambridge Solid State Science Series, Cambridge University Press, 1991.
- [36] Tomizuka, M., Hedrick, J.K., *Advanced control methods for automotive applications*, Vehicle System Dynamics, 24:449-468, 1995.
- [37] Tseng, H.E., Yi, K., Hedrick, J.K., *A comparison of alternative semi-active control laws*, Advanced Automotive Technologies - 1991, DE-Vol. 40, 1991 ASME WAM.
- [38] Tseng, H.E., Hedrick, J.K., *Semi-active control laws - optimal and sub-optimal*, Vehicle System Dynamics, 23:545-569, 1994.
- [39] Vael, G., *The nature and origin of suspension related dynamic phenomena in tractor-semitrailer combinations*, DAF Trucks N.V., The Netherlands, personal communication, 1993.
- [40] Venhovens, P.J.Th., *Optimal control of vehicle suspensions*, Ph.D. thesis, Delft University of Technology, The Netherlands, 1993.
- [41] Vissers, J.H.G., *Real-time implementation of a preview-based control strategy for a semi-active truck suspension*, 2nd Phase Master thesis, Stan Ackermans Instituut, Eindhoven University of Technology, 1997.
- [42] Wirsching, P.H., Paez, T.L., Ortiz, K., *Random vibrations: theory and practice*, John Wiley & Sons, Inc., 1995.

Samenvatting

De veersystemen in een trekker-oplegger combinatie zijn in belangrijke mate verantwoordelijk voor het comfort van de inzittenden, de wegligging, de benodigde veerwegen, de belasting van het wegdek en de belasting van de lading en van componenten die aan het chassis bevestigd zijn. De prestatie van deze veersystemen kan worden verbeterd door het toepassen van geregelde, snel schakelbare dempers.

Gangbare ontwerp methoden voor regelingen gaan uit van kwadratische criteria, die het doel van de regeling weergeven, en lineaire modellen, die het systeem gedrag karakteriseren. De ontwikkeling van regelingen voor schakelbare dempers wordt bemoeilijkt door het niet beschikbaar zijn van geschikte mathematische uitdrukkingen voor begrippen als comfort en wegligging. Verder zorgen de demper dynamica en de niet-lineaire karakteristieken van de schakelbare demper voor een verdere complicatie bij het ontwerpen van regelingen m.b.v. de gangbare methoden.

In dit proefschrift worden model-gebaseerde regelconcepten beschreven voor snel schakelbare dempers, die lijken op 'Model Predictive Control' concepten. Die concepten kunnen een groot scala van criteria aan en kunnen rekening houden met niet-lineariteiten in het veersysteem. Zij gebruiken de demper hetzij als continu variabele demper hetzij als demper met meerdere discrete standen. Alle voorgestelde regelconcepten gaan er vanuit dat het wegdek tussen de voor- en de achterwielen van de trekker op ieder moment bekend is. Deze zogenaamde preview informatie kan door reconstructie worden verkregen uit metingen aan de trekker. Het tijdsinterval waarvoor het wegdek bekend is, het preview interval, wordt verdeeld in een aantal gelijke subintervallen. De stand van de demper, d.w.z. de kracht-relatieve snelheid karakteristiek, wordt steeds constant gehouden over zo'n subinterval.

Om een verdere uitwerking van de regelconcepten mogelijk te maken en de verschillende geregelde veersystemen onderling en met een conventioneel passief veersysteem te kunnen vergelijken, wordt één doelstelling en één model met twee graden van vrijheid als intern voertuig model voor de regelingen gekozen. De gekozen doelstelling behelst het minimaliseren van de maximale absolute chassis versnelling, onder de voorwaarden dat de band niet loslaat en de grenzen van in- en uitvering niet worden bereikt. Indien het loslaten van de band niet kan worden voorkomen, dient de tijd van loslaten te worden geminimaliseerd en indien het bereiken van de grenzen aan de veerweg niet kan

worden voorkomen, dienen de botskrachten zo laag mogelijk te blijven.

Een simulatiemodel met twee graden van vrijheid en één gekozen regelconcept worden gebruikt om geschikte lengtes te bepalen voor de subintervallen en het interval waarna de preview informatie wordt geaktualiseerd. Uit dit onderzoek blijkt dat een betere prestatie voor het semi-actieve systeem dan die voor het passieve systeem alleen verkregen wordt als de lengtes van de subintervallen kleiner zijn dan of gelijk zijn aan de kleinste eigentrillings-periode van het gelineariseerde model. De lengtes van de subintervallen worden daarom iets kleiner gekozen dan deze eigentrillings-periode. Verder neemt de prestatie van het semi-actieve systeem sterk af indien het interval waarna de preview informatie wordt geaktualiseerd langer is dan de genoemde kleinste eigentrillings-periode. De lengte van dit interval wordt daarom gelijk genomen aan de lengte van een subinterval.

Het simulatie model met twee graden van vrijheid wordt eveneens gebruikt om de geregelde veersystemen te vergelijken. Uit dit onderzoek blijkt dat het systeem waarin de dempers twee discrete standen hebben te prefereren is boven het continu variabele demper systeem aangezien het vrijwel gelijke prestaties geeft bij een veel lagere rekeninspanning.

Tenslotte wordt de prestatie van een uitgebreid 3D model van een trekker-oplegger combinatie met conventionele dempers vergeleken met dat van een 3D model waarbij in de ophanging van de achteras van de trekker zowel aan de linker als aan de rechter zijde een demper met twee discrete standen is geplaatst. Deze dempers worden aangestuurd door afzonderlijke regelingen, die elk een intern voertuig model met twee graden van vrijheid gebruiken. Dit interne voertuig model beschrijft het gedrag van de linker of rechter achterzijde van de trekker. Iedere regeling krijgt als preview informatie het wegdek tussen voor- en achterwielen van de trekker aan de zijde van de te regelen demper. Vergelijking van de resultaten voor het conventionele voertuig en het voertuig met geregelde dempers laat zien dat het geregelde systeem in staat is om aan de achterzijde van de trekker de loslaattijd van de banden en een aantal hoge pieken in de chassis versnellingen te reduceren, zowel voor symmetrische als asymmetrische incidentele wegdek aanstotingen. De reductie van de pieken in de chassis acceleratie aan de linker en rechter achterzijde van de trekker leidt wel tot een reductie van de pieken in de belasting op de lading voor symmetrische wegdek aanstotingen en tot een reductie van de vermoeiingsbelasting op de chassis componenten aan de achterzijde van de trekker, maar niet automatisch tot een beter comfort in de cabine en ook niet automatisch tot een reductie van de pieken in de belasting op de lading voor asymmetrische wegdek aanstotingen. Uitgebreidere interne voertuig modellen zullen nodig zijn voor de regelbaar om de prestatie van het ontwikkelde semi-actieve veersysteem te verbeteren met betrekking tot deze twee laatstgenoemde aspecten.

Acknowledgments

I want to thank all the persons who have contributed to the work presented in this thesis.

First, I will express my gratitude to Frans Veldpaus (Eindhoven University of Technology), Jos van Heck (DAF Trucks) and Rudolf Huisman (DAF Trucks) for the support they gave me during the project and for the thoroughness by which they read and edited each part of the thesis. I am also grateful to Jan Kok (Eindhoven University of Technology), who gave me the opportunity to do this research project and also supported me with useful ideas and comments. The discussions with Frans, Jos, Rudolf and Jan were always stimulating and filled with thoughtful criticisms and valuable advises.

Furthermore, I thank prof.dr.ir. P.P.J. van den Bosch (Eindhoven University of Technology) and prof.dr.ir. H.B. Pacejka (Delft University of Technology) for their valuable advises and comments during the preparation of this thesis.

I thank all the students who participated in this research, *i.e.* Maycel van der Aa, Peter Benschop, Maris van Beurden, Rob de Bruijn, Robert Clocquet, Maurice Rienks and Michiel Soede for the research they carried out. I also thank my colleagues for their support and for the pleasant working atmosphere.

This study is performed in the context of the European research project CASCOV, made possible through the CEC Brite/Euram programme. I thank all the members of the CASCOV technical committee for their support during the past four years.

I thank my friends for their support, encouragement and understanding. And last but not least, I thank my family and Carla for their unconditional love, help and understanding.

Hans Muijderman

October 1997

Curriculum Vitae

October 6, 1966	Born in Veldhoven, the Netherlands
1979 - 1985	VWO, Anton van Duinkerkencollege, Veldhoven
1985 - 1991	Student at the Faculty of Mechanical Engineering, Eindhoven University of Technology
1991 - 1992	Military service at the vehicle test department of the land forces (AB/DMKL), Huijbergen
1992 - 1993	Design engineer at Hollandsche Beton- and Waterbouw (HBW), Gouda
1993 - 1997	Research assistant at the Faculty of Mechanical Engineering, Department of Computational and Experimental Mechanics (WFW), Eindhoven University of Technology

STELLINGEN

behorende bij het proefschrift

Flexible objective controllers for semi-active suspensions with preview

1. Het is vaak moeilijker een operationele formulering voor een technisch probleem te vinden dan een oplossing voor een goed gedefinieerd technisch probleem. (dit proefschrift)
2. Het voertuiggedrag op deterministische wegdekken zou eigenlijk op een stochastische manier moeten worden onderzocht. (dit proefschrift)
3. De mogelijkheid tot praktische implementatie van op preview gebaseerde semi-actieve systemen met een flexibel regeldoel wordt sterk vergroot door het combineren van analoge en digitale electronica. (dit proefschrift)
4. De effectiviteit van verkeersdrempels wordt sterk gereduceerd door toepassing van (semi-) actieve veersystemen. (dit proefschrift)
5. Wetenschappers zijn door de publicatiedwang teveel bezig met rapporteren en daardoor te weinig met het vinden van nieuwe methoden en technieken en met het praktisch toepasbaar maken ervan.
6. De invloed van klimatologische omstandigheden op de ontwikkeling van derde-wereld-landen wordt onderschat.
7. De problemen in o.a. België, het Verenigd Koninkrijk, de voormalige Sovjet-Unie en voormalig Joegoslavië zouden moeten leren dat een verenigd Europa, met landen die verschillen in taal en cultuur, zeer waarschijnlijk zal leiden tot grote interne spanningen.
8. Mensen die altijd druk zijn met hun werk dienen zich af te vragen of zij niet te veel aan hun carrière en te weinig aan hun toekomst denken.
9. Fouten vormen ons beter en leren ons meer dan successen.
10. Een promotie onderzoek begin je als vrije vogel en eindig je in een zelf gebouwde kooi.

Hans Muijderman

Eindhoven, oktober 1997